Forensic Investigation of AC and PCC Pavements with Extended Service Life

Volume 3: Petrographic Examination of Blast Furnace Slag Aggregate Concrete Cores taken from PCC Pavements in Cuyahoga County, Ohio

David Lankard, consultant

Report FHWA/OH-2010/004C

for the
Ohio Department of Transportation
Office of Research and Development

and the
United States Department of Transportation
Federal Highway Administration

State Job Number 134280

September 2010

Ohio Research Institute for Transportation and the Environment

1. Report No.	2. Government Accession No.	3. Recipient's Catalog No.
FHWA/OH-2010/004C		

4. Title and Subtitle Forensic Investigation of AC and PCC Pavements with Extended Service Life, Volume 3: Petrographic Examination of Blast Furnace Slag Aggregate Concrete Cores taken from PCC Pavements in Cuyahoga County, Ohio	**5. Report Date** September 2010 **6. Performing Organization Code**
7. Author(s) David Lankard, consultant	**8. Performing Organization Report No.**
9. Performing Organization Name and Address Ohio Research Institute for Transportation and the Environment (ORITE) 141 Stocker Center, Ohio University Athens OH 45701-2979	**10. Work Unit No. (TRAIS)** **11. Contract or Grant No.** State Job No. 134280
12. Sponsoring Agency Name and Address Ohio Department of Transportation Office of Research and Development 1980 West Broad St. Columbus OH 43223	**13. Type of Report and Period Covered** Technical Report **14. Sponsoring Agency Code**

15. Supplementary Notes

Prepared in cooperation with the Ohio Department of Transportation (ODOT) and the U.S. Department of Transportation, Federal Highway Administration

16. Abstract

The purpose of this research was to identify flexible and rigid pavements in Ohio with average and above average performance, and determine reasons for these differences in performance. The identification and implementation of factors linked to extended service life will improve performance statewide. FWD and ride quality profiles were measured to evaluate project uniformity, and material samples were obtained from a selected location on each project and tested in the laboratory to determine material properties. Volume 1 of the report includes: the project selection process, FWD and ride quality data, laboratory results of testing on base, subgrade and asphalt concrete pavement samples, and projected services lives using FWD data and the MEPDG. Volume 2 provides the results of laboratory tests and petrographic examinations on the Portland cement concrete cores. Volume 3 contains petrographic analysis of PCC pavement specimens in Cuyahoga County, Ohio containing Blast Furnace Slag Aggregate.

Flexible and rigid pavements in Ohio receiving no structural maintenance show an average condition rating of 68 after 20 and 30 years of service, respectively. This performance, coupled with no structural distress being observed on the pavements selected for study indicates pavement design procedures used in Ohio are meeting expectations. Among the items recommended to improve pavement performance include: 1) maintaining subgrade uniformity to minimize localized failures, 2) reducing amounts of Portland cement and using larger aggregate in 451 and 452 concrete, while continuing to test aggregate for D-cracking susceptibility, 3) increasing emphasis on ensuring that dowel bars maintain proper alignment during placement of PC concrete, and 4) continuing the use of performance grading and polymers when designing AC mixes on heavily traveled pavements. Other observations regarding the data used to reach these conclusions include: keeping the PMIS database current, retaining construction records for at least the design life of the pavements, being aware that the effect of surface cracks on flexible pavement performance depends upon whether the cracks are top-down or bottom-up, and the PMIS and straight-line diagrams should be consistent in identifying project limits, project numbers and paving materials.

Volume 3 of the report contains petrographic analysis of PCC pavement specimens in Cuyahoga County, Ohio containing Blast Furnace Slag Aggregate.

17. Key Words	18. Distribution Statement
Rigid Pavement Performance, Predicted Pavement Service Life, Forensic Testing, Petrographic Examination of PCC Cores, Blast Furnace Slag Aggregate.	No Restrictions. This document is available to the public through the National Technical Information Service, Springfield, Virginia 22161

19. Security Classif. (this report)	20. Security Classif. (this page)	21. No. of Pages	22. Price
Unclassified	Unclassified	136	

Form DOT F 1700.7 (8-72) **Reproduction of completed pages authorized**

SI* (MODERN METRIC) CONVERSION FACTORS

APPROXIMATE CONVERSIONS TO SI UNITS

Symbol	When You Know	Multiply By	To Find	Symbol
		LENGTH		
in	inches	25.4	millimeters	mm
ft	feet	0.305	meters	m
yd	yards	0.914	meters	m
mi	miles	1.61	kilometers	km
		AREA		
in^2	square inches	645.2	square millimeters	mm^2
ft^2	square feet	0.093	square meters	m^2
yd^2	square yards	0.836	square meters	m^2
ac	acres	0.405	hectares	ha
mi^2	square miles	2.59	square kilometers	km^2
		VOLUME		
fl oz	fluid ounces	29.57	milliliters	mL
gal	gallons	3.785	liters	L
ft^3	cubic feet	0.028	cubic meters	m^3
yd^3	cubic yards	0.765	cubic meters	m^3
NOTE: Volumes greater than 1000 L shall be shown in m^3.				
		MASS		
oz	ounces	28.35	grams	g
lb	pounds	0.454	kilograms	kg
T	short tons (2000 lb)	0.907	megagrams (or "metric ton")	Mg (or "t")
		TEMPERATURE (exact)		
°F	Fahrenheit temperature	5(°F-32)/9 or (°F-32)/1.8	Celsius temperature	°C
		ILLUMINATION		
fc	foot-candles	10.76	lux	lx
fl	foot-Lamberts	3.426	candela/m^2	cd/m^2
		FORCE and PRESSURE or STRESS		
lbf	poundforce	4.45	newtons	N
lbf/in^2 or psi	poundforce per square inch	6.89	kilopascals	kPa

APPROXIMATE CONVERSIONS FROM SI UNITS

Symbol	When You Know	Multiply By	To Find	Symbol
		LENGTH		
mm	millimeters	0.039	inches	in
m	meters	3.28	feet	ft
m	meters	1.09	yards	yd
km	kilometers	0.621	miles	mi
		AREA		
mm^2	square millimeters	0.0016	square inches	in^2
m^2	square meters	10.764	square feet	ft^2
m^2	square meters	1.195	square yards	yd^2
ha	hectares	2.47	acres	ac
km^2	square kilometers	0.386	square miles	mi^2
		VOLUME		
mL	milliliters	0.034	fluid ounces	fl oz
L	liters	0.264	gallons	gal
m^3	cubic meters	35.71	cubic feet	ft^3
m^3	cubic meters	1.307	cubic yards	yd^3
		MASS		
g	grams	0.035	ounces	oz
kg	kilograms	2.202	pounds	lb
Mg (or "t")	megagrams (or "metric ton")	1.103	short tons (2000 lb)	T
		TEMPERATURE (exact)		
°C	Celsius temperature	1.8°C + 32	Fahrenheit temperature	°F
		ILLUMINATION		
lx	lux	0.0929	foot-candles	fc
cd/m^2	candela/m^2	0.2919	foot-Lamberts	fl
		FORCE and PRESSURE or STRESS		
N	newtons	0.225	poundforce	lbf
kPa	kilopascals	0.145	poundforce per square inch	lbf/in^2 or psi

* SI is the symbol for the International Symbol of Units. Appropriate rounding should be made to comply with Section 4 of ASTM E380.

(Revised September 1993)

FINAL REPORT

FORENSIC INVESTIGATION OF AC AND PCC PAVEMENTS WITH EXTENDED SERVICE LIFE: Volume 3: Petrographic Examination of Blast Furnace Slag Aggregate Concrete Cores taken from PCC Pavements in Cuyahoga County, Ohio

State Job No. 134280(0)

By

Dr. David Lankard
Lankard Materials Laboratory, Inc.
Columbus, Ohio

July 20, 2010

Prepared in Cooperation with the Federal Highway Administration and the Ohio Department of Transportation

FORENSIC INVESTIGATION OF AC AND PCC PAVEMENTS WITH EXTENDED SERVICE LIFE: Volume 3: Petrographic Examination of Blast Furnace Slag Aggregate Concrete Cores taken from PCC Pavements in Cuyahoga County, Ohio

TABLE OF CONTENTS

APPENDICES

LIST OF TABLES (APPENDIX A)

LIST OF FIGURES (APPENDIX B)

LIST OF FIGURES CONT'D (APPENDIX B)

LIST OF FIGURES, CONT'D (APPENDIX B)

LML REPORT NO. 5536N

ON

FORENSIC INVESTIGATION OF AC AND PCC PAVEMENTS WITH EXTENDED SERVICE LIFE: Volume 3: Petrographic Examination of Blast Furnace Slag Aggregate Concrete Cores taken from PCC Pavements in Cuyahoga County, Ohio

TO

OHIO RESEARCH INSTITUTE FOR TRANSPORTATION AND THE ENVIRONMENT (OHIO UNIVERSITY, ATHENS, OHIO)

DR. DAVID LANKARD
LANKARD MATERIALS LABORATORY
COLUMBUS, OHIO

July 20, 2010

BACKGROUND

Beginning in May 2009, Lankard Materials Laboratory (LML) began a study in support of a program, which is titled, "Forensic Investigation of Asphaltic Concrete (AC) and Portland Cement Concrete (PCC) Pavements with Extended Service Life." This program is jointly sponsored by the Federal Highway Administration, the Ohio Department of Transportation, and the Ohio Research Institute for Transportation and the Environment at Ohio University in Athens, Ohio. The program is founded on the reasoning that valuable insights could be gained by identifying the factors that have contributed to satisfactory levels of performance of AC and PCC pavements in the ODOT system. Over the period May, 2009 through April, 2010, LML conducted petrographic examinations and other studies of cores taken from 20 different PCC pavements sites in the ODOT system whose performance have been characterized as average or excellent in service (Lankard, 2010). The material and design variables examined in our work as regards their contribution to a satisfactory level of performance included,

- The type(s) of cements used in the concretes.
- The water to cementitious material ratio (w/cm) of the cementitious phase.
- The cement content of the concretes.

- Coarse aggregate type and size.
- Quality of the cement paste/aggregate bond.
- The occurrence and degree of cement-aggregate reactions.
- Resistance of the concrete to the effects of freezing and thawing.
- Fine aggregate type and constituents
- Parameters of the entrained air void system.
- Concrete density (unit weight).
- Control joint spacing.
- Control joint sealant material.
- The presence or absence of steel mesh reinforcement
- Base material
- Base design (free-draining or not).

In addition to the above factors, which were considered at LML, Ohio University provided (on companion cores) information on compressive strength, splitting tensile strength, and static modulus of elasticity, which is included in our report (Lankard, 2010). The results of the LML phase of the study is in the process of publication as Volume 2 of the subject program (Lankard, 2010).

In November, 2009, the Ohio Department of Transportation requested that Ohio University add to the subject program by including petrographic examinations (and other tests) on cores from four ODOT pavement projects in ODOT District 12 (specifically Cuyahoga County), which were constructed with concretes containing blast furnace (BF) slag as the coarse aggregate. It was intended that the study of these slag aggregate concretes would provide additional input to an ongoing FHWA project that is addressing unusual forms of deterioration in pavements constructed with slag aggregate concretes in Michigan (FHWA Draft Interim Report, 2009). Eight cores for this purpose were provided to LML by ODOT on March 3, 2010 from pavements that also show the unusual form of distress. The sites in Cuyahoga County include State Route 91 (One Site - 2 cores), State Route 176 (One Site - 2 cores), and State Route 175 (Two Sites - 2 cores from each Site). At each Site one core was taken from a distressed area and a second core was taken in close proximity to the distressed core in an area showing no distress. A summary of site information and other data on the eight cores is given in Table A-1 (Appendix A).

The information generated to date on the cited ongoing FHWA study of slag aggregate pavement concretes in Michigan has been compiled as a Draft Report (FHWA Draft Interim Report, 2009), which is currently under review. The over-riding material-related issue as expressed in this report is,

> *The role of air cooled blast furnace slag (ACBFS) aggregates in materials-related distress (MRD) in Michigan pavements has not yet been fully resolved.*

In the work done to date by other researchers (cited in [Draft Interim Report, 2009]) at least three potential sources of distress have been cited to explain the unique distress observed in Michigan pavements prepared with concretes containing air-cooled blast furnace slag aggregates, including,

1. <u>Alkali-silica reaction</u> activity (ASR), affecting ASR-prone rocks and minerals in the fine aggregate phase of the concrete.

2. <u>Internal sulfate attack</u>, with the precursor source of sulfate being the sulfides (mainly calcium sulfide) residing in the slag aggregate particles.

3. <u>Freeze/thaw damage</u> resulting from malfunctioning of the entrained air void system due to in-filling of the voids with secondary deposits (ettringite).

It is noted in the FHWA Draft Interim Report (2009) that,

> *"In-depth studies of the potential impact of calcium sulfide dissolution, alkali-silica reactivity (ASR), and internal sulfate attack have not been conducted and thus a relationship between the blast furnace slag aggregates and materials-related distress is only speculative at this juncture."*

The results obtained from our petrographic examination and other tests on the ODOT Cuyahoga County, Ohio pavement cores may shed some light on this matter (as discussed in the remainder of the present report). The structure of our report is summarized below.

- The next Section of the report provides a description of the four ODOT Cuyahoga County pavement concretes examined in our study.

- This is followed by a review of our examination and testing procedures, along with a description of the materials and properties of the core concretes.

- A brief description is then provided from a historical perspective of the unique form of distress experienced in the PCC pavements containing blast furnace slag aggregates (in Michigan and Ohio).

- The next Section of the report is devoted to a description of the cracking exhibited by the eight slag aggregate concrete cores examined here. A proposed mechanism is given for the cracking distress involving both internal sulfate attack and alkali-silica reaction activity.

- The following two Sections of the report provide detailed analyses of (1) internal sulfate attack, and (2) alkali-silica reaction activity as they are operative in these slag aggregate concretes.

- The final Section of the report summarizes the results of our study and provides a listing of the conclusions derived from the findings as well as a listing of recommendations for future studies and implementations.

- Throughout the present report, data from our 2009 forensic study are included to support a conclusion or a point of view where it is useful and appropriate to do so (Lankard, 2010).

PROJECT CONCRETES

The ODOT pavement sites for the present study are in Cuyahoga County, Ohio. They include (1) State Route 91 at one location, (2) State Route 175 at two locations, and (3) State Route 176 at one location. All of the cores have a diameter of 4 in. (10 cm), and were taken through the full depth of the pavements. Table A-1 in Appendix A provides information on (1) core length, (2) coring site and location, (3) the date of placement, and (4) the condition of the cores as-received at our laboratory. The mix designs of the core concretes are given in Tables A-2, A-3, and A-4 in Appendix A.

All of the concretes contain blast furnace (BF) slag as the coarse aggregate. The slag aggregate was obtained from two sources; both in the Cleveland, Ohio area. The fine aggregate in the concretes is a natural sand obtained from two sources (Table A-5, Appendix A).

State Route 91

This pavement concrete is ODOT's Class C concrete as shown in Table A-2. This is an air-entrained concrete containing 600 lb of portland cement per cubic yard (356 kg/m^3), with a maximum water to cementitious material ratio (w/cm) of 0.50. This project was constructed in 2002.

State Route 175

This pavement concrete is ODOT's High Strength concrete as shown in Table A-4. This is an air-entrained concrete containing 800 lb of portland cement per cubic yard (475 kg/m^3), with a maximum water to cementitious material ratio (w/cm) of 0.42. This concrete was used at both of the SR 175 coring site locations used for the present study. This project was constructed in 1999.

State Route 176

This pavement concrete is ODOT's Class C Option 1 concrete as shown in Table A-3. This is an air-entrained portland cement/fly ash concrete containing 510 lb of portland cement and 90 lb of Class C fly ash per cubic yard (303 and 53 kg/m^{3}respectively), with a maximum water to cementitious material ratio (w/cm) of 0.46. This project was constructed in1994.

EXAMINATION PROCEDURES AND DESCRIPTION OF THE CORE CONCRETES

The eight cores were taken full depth through the wearing surface of the pavements and were provided to LML in sealed plastic bags. As shown in Table A-1 (Appendix A) pavement thickness is 9 in. to 10 in.(23 to 25 cm) on SR 91; 9 in. to 10 ½ in.(23 to 27 cm) on SR 175; and 11 ½ in. (29 cm) on SR 176. For convenience and ease of discussion the eight cores were labeled Numbers 1 through 8 at our laboratory (Table A-1).

The examination and testing of the PCC pavement cores was conducted following relevant guidelines of the following American Society for Testing and Materials (ASTM) Standard Practices and Standard Test Methods.

- ASTM C 856 is "Standard Practice for the Petrographic Examination of Hardened Concrete."
- ASTM C 457 is "Standard Practice for Microscopical Determination of Parameters of the Air-Void System in Hardened Concrete." The modified point count method was used.
- ASTM C 642 is "Standard Test Method for Specific Gravity, Absorption, and Voids in Hardened Concrete."

The examination and testing of the cores provided the opportunity for,

- Characterization of the condition of the cores in the as-received state.
- Characterization of the cementitious phase of the concretes.

- Measurement of the cement paste content of the concretes.
- Characterization of the fine and coarse aggregate phases of the concretes.
- Measurement of the coarse aggregate content of the concretes.
- Characterization of the entrained air-void system of the concretes.
- Measurement of the density of the concretes.
- Characterization of pre-existing fractures in the concretes.
- Creation and examination of "new" fractures in the cores.
- Analysis and characterization of distress mechanisms.

The primary tool used in the petrographic examination of the cores is the stereomicroscope (Olympus SZX-12) at magnifications from 7X to 100X. Thin sections were made on several of the core concretes and examined using an optical polarizing microscope (Olympus CX-31). Scanning electron microscope (SEM) work was done using a JEOL Model JSM-840 with EDX capability.

Detailed information on the properties and proportioning of the concretes was obtained on the "No Distress" core from each of the four sites. All of the "No Distress" cores were received in one piece. An example of one of the "No Distress" cores is shown in Figure 1 for State Route 91. The dashed lines in Figure 1 show the location of saw-cuts that were made to provide a ¾ in. thick slice on which the saw-cut surfaces were lapped in accordance with the ASTM C 457 procedure. Slabs were prepared in this manner for seven of the eight cores. The "Distress" core taken from State Route 175 (Core 3) was examined using other techniques.

Cementitious Phase of the Core Concretes

The cementitious constituents of the core concretes are in compliance with those prescribed for the project concretes (Tables A-2, A-3, and A-4). In all of the core concretes the cement paste phase is variable in color and ranges from the normal gray that is typical for portland cement concretes to a dark green that is commonly seen in concretes that contain ground granulated blast furnace (GGBF) slag cement as a cementitious ingredient. Our examination of thin sections of the core concretes showed that the green coloration was derived from the BF slag coarse aggregates and not from GGBF slag cement.

The Water to Cementitious Material Ratio (w/cm) of the Cementitious Phase

Petrographic estimates of w/cm were made on the basis of a number of features of the hardened cement paste phase that reflect differences in w/cm. These features include (1) color, (2) hardness, (3) rate of water absorption, (4) relative abundance of unhydrated portland cement grains, and (5) the appearance of fresh fracture surfaces. It is commonly thought that a petrographic estimate of w/cm made by a qualified petrographer is within ± 0.03 of the actual value. Others place this range at ± 0.05.

There is some variability in w/cm in the core concretes on a microscopic level. In particular, the w/cm of a thin layer of cement paste along the outer surface of the slag aggregate particles is often lower than the "typical" values, which are given below.

- SR 91 Concrete (Core 2) = 0.44 (Target Value = Maximum of 0.50)
- SR 175 Concrete (Core 4) = 0.43 (Target Value = Maximum of 0.43)
- SR 175 @ Concord (Core 6) = 0.44 (Target Value = Maximum of 0.43)
- SR 176 Concrete (Core 8) = 0.47 (Target Value = Maximum of 0.46)

Within our ability to estimate w/cm it is concluded that all are in reasonable compliance with the target values of the mix designs.

Cement Paste Content of the Concretes

The cement paste content is a measured value that is obtained as part of the ASTM C 457 procedure. In the present study the modified point count method of ASTM C 457 was used. The measured cement paste content of the core concretes representing each of the four coring sites is shown in Table A-8 in Appendix A. The values, which are in volume percent, are summarized below.

- SR 91 Concrete (Core 2) = 26.0 % (Theoretical Value = 29.2 %)
- SR 175 Concrete (Core 4) = 33.5 % (Theoretical Value = 35.2 %)
- SR 175 @ Concord (Core 6) = 33.1 % (Theoretical Value = 35.2 %)
- SR 176 Concrete (Core 8) = 29.6 % (Theoretical Value = 28.3 %)

Carbonation of the Cementitious Phase of the Core Concretes

A hardened portland cement-based concrete surface exposed to the atmosphere can experience carbonation. Carbonation is the reaction of atmospheric carbon dioxide (CO_2) with the hydrated portland cement phases, most particularly calcium hydroxide. The pore water solution in portland cement concrete is highly basic, with a pH typically in the range of 13 to 14. When carbonation occurs, the pH is reduced, often to a neutral value of 7 or even lower.

In pavement applications the portions of the pavement that can experience carbonation are the pavement wearing surface and concrete that is exposed along a joint or a vertical crack in the concrete. In the present study the depth of carbonation of the wearing surface of the pavement cores was measured by applying a pH indicating solution (phenolphthalein) to fresh saw-cut surfaces. The saw-cuts are made perpendicular to the plane of the wearing surface (as shown in Figure 2). The phenolphthalein (in an alcohol solution) is applied in a light mist form to the concrete surface. If the surface has a pH above 10 (i.e. is not carbonated), the phenolphthalein produces a bright red color. If the pH is below 10, there is no color change in the concrete and the concrete exhibiting this behavior is judged to be carbonated. The actual pH of the concrete was checked by applying a universal indicating solution to the fresh saw-cut surfaces of the cores. The universal indicating solution is Rainbow Indicator, a proprietary product produced by Germann Instruments Company in Evanston, Illinois. Through the use of distinctive color changes, this indicating solution can identify pH regions ranging from 5 to 13.

Figure 2 shows a saw-cut surface of "No-Distress" Core 2 (SR 91) and Core 4 (SR 175) following the application of the phenolphthalein solution. The saw-cuts are perpendicular to the plane of the pavement wearing surface. No carbonation has occurred in the cementitious phase in those portions of the surface that are red in color. The only carbonation in these cores is in portions of a thin layer (0 to 1 mm) of the topmost layer of the wearing surface. A similar result was obtained on most of the other cores examined in the study. An exception is Core 1 (SR 91 – Distress), which was taken through a joint crack and which shows some shallow carbonation along the topmost portions along the length of the crack. The global absence of any significant amount of carbonation of the wearing surface is attributed in large part to the good quality (low w/cm) of the cementitious phase of the core concretes.

The Fine Aggregate Phase of the Core Concretes

The fine aggregate phase in the core concretes is a natural sand from one of two sources (as shown in Table A-5 (Appendix A). The rock and mineral species in the sands were identified in the petrographic examination. They are listed in Table A-6 (Appendix A) in order of decreasing abundance.

The dominant mineral species in the core sands is quartz. The second most abundant mineral is siltstone. Chert is present in all of the sands and is rated as being the 6th or 7th most abundant rock type. As will be discussed in detail later in the present report, alkali-silica reaction (ASR) activity was identified in chert and siltstone particles in the core concretes.

For comparative purposes the constituents of the natural sands in the twenty ODOT pavement concretes examined in the precursor study to the present one (Lankard, 2010) are listed in Table A-7 (Appendix A) in order of decreasing abundance. Quartz is the dominant mineral species in all twenty of these concretes. Siltstone is the 2nd or 3rd most abundant rock type in eighteen of the twenty concretes and chert is present in all but one of the twenty sands, ranging from 3rd most abundant to 9th most abundant. On average for the twenty concretes, the chert constituent in these sands is the 5th to 6th most abundant mineral type.

The dominant rock and mineral species (quartz and siltstone) are comparable in the natural sands from our two projects. The relative abundance of chert is also similar (ca. 6th most abundant).

The Coarse Aggregate Phase of the Core Concretes

The coarse aggregate phase in the core concretes is a blast furnace slag from one of two sources (as shown in Table A-5 (Appendix A). Both slag sources are in the Cleveland, Ohio region.

In Core 2 (SR 91) and in Cores 4 and 6 (SR 175) the nominal maximum particles size is ¾ in. (19 mm). The angular particles are compact to elongate in shape and typically range from brownish gray to medium dark gray in color. When examined in two dimensions on a lapped surface the shortest dimension of the largest of the elongate particles is less than ¾ in. (19 mm), and the longest dimension is typically less than 1 in. (25 mm).

In the Core 8 concrete (SR 176) the nominal maximum particles size is 1 in. (25 mm). The angular particles are compact to elongate in shape and typically range from brownish gray to medium dark gray in color. When examined in two dimensions on a lapped surface the shortest dimension of the largest of the elongate particles is frequently greater than ¾ in. (19 mm) and the longest dimension is typically 1in. to 1 ¼ in. (25 mm to 32 mm).

The coarse aggregate content of the core concretes was measured using the modified point count method of ASTM C 457, with the following results (as volume percent). The measured values are in reasonable compliance with the mix design values.

- SR 91 Concrete (Core 2) = 33.4 % (Theoretical Value = 34.6 %)
- SR 175 Concrete (Core 4) = 33.3 % (Theoretical Value = 35.2 %)
- SR 175 @ Concord (Core 6) = 36.4 % (Theoretical Value = 35.2 %)
- SR 176 Concrete (Core 8) = 33.7 % (Theoretical Value = 35.6 %)

Air Void Parameters and Density of the Core Concretes

All four of the core concretes are air entrained. ASTM C 457 characterization data on the air void content, air void spacing factor, and air void specific surface area are given in Table A-8 (Appendix A). The target air content for the ODOT pavement concretes is 6 % ± 2 %.

Density measurements were made on the core concretes following a 48 hour water soaking period using the water immersion procedure of ASTM C 642. A density measurement made on water-saturated concrete is expected to correlate with the original unit weight of the concrete in the fresh state.

SR 91 (Core 2)

This core concrete has a total air void content of 6.9 percent; a spacing factor of 0.0054 in. (0.13 mm); and a specific surface area of 703 in^2/in^3 (28 mm^{-1}). The water-saturated density of the core concrete is 140.5 lb/ft^3 (2251 kg/m^3). The theoretical unit weight of the Core 2 concrete at an air content of 6 % is 139.1 lb/ft^3 (2229 kg/m^3).

SR 175 (Core 4)

This core concrete has a total air void content of 7.0 percent; a spacing factor of 0.0038 in. (0.09 mm); and a specific surface area of 1197 in^2/in^3 (48 mm^{-1}). The water-saturated density of the core concrete is 139.2 lb/ft^3 (2230 kg/m^3). The theoretical unit weight of the Core 4 concrete at an air content of 6 % is 132.6 lb/ft^3 (2125 kg/m^3).

SR 175 @ Concord (Core 6)

This core concrete has a total air void content of 3.73 percent; a spacing factor of 0.0040 in. (0.10 mm).; and a specific surface area of 1487 in^2/in^3 (60 mm^{-1}). The water-saturated density of the core concrete is 143.4 lb/ft^3 (2298 kg/m^3). The theoretical unit weight of the Core 6 concrete at an air content of 6 % is 132.6 lb/ft^3 (2125 kg/m^3).

SR 176 (Core 8)

This core concrete has a total air void content of 6.9 percent; a spacing factor of 0.0052 in. (0.13 mm); and a specific surface area of 835 in^2/in^3 (34 mm^{-1}). The water-saturated density of the core concrete is 139.3 lb/ft^3 (2232 kg/m^3). The theoretical unit weight of the Core 8 concrete at an air content of 6 % is 134.3 lb/ft^3 (2152 kg/m^3).

The data presented in this Section of the report support a conclusion that the four pavement concretes examined here are in reasonable compliance with the mix design requirements and values from the point of view of (1) cementitious constituents, (2) cement content, (3) not exceeding the target w/cm, (4) coarse aggregate type (slag), and (5) coarse aggregate content. All of the concretes are air entrained and are in compliance with the specified value, with the exception of the Core 6 concrete in which the air content is low (3.7 %). The air content also shows considerable within core variability in both cores from the SR 175 @ Concord Site (Cores 5 and 6).

It is noted that for the four SR 175 cores and the SR 176 cores the measured density is considerably in excess of the theoretical unit weight value. The measured total air content of the Core 6 is 3.7 %, accounts in part for the density difference in this core concrete. The density difference for the others is not clear.

With the material characterization data as background, the nature of the distress in the ODOT Cuyahoga County, Ohio pavement concrete will be described in detail and analyzed in the remaining sections of the present report.

CHARACTERIZATION OF DISTRESS IN SLAG AGGREGATE CONCRETE PAVEMENTS

Examples of the cracking distress that is uniquely associated with pavement concretes containing BF slag coarse aggregates are shown in Figure 3 (Figures are presented in Appendix B). The top photograph shows this distress in a Michigan pavement as reported in a 2003 Transportation Research Board paper (Van Dam, 2003). The bottom photograph was taken in 2009 of a pavement in Cuyahoga County, Ohio from which cores examined in our study were taken (Ohio State Route 176).

The salient features of this type of cracking distress as revealed in past studies are,

- The cracks have formed in relatively young pavements (≤ 15 years of service).
- The cracking distress is most often (but not always) confined to the concrete adjacent to transverse control joints. The distress has also occurred in shoulder pavements.
- The control joints themselves in the affected areas are subject to the distress.
- The crack pattern as expressed in plan view on the pavement wearing surface is typically characterized as either “map cracking”, or “pattern cracking”.
- In the early stages of the distress the dominant orientation of the cracks as expressed on the pavement wearing surface is longitudinal (see the bottom photograph in Figure 3)
- In the more advanced stages of the distress, intersecting transverse cracks have formed and there is an associated crumbling and spalling of the wearing surface concrete nearest the control joint (see the top photograph in Figure 3).

As a related aside, BF slag has been used as the coarse aggregate in pavement concretes in Michigan and Ohio (and other states) for many decades. Many of these pavements have performed satisfactorily. In fact, three of the ODOT pavements examined in our 2009 study (Lankard, 2010), in which the pavement performance was rated as “Average” or “Excellent” contain slag aggregate. These pavements, which range in age from 15 to 19 years, are factored into our discussions in later Sections of the present report.

The remainder of the report is devoted to a description of the distress features in the core concretes taken from the four ODOT Cuyahoga County, Ohio pavements containing BF slag coarse aggregates and relating these features as discerned in the petrographic examinations to the mechanisms of distress.

CRACKING IN THE CUYAHOGA COUNTY, OHIO PAVEMENT CORES

Two cores were taken from each of four slag aggregate PCC pavement coring sites in Cuyahoga County, Ohio. One of the two cores was taken at a location on or very near a transverse control joint, where the distress is present as longitudinal and/or map cracking that can be seen on the pavement wearing surface. These locations are designated as the "Distress" locations. The companion second core at the four coring sites was taken at a "No Distress" location within 3 to 6 ft. (0.9 to 1.8 m) of the "Distress" core. At the "No Distress" locations the cracks that could be observed on the pavement wearing surface are either not present or are few in number and very tight. As will be shown, at least two of the "No Distress" cores show a less advanced stage of the sub-surface distress exhibited by the "Distress" cores.

The cores taken from the "Distress" locations (Table A-1) are listed below,

- Core 1 – SR 91 (Station 100+50)
- Core 3 – SR 175 (Station 269+80)
- Core 5 – SR 175 @ Concord (Station 270 + 80)
- Core 7 – SR 176 (Station 107)

Figures 4, 5, 6, and 7 show two views of the four "Distress" cores. The top photograph shows the full length of the core and the bottom photograph is a plan view of the wearing surface. Cracks that could be observed through visual and stereomicroscopic examinations of the as-cored surfaces of the cores are marked with a black marking pen in the top photographs.

Core 1 (Figure 4) was taken *through* a transverse control joint. The other three "Distress" cores were taken within 1 ft. to 4 ft. (0.3 m to 1.2 m) of a control joint and the following discussion focuses on the distress exhibited by these cores as revealed in their examination in the as-received condition. The features are similar in the cores and include,

- There are both "vertical" and "horizontal" cracks in the cores taken from the pavements adjacent to, but not directly over a control joint.

- In this report we define a "vertical" crack as a crack whose fracture plane is perpendicular to the plane of the wearing surface of the pavements. These cracks are those that can be seen on the wearing surface of the pavements (as seen in the bottom photographs of Figures 5, 6, and 7).

- In this report we define a "horizontal" crack as a crack whose fracture plane is parallel to the plane of the wearing surface of the pavements. These are sub-surface horizontal cracks that can not be seen on the wearing surface of the pavements.

- In these cores the vertical cracks are typically shallow and many are so tight that they can't be seen with the unaided eye.

- In plan view on the wearing surface, the vertical cracks are parallel, perpendicular, and at a diagonal to the texture lines of the wearing surface. In service the wearing surface texture lines have a transverse orientation. Typically, the widest vertical cracks are perpendicular to or at a diagonal to the texture lines (i.e. these cracks have primarily a longitudinal orientation).

- The sub-surface horizontal cracks as observed on the as-cored surfaces of the "Distress" cores are most numerous and widest within the interval of ca. ½ in. to 3 in. (12 mm to 76 mm) below the plane of the wearing surface.

- Some of the horizontal crack fracture planes are contiguous across the full cross-sectional area of the cores. For Core 3 (Figure 5) and Core 5 (Figure 6) this resulted in a separation of the top ca. 2 in. (5 cm) portion of the core from the bottom portion.

- Others of the horizontal crack fracture planes are discontinuous as can be seen in the top photographs of Figures 5, 6, and 7.

- No sub-surface horizontal cracks were detected in the examination of the as-cored surfaces of the cores at depths below around 3 in. (8 cm). The horizontal cracks do go deeper into the cores as revealed in the subsequent examinations on lapped surfaces.

Sub-Surface Horizontal Cracking in the "Distress" Cores

The as-cored surfaces of the cores have a relatively rough texture. Because of this, only the widest cracks can be detected on as-cored surfaces, even under microscopic examination. The same is true in the examination of saw-cut surfaces. Lapping of the saw-cut concrete surfaces to greater and greater degrees of flatness reveals the more narrow cracks, if they are present. The dashed lines in the top photograph of Figure 1 show the location of saw-cuts that were made on the cores in the present study. These saw-cuts yield "slab-shaped" samples that are about ¾ in. (19 mm) thick, which are the full length of the core. The saw-cut surfaces of the slab are lapped (polished) on a steel wheel using successively finer polishing grits. Subsequent stereomicroscopic examination of the lapped core surfaces did reveal the presence of many more horizontal cracks in the "Distress" cores. This comparison is shown in Figures 8 and 9, in which the top photograph shows the location of the horizontal cracks that were detected visually and microscopically on the as-cored surfaces of the cores and the bottom photograph shows one of the lapped surfaces of the same core on which the cracks detected in the stereomicroscopic examination are marked with a black marking pen.

Figure 8 shows the distribution of the sub-surface horizontal cracks in Core 5, which is the core taken from a "Distress" location on the State Route 175 @ Concord pavement. Sub-surface horizontal cracks were detected on the as-cored surfaces to a depth of ca. 2.5 in. (6.4 cm) below the wearing surface (top photograph in Figure 8). Sub-surface horizontal cracks were detected on the lapped surfaces to a depth of ca. 7 in. (18 cm) below the wearing surface (bottom photograph in Figure 8).

Figure 9 shows the distribution of the sub-surface horizontal cracks in Core 7, which is the core taken from a "Distress" location on the State Route 176 pavement. Sub-surface horizontal cracks were detected on the as-cored surfaces to a depth of ca. 3 in. (7.6 cm) below the wearing surface (top photograph in Figure 9). Sub-surface horizontal cracks were detected on the lapped surfaces to a depth of ca. 10 in. (25 cm) below the wearing surface (bottom photograph in Figure 9).

Microscopic examination of the sub-surface horizontal cracking in the six "Distress" cores from the three State Route 175 and 176 coring sites revealed the following common features:

- The <u>dominant orientation</u> of the crack fracture planes is parallel to the plane of the wearing surface (referred to here as <u>sub-surface horizontal cracks</u>). This feature is shown in Figures 8 and 9.

- The <u>horizontal cracks begin</u> at a depth of ca. ¾ in. (19 mm) below the wearing surface. This feature is shown in Figures 5 through 9.

- The <u>greatest concentration</u> or clustering of the horizontal cracks is in the interval depth of ¾ in. (2 cm) to 3 in. (7.6 cm) below the wearing surface. This feature is shown in Figures 5, 6, 8, and 9.

- Relative to the top 3 in. (7.6 cm) thickness of the cores, <u>horizontal cracks that are present at depths below 3 in.</u> (1) are many fewer in number, (2) are significantly more narrow, and (3) tend to gradually trend from a horizontal orientation to a diagonal orientation. These features are shown in Figures 8 and 9.

- Virtually all the horizontal cracks pass around, rather than through the slag coarse aggregate particles. Examples of this microstructural features can be seen on a global scale in the bottom photographs of Figures 8 and 9. Enlarged views of this feature are shown in Figure 10.

- Within the top 3 in. (8 cm) thickness of the cores the horizontal cracks commonly pass around, rather than through fine aggregate particles. An example of this microstructural feature is shown in the top photograph of Figure 11. However, examples where the horizontal cracks pass through fine aggregate particles are not uncommon, as shown in the bottom photograph of Figure 11, where the crack passes through a siltstone fine aggregate particle.

- In those instances where the horizontal cracks in the top 3 in. (8 cm) of the cores pass through the fine aggregate particles, the particles in question are most often fine-grained siltstones. Less frequently, the intersected fine aggregate particles are chert. As will be discussed some of these particles show evidence of alkali-silica reaction (ASR) activity.

- In the top 3 in. (8 cm) of the cores some of the widest horizontal cracks cover the full width of the core. Tighter cracks in this portion of the core are most often discontinuous (that is, when viewed in two dimensions on the lapped surfaces, they do not pass through the full width of the core).

- At depths below 3 in. (8 cm) in the cores virtually all of the horizontal cracks are discontinuous and they pass around, rather than through fine and coarse aggregate particles.

Sub-Surface Horizontal Cracking in the "No Distress" Cores

Two of the companion cores (Cores 6 and 8) taken in areas of "No Distress" in close proximity to the "Distress" cores (see Table A-1) also show some of the sub-surface horizontal cracks. An example is provided by Core 6, which is the "No Distress" core taken at the SR 175 @ Concord pavement site. Core 6 was received in one piece in good condition. No sub-surface horizontal cracks could be seen on the cored surfaces.

Core 6 was sectioned (saw-cut) and lapped in the same manner as described previously. The examination of the lapped surfaces revealed the presence of a few horizontal cracks and a few shallow vertical cracks. These cracks are shown in Figure 12, which shows two views of a lapped surface of Core 6. The sub-surface horizontal cracks are very tight and can only be seen with the aid of the microscope. These cracks are present in a discontinuous form in the top ¾ in. to 1 ¼ in. thickness of the core (19 mm to 32 mm). These horizontal cracks are marked with a black pen in the top photograph of Figure 12. One of the cracks goes through a slag coarse aggregate particle.

The bottom photograph in Figure 12 is an enlarged view (10X) of a lapped surface of Core 6 showing horizontal cracks that (1) pass around a slag coarse aggregate particle, and (2) pass through several fine aggregate particles (chert and siltstone). The microstructural features of these cracks are similar to those described previously for the core taken from the "Distress" location of the State Route 175 @ Concord Site (Core 5). On the basis of the microstructural evidence it is judged that the sub-surface horizontal cracking in Core 6 is an "early stage" of the more extensive cracking shown in Core 5 (Figure 8).

Vertical Cracking in the Cores

The term "vertical crack" or "vertical cracking" as used in the present report refers to cracks that can be seen on the exposed wearing surface of the pavement slabs, in which the crack fracture planes are perpendicular to the plane of the pavement wearing surface. Often, cracks such as these are tight and shallow and are referred to as "crazing" or "craze" cracks. Craze cracks are typically attributed to restrained drying shrinkage or carbonation shrinkage strains. As discussed below, this is not the case for most of the vertical cracks observed on the wearing surface of the ODOT Cuyahoga County cores.

Vertical cracks are present in both the "Distress" and the "No-Distress" ODOT cores. The bottom photograph in Figure 1 is a plan view of the "No Distress" core (Core 6) from the SR 175 @ Concord pavement site, showing a tight, longitudinally oriented vertical crack. Similar expressions of vertical cracking are shown for the "Distress" cores in the bottom photographs of Figure 5 (Core 3), Figure 6 (Core 5), and Figure 7 (Core 7).

The petrographic observations discussed below support an opinion that these vertical cracks formed as a consequence of the prior formation of the sub-surface horizontal cracks described earlier for these cores. Examples of vertical cracking in the ODOT cores are shown in Figures 13, 14, and 15, which are enlarged lapped surface views perpendicular to the plane of the wearing surface of Cores 5, 6, and 8. The wearing surface is at the top in the photographs. Reference is made here to <u>"near-surface" slag coarse aggregate particles</u>. As used here, this term means slag aggregate particles that lie just under the plane of the wearing surface (at shallow depths ranging from less than 1 mm to 10 mm).

<u>The top photograph in Figure 13</u> shows a near-surface slag coarse aggregate particle (A) in Core 5 (taken from a "Distress" location in SR 175 @ Concord) 5, which is around ¼ in. (5 to 6 mm) below the plane of the wearing surface. The red arrows in the photograph point to the paths of vertical cracks (four of them), and diagonal cracks (two of them). Salient features of the cracks as viewed in two dimensions on the lapped surface shown in Figure 13 are:

- All the cracks are tight. For the cracks with the greatest width it is possible to see that the crack width is wider at the top than it is at the bottom.

- The cracks typically pass around, rather than through the fine aggregate particles.

- The vertical cracks terminate at the point of contact with the slag aggregate particle. There are no cracks in the slag aggregate particle.

- Three of the four vertical cracks penetrate the wearing surface in plan view. These are the cracks that can be seen on the pavement wearing surface in service.

- As viewed in two dimensions on the lapped surface, the crack along the left side of the slag aggregate particle continues along that side and most of the bottom surface of the particle.

<u>The bottom photograph in Figure 13</u> shows a near-surface slag coarse aggregate particle (A) in Core 6 (taken from a “No Distress” location in SR 175 @ Concord), which is 2.5 mm below the plane of the wearing surface. In this example there is a single vertical crack (red arrows) that passes through the aggregate particle and downward into the cementitious matrix underlying the aggregate particle. The crack width is wider at the top than it is at the bottom. The bond between the aggregate particle and the cementitious matrix is uninterrupted.

<u>The left-hand photograph in Figure 14</u> shows a near-surface slag coarse aggregate particle (A) in Core 6, (taken from a “No Distress” location in SR 175 @ Concord), which is ca. ¼ in. (5 mm) below the plane of the wearing surface. The red arrows in the photograph point to the paths of vertical cracks that pass through both the slag aggregate particle and the cementitious matrix phase of the concrete. Salient features of the cracks as viewed in two dimensions on the lapped surface in Figure 14 are,

- The crack pattern in the slag aggregate particle (A) is complex, but the cracking is confined to the particle. The cracks are wider at the top than at the bottom.

- The crack in the aggregate particle originates as a single crack at the bottom of the particle then forks at the site identified with the red dot. The two forks of the crack pass upward into the particle, but do not pass into the matrix.

- The vertical crack in the matrix is ½ in. (12 mm) long and it too is wider at the top than at the bottom. The crack typically passes around, rather than through the fine aggregate particles. The crack penetrates the plane of the wearing surface.

- There is a small amount of a white exudate material present on the surfaces of three fine aggregate particles located directly under the slag aggregate particle (identified with yellow dots on the particles).

The right-hand photograph in Figure 14 shows a near-surface slag coarse aggregate particle (A) in Core 7 (taken from a "Distress" location in SR 176) , which is less than 1 mm below the plane of the wearing surface. The red arrows point to a vertical crack that passes through the full thickness of the slag aggregate particle and passes into the cementitious matrix above and below the aggregate particle. The vertical crack intersects a large void in the middle of the aggregate particle. Sub-surface horizontal cracks in the cementitious matrix underlying the slag aggregate particle are marked with a black marking pen.

The left-hand photograph in Figure 15 shows a near-surface slag coarse aggregate particle (A) in Core 7 (taken from a "Distress" location in SR 176) , which is less than 0.5 mm below the plane of the wearing surface. The red arrows in the photograph point to the path of a vertical crack through the aggregate particle (which penetrates the wearing surface). There are sub-surface horizontal cracks in the cementitious matrix that lie directly under the slag aggregate particle (which have been marked with a black marking pen).

The right-hand photograph in Figure 15 shows a near-surface slag coarse aggregate particle (A) in Core 8 (taken from a "No Distress" location in SR 176) , which is around 0.4 in. (10 mm) below the plane of the wearing surface. The red arrows in the photograph point to the path of a vertical crack that passes through the top half of the slag aggregate particle and continues on through the cementitious matrix phase to penetrate the plane of the wearing surface.

Proposed Mechanism of the Cracking Distress in the Cores

The proposed mechanism of the cracking distress in the slag aggregate concretes where this cracking was observed ("Distress" Cores 3, 5 and 7 and "No Distress" Cores 6 and 8) is explained with the aid of the examples shown in Figure 16. Figure 16 shows photographs of lapped surface views at the wearing surface elevation, (perpendicular to the plane of the wearing surface) in "Distress" Cores 5 (SR 175 @ Concord) and 7 (SR 176). The photographs in Figure 16 show the full width of the cores, which is around 4 inches (10 cm). The petrographic evidence described in the current Section of our report support a conclusion that the following cracking mechanism is in play in the cores examined here. Two types of cracking were identified including (1) shallow vertical cracks with fracture planes oriented perpendicular to the plane of the wearing surface that penetrate the pavement wearing surface, and which frequently pass into and/or through near-surface slag aggregate particles, and (2) sub-surface horizontal cracks, whose fracture planes are oriented parallel to the plane of the pavement wearing surface.

With reference to Figure 16, it is proposed that multi-axial expansive stresses developed in service within the cementitious phase of the core concretes; initially in the top 3 inches (8 cm) or so of the pavement slabs. The internal expansive stresses initially created sub-surface horizontal cracks. As will be shown, there are two distress phenomena that are involved in the creation of the expansive internal stresses in the core concretes, and they are,

- Expansive stresses associated with alkali-silica reaction (ASR) activity in the core concretes.
- Expansive stresses associated with internal sulfate attack in the core concretes.

The petrographic evidence confirming the involvement of the cited distress mechanisms is described in detail in the next sections of the report. The actual mechanics of the cracking distress can be explained with reference to Figure 16.

1. Expansive stresses resulting from internal sulfate attack create sub-surface horizontal cracks within the cementitious matrix phase of the core concretes. In the early life of the pavements this activity is confined to the top 3in. (8 cm) or so of the pavement slabs (although the topmost ¾ in. (19 mm) layer may not be affected.

2. As illustrated by the red arrows in Figure 16, the “direction” of the strains created by the internal expansive stresses is upward toward the free surface, which is the wearing surface of the pavement slabs (i.e. along the path of least resistance). In the process, the cementitious matrix phase is “lifted-off and away from” some of the slag aggregate particles, creating a separation at the paste/aggregate bond line (Figures 8, 9, 10, 11, 12, 14, 15, and 16).

3. The internal sub-surface expansive stresses create a condition of tensile strains in the immediate wearing surface layer as shown by the double yellow arrows in Figure 16. This condition results in the formation of tensile cracks (vertical cracks) in the immediate wearing surface of the pavement slabs (Figures 13, 14, and 15).

4. The horizontal cracks originating along the cement paste/slag aggregate boundaries subsequently pass into the adjacent cementitious phase. The presence of these cracks provides access routes for water movement into the cementitious phase. At some point alkali-silica reaction (ASR) activity is initiated in those areas where both potentially reactive particles (such as chert) and high moisture levels are present.

5. With increasing service time both the horizontal and the vertical cracks in the pavements widen and propagate, resulting ultimately in spalling (material loss). This condition is most prevalent

in the concrete adjacent to joints and transverse cracks, where access to moisture is high, and repetitive traffic loads are most eccentric.

The petrographic evidence supports a conclusion that the vertical cracks depicted in Figures 13, 14, and 15 originate below the plane of the wearing surface due to the stresses resulting from internal sulfate reactions. In some cases the cracks begin on the underside of near-surface slag aggregate particles and are propagated upward through the particles and, in some cases through the thin mortar layer overlying the aggregate particle. Where the orientation of the slag aggregate particle is as shown in the top photograph of Figure 13, the upward pressure creates multiple vertical cracks in the mortar overlying the aggregate particles.

The slag aggregate particles are literally high-fired ceramic compositions that possess a high level of strength. When we intentionally created new fractures in the core concretes the resultant fracture surfaces showed fracture of the coarse aggregate particles as the dominant failure mode. It is reasonable to assume that classical crazing cracks in the wearing surface of the core concretes would not possess the level of force required to penetrate and pass through the high strength slag particles. This would be particularly true in the early life of the pavements where drying shrinkage and carbonation shrinkage strains would be highest, and the strength of the cementitious phase the lowest.

Table A-9 summarizes the condition of vertical and horizontal cracking distress in the ODOT slab aggregate PCC pavement cores. The extent of sub-surface horizontal cracking is ranked on the basis of categories of Heavy, Moderate, Light, and None. Vertical cracks are assessed as to whether or not they pass through near-surface slag coarse aggregate particles.

In the next Sections of the report the petrographic evidence for the proposed sources of the distress mechanisms (ASR and internal sulfate attack) are discussed. The conditions giving rise to internal sulfate attack are discussed first as it appears that the initial distress in the ODOT pavement concretes is due to this distress mechanism. This is followed by a discussion of the evidence for ASR activity and its consequences in the core concretes.

INTERNAL SULFATE ATTACK IN THE SLAG AGGREGATE CORES

Previous researchers have speculated that internal sulfate attack is one of the contributing factors to distress in slag aggregate PCC pavements in Michigan (FHWA Draft Interim Report, 2009). The results of the present study support a conclusion that this distress mechanism is also operative in Ohio Department of Transportation (ODOT) slag aggregate PCC pavements that show this unique form of distress.

In this Section of the report attention is first given to the source of the sulfates that create the chemical environment that is required for the internal sulfate reactions to take place. This is followed by a description of the petrographic evidence that supports the conclusion that this distress mechanism is operative in the ODOT cores examined here.

The Source of Sulfates Involved in Internal Sulfate Attack in the Core Concretes

Previous studies have shown that the primary constituents of blast furnace slags are oxide-forms of calcium, silica, alumina, and magnesia. The cited FHWA study (FHWA, 2009) reports that these four oxides account for approximately 95 percent of the chemical species in these slags. The other 5 percent is accounted for by various forms of sulfur, manganese, iron, titanium, fluorine, sodium, and potassium.

A portion (variable) of the chemical species present in air cooled BF slag is glassy (non-crystalline). The most prevalent crystalline mineral in blast furnace slags is melilite, which is a solid solution between gehlenite ($2CaO.MgO.2SiO_2$) and akermanite ($2CaO.Al_2O_3.SiO_2$). Other calcia-alumina silicate and calcia-magnesia silicate minerals may also be present in variable amounts in blast furnace slags.

Data from the National Slag Association shows that calcia (CaO) and silica (SiO_2) are the dominant oxide constituents of blast furnace slags, comprising 60 to 80 percent of the total. Sulfur bearing compounds are reported to have a typical range of 1.0 to 1.9 percent, with individual values as low as 0.6 percent and as high as 2.3 percent. The cited FHWA report (2009) indicates that the most common form of sulfide in blast furnace slags is calcium sulfide (CaS), which is the mineral oldhamite. One of the papers cited in the FHWA report (2009) shows that the dissolution of oldhamite dendrites in blast furnace slag is a source of gypsum and ettringite precipitation (Hammerling, 2000).

Green Coloration as a Marker for Sulfides Derived from the Slag Aggregates

The findings of our study support the conclusion that sulfur compounds (in the form of sulfides and sulfates) can be leached from the blast furnace slag aggregates in PCC pavement concrete and are subsequently distributed throughout the cementitious matrix of the concretes via moisture migration. A very useful indication that this phenomenon has occurred is a color change in the cementitious phase of portland cement-based concretes containing either (1) ground granulated blast furnace slag cement, or (2) air cooled blast furnace slag aggregates. In these concretes the normal gray color of the cementitious phase of the concretes takes on a distinctive green color.

The Slag Cement Association (SCA) attributes the green coloration to "*the oxidation state of sulfide compounds during portland cement/slag cement hydration.*" On exposure of the concrete to air the color dissipates and eventually no remnants of the green coloration remain.

Hime and Erlin comment on the green coloration as follows (Hime, 2008),

> *"Concrete made with portland cement manufactured using iron slag as a component of its raw feed, and concrete made using ground granulated blast furnace (slag), initially will result in a bluish-green paste. With time, the color will change to a warm-tone brown that results when an iron sulfide component oxidizes"*

Calcium sulfide (CaS) is the primary source of sulfide contributed by the blast furnace slag component (Draft Report, October 2009). However, calcium sulfide is white in color. Hime (Hime, 2008) attributes the green coloration to iron sulfide. Iron sulfide in leachable form may be present in small amounts as a minor slag mineral, or it may be formed subsequently in a portland cement-based concrete as a result of in-situ reactions of iron compounds with some form of sulfide/sulfate in the cementitious system. Iron (II) hydroxide (ferrous hydroxide) is a compound produced when iron (II) ions, from a compound such as iron (II) sulfate react with hydroxide ions. Reportedly, iron (II) hydroxide is white in color, but even traces of oxygen impart it with a greenish tint. This material is also known as "green rust" and it can be seen in some cases of rebar corrosion on freshly exposed concrete surfaces. On an unusual but related note, it has been observed that when eggs are boiled for a long time, the yolk's surface turns green. This is reportedly due to iron (II) sulfide, which forms as iron from the yolk comes in contact with hydrogen sulfide released from the egg white by the heat (Belle Lowe, 1937).

In any event, the green coloration in slag-containing portland cement-based concretes is a useful marker, that (1) confirms the presence of sulfides in the concrete and (2) reveals the extent of the distribution of the sulfides in the concrete. The green coloration confirms that (1) the highly alkaline and moist environment of the concrete has leached sulfides from the slag, and that (2) the dissolved sulfides have moved throughout the cementitious phase of the concrete, as a result of moisture cycling. When this phenomenon occurs in portland cement/slag cement concretes the green coloration is typically uniform throughout the cementitious matrix. When this phenomenon occurs in slag aggregate concretes, the green coloration is not as uniform due to the point-sources of the sulfide/sulfate phases in the larger slag aggregate particles.

One of the ODOT pavements that we studied in 2009 is a portland cement/limestone coarse aggregate concrete pavement for which the base material is blast furnace slag. When the 12 in. (30 cm) core was sectioned perpendicular to its wearing surface, it was observed that the bottom 0.5 in. (12 mm) or so of the cementitious phase of the limestone aggregate pavement concrete showed the green coloration. This condition is direct verification that sulfides were leached from the slag base, and they subsequently moved a short distance into the cementitious phase of the pavement concrete. Although the green "marker" phase in this scenario is the iron sulfides, it is expected that calcium sulfide, which is the dominant sulfide phase, would be experiencing the same dissolution from the slag and subsequent transportation in soluble form via water movement into the cementitious phase of the concrete.

Concretes containing BF slag either as slag cement or as slag aggregates will retain the green color throughout the full thickness of the member until the concrete has experienced a period of drying and subsequent contact with air (i.e., oxidation). Figure 17 is a photograph of a lapped surface of Core 6 (SR 175 @ Concord), which is 10 ¼ in. (26 cm) long. The surface is perpendicular to the plane of the wearing surface. In this core the green color has been lost in the top 1 in. to 2 in. (2.5 to 5 cm) thickness of the core due to oxidation of the sulfide phases. Below the arrows in Figure 17 the cementitious phase of the core is darker, and the color is green (although this is not obvious in the photograph).

The color variation shown in Figure 17 is typical for slag-containing concretes that are taken from service. The portion of the concrete that is exposed to the elements (a wearing surface or a formed surface) experiences drying and subsequent contact with air and with periods of re-wetting. The sulfides from the slag that are present in the cementitious phase in this portion of the concrete can oxidize and the green color is then diminished or eliminated. The depth of the color-free layer is dependent on several variables including entrained air content and water-cement ratio. The higher the air content and the higher the w/c, the greater will be the depth of the color free zone.

The eight ODOT pavement cores examined here have length ranging from around 9 to 11 inches (23 cm to 28 cm). When the saw-cuts were first made on the cores as shown in Figure 1 the newly exposed surfaces were examined for evidence of the green coloration. In the pavement concretes the oxidation of the sulfides is expected to occur first in the portion of the concrete exposed to the elements; that is at and near the wearing surface. That is the case for the cores examined here. In all cases the top 2 to 3in. (5 to 8 cm) thickness of the cores had the normal gray color of PCC, indicating that the sulfides in this portion of the core had oxidized to the sulfate form. At depths below about 3 in. (8 cm) in the cores the green coloration was evident, although the intensity of the degree of "green-ness" is variable and non-uniform in some of the cores.

As noted previously the "Distress" cores examined here were taken from sites either right on or within a few feet of a transverse joint. Relative to regions of the concrete farther removed from the joints, the pavement concrete nearest the joints would have a greater accessibility to both moisture and air as cyclic wetting and drying can take place at two locations (1) on the exposed wearing surface of the pavement, and (2) along the joint fracture plane. For the top 2 to 3 in. (5 cm to 8 cm) thickness of the pavement at these sites the conditions are present for (1) oxidation of the sulfides to sulfates, and (2) a supply of water for the internal sulfate reactions. As shown previously (Figures 5, 6, 7, 8, 9, 12 and 16)) this is the case for the cores examined here where the most extensive and destructive sub-surface horizontal cracking has occurred in the top 3 in. (76 mm) or so of the cores. It is important to note that the very top ¾ in. (19 mm) or so of the cores is relatively free of the horizontal cracking. This can be explained by an overall dryer condition here as this is right below the evaporation surface of the pavement (assuming that the moisture level controls the internal sulfate reactions).

Historical Forms of Internal Sulfate Attack

There are two forms of internal sulfate that have been well known and well researched for many years. They include (1) classic sulfate attack, and (2) delayed ettringite formation (DEF). Both of these phenomena involve destructive chemical changes that take place in hardened portland cement-based concrete; often many months or years after the concrete has been in service. For both forms of distress the principal chemical change involves the reaction of sulfate phases with calcium aluminate hydrate phases (including the monosulfate, AFm) to form a new phase, which is ettringite. Ettringite is a calcia-alumina sulfate hydrate phase that has a large molecular structure due to large amounts of chemically held water. When this phase forms within the cementitious matrix the resultant in-situ increase in volume caused expansive stresses that can crack the matrix. In the case of classic sulfate attack the source of sulfates is external; most often derived from sulfate-rich groundwaters in contact with the concrete. In DEF cases the sulfate is already present in the concrete in one form, but is re-released in reactive form within the cementitious matrix after the concrete has been in service and comes into contact with water.

As described in preceding sections the external source of sulfates in slag aggregates concretes is the sulfides/sulfates that are leached from the slag particles and move via moisture migration into the cementitious matrix phase of the concretes.

Petrographic Evidence for Internal Sulfate Attack in the Core Concretes

The findings from our study and that of others provides strong evidence that the conditions under which external sulfate attack can occur are present in slag aggregate pavement concretes; namely (1) there is an external source of sulfates, (2) a number of different calcium aluminate hydrate phases are present, and (3) there is a constant supply of moisture. The petrographic evidence supporting a conclusion that destructive internal sulfate reactions *have been and are operative* in the ODOT pavement cores that we examined is summarized as follows,

- Relative to PCC limestone and gravel aggregate concretes that we have examined, the extent of <u>secondary deposits of ettringite in-filling of air voids</u> is significantly higher. Examples of entrained air voids that are partially or completely filled with ettringite are shown in Figure 18 (for Cores 6 and 8).

- The dominant condition of the <u>sub-surface horizontal cracking in the cores</u> is a separation of the cementitious matrix from the slag aggregate particles at and near the cement paste/aggregate bond line (see Figures 8, 9, 10, 11, 15, and 16). It is a diagnostic microstructural feature of internal sulfate attack for gaps to form between the cement paste and aggregate particles. The internally expanding cementitious phase literally grows outwardly away from the aggregate particle with which it was formerly in contact.

- New cracks have formed in some of the ODOT Cuyahoga County cores during their weeks of storage in our laboratory. The conditions of storage and the nature of the cracking supports a view that the new cracks formed as a result of expansions associated with on-going internal sulfate reactions.

In-Filling of Entrained Air Voids with Ettringite

Examples of entrained air voids that are partially or completely filled with ettringite are shown in Figure 18 (for Cores 6 and 8). Confirmation that the in-filling is ettringite was made based on the acicular habit of the deposits as viewed in the stereomicroscopic examinations, and in some cases by EDX analyses. The in-filling of the air voids in and of itself is not considered to be a destructive phenomenon. However, the abnormally large amount of ettringite in air voids in some of the slag aggregate cores examined here confirms that a substantial external source of sulfate has become available in these concretes. It is logical to assume that the new sulfate is not confined to the air void deposition sites. In the cores examined here the ones taken from a “Distress” location (located on or near a transverse joint) have the highest levels of in-filled air voids. It is expected that the primary reasons for this are (1) the greater availability of moisture and air for the concrete at or near the joints, and (2) the increased occurrence of cyclic wetting and drying at these locations. However, even the companion cores taken from the “No Distress” locations in the present study have some level of ettringite in-filling.

It is relatively easy to identify petrographically the presence of entrained air voids that have ettringite crystals in them. It is difficult to quantify the “extent” or the “degree” of this condition as this involves (1) estimating the percentage of the total air void population that shows this condition, and (2) dealing with the fact that the condition can range from a very minor amount of in-filling to complete filling of the air void space. An attempt is made to address this issue in Table A-9, where the locations in the core where any in-filled air voids are present is listed, along with comments on the infilling condition as very light, light, moderate, or heavy. There is some amount of ettringite in-filling of air voids throughout most of the length of cores, with the exception of two of the “No Distress” cores (Cores 2 and 4).

It is a commonly accepted view that the in-filling of entrained air voids with a secondary deposit can have an adverse effect on the durability of concretes that experience this phenomenon. This can occur inasmuch as the intended function of the air voids can be compromised when their void space is filled. This situation has occurred in Core 1, which was taken *through* a transverse control joint in a "Distress" location on State Route 91. A lapped surface view of Core 1 perpendicular to the plane of the wearing surface is shown in Figure 19. A cone-shaped region of material has spalled from the top of the joint area and there is a significant amount of cracking adjacent to the spall. These cracks are parallel to the sides of the existing spall (and to each other), and most of the cracks pass through, rather than around the slag aggregate particles. Most of the entrained air voids in this portion of the core are completely in-filled with ettringite. The conditions and features just described support a conclusion that the cone-shaped cracking and spalling in Core 1 is due in large part to freeze/thaw cycling of the concrete following the loss of functionality of the air void system due to the in-filling. However, even though the Core 1 concrete does not show the vertical and sub-surface horizontal cracking described previously for the cores taken from State Routes 175 and 176, there is some evidence that internal sulfate attack has occurred at the Core 1 site.

Creation of Sub-Surface Horizontal Cracking in the Slag Aggregate Cores

As can be seen in Figures 8, 9, 10, 11, 15, and 16, a great majority of the sub-surface horizontal fracture planes in the ODOT pavement cores *pass around rather than through* slag coarse aggregate particles. Enlarged views of this microstructural feature are shown in Figures10 and 11. As viewed in two dimensions on these lapped surfaces the cracks follow the profile of the aggregate particles, but most often a small layer of cementitious material remains adhered to the particles. That is, the fractures frequently occur *within the cementitious phase of the concrete*, very close to but not right at the cement paste/aggregate bond line. The petrographic evidence supports a conclusion that this separation is caused by the growth of ettringite at and near the boundary of the aggregate particles with the adjacent cementitious material. It is expected that both sulfates and sulfides are released by the slag aggregate. In contact with water and the atmosphere, the sulfides are oxidized to sulfates. In the presence of water, the new source of sulfate reacts with the various forms of calcium aluminate hydrates (including the monosulfate, [AFm]) in the cementitious phase of the concrete to form ettringite. The expansive stress resulting from these reactions literally lifts the cementitious material off of the slag aggregate particles.

Creation of Sub-Surface Horizontal Cracking in the Core 3 Concrete

Figure 20 shows two views of Core 3 (taken from a "Distress" location on SR 175) which will be used to explain the next step in our analysis of factors involved in the sub-surface cracking in the ODOT pavement cores. The top photograph in Figure 20 shows the as-received core, which came in two pieces, separated by a full core width fracture located about 1 ½ in. (4 cm) below the plane of the wearing surface. Pre-existing sub-surface horizontal fractures that could be detected on the as-cored surfaces are marked with a black marking pen. Subsequently, we opened up the not-yet exposed fracture surfaces (blue arrows) by inserting a small chisel into the fracture and tapping with a small hammer until full separation occurred across the width of the core. The effort required to "open-up" the pre-existing fractures varied. It became clear that the fracture plane in some cases was not contiguous. There were some areas that had not yet physically separated at the time of our effort to open up the crack. This was confirmed by the effort required to fully separate the core pieces and by the fact that some of the fine aggregate particles showed "clean" fracture surfaces (meaning our efforts caused a new fracture surface at these locations. Overall, however, the bulk of the fracture surface was covered with white secondary deposits. These features just discussed are shown in the bottom photograph of Figure 20. The colored dots on the photograph identify the sites of four types and/or condition of aggregate particles, as follows,

- Yellow Dots = Slag Coarse Aggregate Particles that have partially or completely pulled out of the cementitious matrix phase of the concrete.
- Blue Dots = Siltstone fine aggregate particles that are fractured and which have a coating of a secondary deposit.
- Green Dots = Siltstone fine aggregate particles that are cleanly fractured and which do not have a coating of a secondary deposit.
- Red Dots = Chert fine aggregate particles that are fractured and which have a coating of a secondary deposit.

The area above the dashed line in the bottom photograph of Figure 20 is the remnants of one of the fracture planes that formed a pre-exposed fracture on the as-received core.

Relative to the total area occupied by the aggregate particles on the newly-exposed pre-existing horizontal fracture surface (bottom photograph of Figure 20), the largest percentage is represented by the nine slag coarse aggregate particles (yellow dots). All nine of these slag aggregate particles either completely or partially pulled out of the cementitious matrix phase of the concretes. In the portion of the pavement cores at depths *below* the greatest concentration of sub-surface horizontal fractures (around 3 in. (76 mm) below the wearing surface) the mode of failure when the concrete was intentionally loaded to failure by us in our study was virtually always *through* the slag aggregate particles. In the example shown in Figure 20 and in the other instances of pre-existing subsurface horizontal cracking, the failure mode was overwhelmingly via aggregate pullout. Microscopic examinations of the newly-exposed pre-existing horizontal fracture surfaces explain this difference in failure mode.

<u>Figure 21 shows enlarged views (7X and 16X) of one of the newly-exposed pre-existing horizontal fracture surface in Core 3.</u> The top photograph is a 7X view of a slag coarse aggregate particle (A) that has separated from the cementitious material with which it was formerly in contact. The red arrows show the cement paste/aggregate boundary. The red dots in the photograph are placed on remnants of the cement paste and secondary deposits of ettringite that remain adhered to the surface of the slag aggregate particle after it separated from the cementitious matrix. The bottom photograph in Figure 21 shows a 16X view of the same slag aggregate particle.

<u>Figure 22 is the slag coarse aggregate particle shown in Figure 21 at magnifications of 40X and 90X.</u> At these magnifications it is seen that the entire surface of the slag particle is covered with a layer of acicular crystals, which, as will be shown, are ettringite. Red dots in the photographs are placed on small patches or clumps of white material that are adhered to the aggregate particle surface. These clumps of material will be shown to be remnants of the cement paste in contact with the aggregate particle. These clumps of cement paste also contain the acicular crystals.

Figures 23 through 28 are scanning electron microscope (SEM) images and companion energy dispersive x-ray spectroscopy (EDX) spectra of the material shown in the corresponding image on that page. The materials examined here are the small clumps of white material that was adhered to the pulled-out slag aggregate particle shown in Figures 21 and 22. The white material was removed from the surface of the aggregate particle using small needles and was deposited on conductive carbon tape for the SEM/EDX analysis. Carbon was also used as the conductive coating material for the examination.

Figure 23 is an SEM/EDX scan and spectrum of a small clump of the white material at a magnification of 100X. Even at this relatively low magnification the distinctive shape of the acicular ettringite fibers can be seen. The smooth surface on the clump is remnants of the carbon coating. In areas where this is not present the clump has the appearance of a "brillo pad", with individual fibers held in a matrix. As will be shown the matrix material is hydrated portland cement. The EDX analysis shows the presence of the elements of calcium (Ca), sulfur (S), silicon (Si), and aluminum (Al). Prior knowledge of the constituents of the concrete and the identification of elemental oxygen (O) confirm the presence of these elemental constituents as a form of the oxides. For this sample the contribution of ettringite to the spectrum is calcia, alumina, and sulfate. The portland cement constituent contributes calcia and silica to the spectrum. In some cases low levels of silica are also provided by the ettringite constituent in which it is not uncommon to find silica (in some cases the fibers may be a solid solution of ettringite and thaumasite).

Figure 24 is an SEM/EDX scan and spectrum of a small clump of the white material at a magnification of 5000X. This image shows a small clump of the acicular fibers, and a spot elemental analysis was done at the indicated site (+) on the largest fiber. In this analysis the silica is present in trace amounts. In spot analyses on other fibers the silica content showed a fiber to fiber variability, but the silica always had the shortest peak height, relative to Ca, S, and Al.

Figures 25 through 28 show a progression of greater and greater magnifications of the same small clump of the white material excavated from the pulled-out surface of the slag aggregate particle shown in Figures 21 and 22.

Figure 25 is an SEM/EDX scan and spectrum of a small clump of the excavated white material at a magnification of 500X. The bulk of the area of the image is dominated by loose ettringite fibers. In the northwest corner of the image analysis frame is a still smaller clump of the fibers that have the aforementioned agglomerated "brillo pad" appearance. This agglomerated clump of the white material is examined at higher magnifications in Figure 26 (750X), Figure 27 (2000X), and Figure 28 (20,000X)

Figure 26 is an SEM/EDX scan and spectrum at 750X of the agglomerated clump of the excavated white material shown in the northwest corner of the SEM image shown in Figure 25. Again, the bulk of the area of the image is dominated by ettringite fibers, and the EDX spectrum is similar to that shown in Figure 25 for the larger scan field.

<u>Figure 27 is a 2000X SEM/EDX scan and spectrum of the agglomerated clump of the excavated white material shown in the northwest corner of the SEM image shown in Figure 25</u>. At this magnification the matrix material in the agglomerated clump can be clearly seen. An EDX spot analysis was made on the matrix material at the site of the (+). Here the elemental analysis is clearly different from the scans showed in Figures 25 and 26, which mainly show the elemental constituents of the ettringite constituent. The elemental scan shown in Figure 27 is a marker for portland cement with calcia dominating the spectra, followed by silica. Other expected constituents of portland cement are also present including aluminum (Al), magnesium (Mg), potassium (K), sodium (Na), iron (Fe), and sulfur (S). As will be shown, the matrix material also contains additional ettringite, which makes a contribution to the aluminum and sulfur peaks in the spectra. This feature is shown in Figure 28.

<u>Figure 28 is a 20,000X scan and spectra of the matrix material of the agglomerated clump of the excavated white material shown in the northwest corner of the SEM image shown in Figure 25</u>. The elemental analysis spectrum is similar to that shown in Figure 27. At the magnification of 20,000X it is possible to see the acicular ettringite fibers embedded in the hydrated portland cement matrix. As seen by the scale on the image in Figure 28 the length of the fibers is around 1 µm, and the fiber diameters are around 0.1 µm.

<u>Creation of Sub-Surface Horizontal Cracking in the Core 1, 5, and 7 Concretes</u>

The microstructural features implicating destructive internal sulfate reactions in the cracking distress of the Core 3 pavement (shown in Figures 20 through 28) were also seen in the other three "Distress" cores (Cores 1, 5, and 7), and in two of the slag aggregate cores taken from a "No Distress" location (Cores 6 and 8). Figure 29 shows examples for the "Distress" cores taken from State Route 175 @ Concord (Core 5) and State Route 176 (Core 7).

Both photographs in Figure 29 are enlarged views of a slag coarse aggregate particle that has pulled out of the adjacent cementitious matrix of the concrete along a sub-surface horizontal fracture surface. The top photograph in Figure 29 is a 90X view of the Core 5 concrete and the bottom photograph is a 50X view of the Core 7 concrete. Both aggregate particles lie at a depth of 2 ½ to 3 in. (6 to 8 cm) below the plane of the wearing surface of the cores. Red dots in the photographs are placed on remnants of the cement paste that remain adhered to the slag particle after it was pulled from the matrix. The acicular crystals are ettringite fibers, which are embedded in the cement paste and which cover the surface of the aggregate particle.

During the preparation and examination of the core concretes for the petrographic study it was observed that new sub-surface cracks appeared to be forming in some of the cores after they had been saw-cut and lapped and subsequently stored in sealed plastic Zip-Loc bags. After this phenomenon was first suspected it became a major focus of our study. This led to the generation of a considerable body of petrographic evidence that validates the conclusion that latent expansions and cracking did occur in the core concretes. This evidence is discussed in the next Section of the report.

Latent Expansions and Cracking in the Core Concretes

With the exception of Core 3, the other seven slag aggregate cores were prepared for the petrographic examination by saw-cutting and lapping (which followed the initial examination of all the cores in the as-received condition). The core saw-cutting step, as illustrated in Figure 1, yields three pieces including a center slab section that is about ¾ in. (19 mm) thick, and two end pieces with a hemispherical cross section. The saw-cutting step creates new surfaces of the concrete that have not yet been exposed to the atmosphere. These newly exposed surfaces are now subject to oxidation, which results in the sulfides in the cementitious phase being converted to sulfate. This phenomenon can be followed as a gradual fading of the green color of the cementitious phase.

Following the saw-cutting steps, both saw-cut surfaces of the slab sample are lapped on a steel wheel, with water as the lapping medium. For the cores examined here, the time for the lapping operation for a single slab is 1 to 1 ½ hours. During this time the slab sample absorbs water and the water content of the concrete reaches a higher level than it had in the field in service at the time of coring.

Immediately or shortly following the final lapping step the slab sample is microscopically examined to learn the extent and the nature of the cracking distress. Following this initial examination the slab sample is placed in a sealed Zip-Loc bag and stored prior to subsequent examinations over the following weeks. It was during these subsequent examinations that we suspected that new cracks had formed during the period of storage of the wet slabs in the sealed bags. It was further suspected that the cracking was due to latent expansions in the core concrete pieces brought about by the “new” environment that they were placed in (i.e., exposed to the atmosphere and moisture, with a new supply of sulfates). Once our suspicions were aroused, we conducted some additional experiments to provide further confirmation.

<u>Latent Expansions and Cracking in Core 5 (SR 175 @ Concord)</u>

Core 5 was taken from State Route 175 @ Concord at a "Distress" location. As shown in Figure 8 Core 5 was received in two pieces, which are separated by a full core width fracture, whose location 2 in. (5 cm) below the plane of the wearing surface is shown by the arrow in Figure 8. The two core pieces have matching surfaces and the core was "re-assembled" by gluing the pieces together with an epoxy adhesive (a procedure we have used many times in a similar situation to recreate the spatial relationships of the core concrete in service). The saw-cuts were made after the epoxy cured. One of the lapped surfaces of the slab section of Core 5 is shown in the bottom photograph of Figure 8. The sub-surface horizontal cracks that could be detected microscopically on the as-lapped surface are marked with a black marking pen.

When Core 5 was re-examined after a two week storage period it was suspected that new cracks had formed. An example of one of these cracks is shown in Figure 30. As viewed in two dimensions on the lapped surface the crack is (1) hairline in width, (2) a few millimeters long, and (3) passing around fine aggregate particles.

It was also observed during the examination after the two week storage period that the epoxy adhesive layer had stretched and cracked. This feature is shown in Figure 31. Normally, the epoxy adhesive used for this purpose remains intact following the lapping procedure. The views shown in Figure 31 show tears within the epoxy layer, with the epoxy on both sides of the tears still adhered to the concrete. The shape of the tears in the epoxy layer strongly suggests that they were formed by strains that occurred perpendicular to the long axis of the tears. A feasible source of these strains is a stress associated with renewed formation of ettringite within the cementitious phase of the concrete (see Figure 16).

Following the revelations just described, a renewed study was made of one of the hemispherical cross section pieces of Core 5 (identified here as "Piece 5-1 for ease of discussion). The initial saw-cuts were made on Core 5 on April 9, 2010. Piece 5-1 absorbed some water during the saw-cut and it was placed in a Zip-Loc bag after the cut was made. We re-examined it on April 28, 2010 after 19 days of storage in the bag. Microstructural features observed on the saw-cut surface at this time support the speculation of the latent expansion/cracking phenomenon as shown in Figure 32.

Figure 32 shows two views (7X and 50X) of the saw-cut surface of Piece 1 of Core 5 after 19 days in the sealed plastic bag. The green arrows in the top photograph point to the pre-existing horizontal fracture in Core 5 that was re-glued with the epoxy adhesive. The blue arrows point to a crack that passes along the cement paste/aggregate (A) bond line and on into the cementitious phase. At the site of the red arrow the crack passes through a small dark mafic mineral fine aggregate particle (M). As shown in the bottom photograph of Figure 32 the crack passes *through* the fine aggregate particle. The largest part of the aggregate particle is present above the crack and the smallest part is below the crack. This artifact is proof that *the crack occurred after the saw-cut was made.* The small particle would undoubtedly been dislodged during the saw-cutting step if the crack had been present at that time.

Piece 1 of Core 5 was lapped on April 29, 2010 and examined immediately after lapping. The top photograph in Figure 33 shows a 16X view of the lapped surface at a location 2 in. (5 cm) below the wearing surface at the site of the epoxy re-assembly seam (green arrows). The epoxy layer is intact and a number of horizontal cracks can be seen passing through the cementitious matrix above and below the epoxy seam. After the microscopic examination on April 29, 2010 the core piece containing water absorbed from the lapping operation was placed in a sealed Zip-Loc bag. The core piece was left undisturbed until May 18, 2010 when it was re-examined. The bottom photograph in Figure 33 shows the same site as the top photograph after the 19 day storage period. Expansive strains in the concrete during this time have (1) widened the existing cracks in the cementitious phase, (2) created some new cracks in the cementitious phase, and (3) created tears in the epoxy seam.

Latent Expansions and Cracking in Core 7 (SR 176)

Core 7 was taken from State Route 176 at a “Distress” location. As shown in Figure 9 Core 7 was received in one piece. Following the work on Piece 1 of Core 5, a similar experiment was carried out on Piece 1 (hemispherical cross section) of Core 7. The saw-cut surface of Piece 1 of Core 7 was lapped on May 3, 2010 and the sub-surface horizontal cracks were marked with a black pen shortly after the completion of the lapping operation as shown in the top photograph of Figure 34. While retaining most of the water absorbed in the lapping operation the core piece was sealed in a Zip-Loc bag and left undisturbed for 11 days. The core piece was removed from the plastic bag and the lapped surface was re-examined on May 14, 2010. New cracks had formed during the 11 day storage period and they were marked with a red marking pen as shown in the bottom photograph of Figure 34.

The discussion presented in this Section of the report provides strong evidence in support of a conclusion that in the presence of moisture and the atmosphere, newly exposed surfaces of the slag aggregate concretes experienced latent expansions and cracking distress. Knowledge of the constituents of the concretes supports a conclusion that the expansive stress creating the cracking is derived from internal sulfate reactions. (End of Internal Sulfate Attack Section)

ALKALI-SILICA REACTIONS (ASR) IN THE PAVEMENT CORES

Researchers investigating the cause of cracking in slag aggregate PCC pavements in Michigan reported that it was common to find evidence of alkali-silica reaction (ASR) activity in these concretes, along with evidence pointing to an involvement of internal sulfate attack (FHWA, 2009; Van Dam 2003). This connection between internal sulfate attack and ASR in concretes experiencing deterioration had also been noted and discussed by researchers engaged in a study of delayed ettringite formation (Hime, 2000). In both the Michigan pavement studies and the DEF studies there is no clear consensus about which of the two potential distress mechanisms initiates the problem and which is subsequently the dominant distress mechanism.

Hime (Hime, 2000) does offer an explanation as to why it can be expected that the initiation of internal sulfate attack could create a chemical environment in which previously dormant ASR activity would be expected to develop. In discussing the difficulties encountered in distinguishing between ASR and DEF reaction products in a petrographic examination, Hime states,

> *"Difficulties arise not only from the similarity of ASR and DEF "gels", but also from their occurrence together. Even when the concrete contains historically innocuous aggregates, ASR gel may be produced in small quantities in association with DEF or other forms of sulfate attack. This may be due to the increase in available alkali hydroxides when alkali sulfates dissolve in the paste and react with calcium hydroxide and aluminates to form ettringite, which does not incorporate sodium or potassium in its crystalline structure."*

The situation described by Hime also prevails in our present study of the slag aggregate concretes from the three Cuyahoga County Ohio pavement sites. Evidence of ASR activity was commonly found in our study in the form of,

- Alkali-silica gel present as a secondary deposit on void surfaces in the concretes.
- Alkali-silica gel present in association with chert and siltstone fine aggregate particles.
- Alkali-silica gel present as exudate which formed on lapped surfaces of the core concretes, which had experienced a brief period of drying at the conclusion of the lapping operation.
- Diagnostic cracking in chert and siltstone fine aggregate particles with an association of ASR gel.
- "Staining" of cement paste in contact with chert and siltstone fine aggregate particles that show other features of ASR activity.
- In a few cases, advanced gelatinization of reacted chert fine aggregate particles.

The petrographic evidence for the ASR activity just described is presented in the following text and is supported with photographs of the features of interest. The ASR gel was identified on the basis of both its appearance in the microscopic examinations and EDX elemental analyses of material excavated from the core samples. Aged ASR gel as deposited in air voids and cracks is often white and opaque and does not show any well-defined crystal structure. Frequently the gel is glassy and translucent. Both types of gel deposits may show extensive map or pattern cracking (on the microscopic level) in those instances where the gel is desiccated. The typical EDX signature spectrum for ASR gel includes silica (Si) which usually shows the greatest peak height, along with calcium (Ca), potassium (K), and sodium (Na). It is not unusual to detect the presence of small amounts of aluminum (Al) and magnesium (Mg) in the ASR gel reaction product as well. As indicted by peak heights, large variability is encountered in the proportions of calcium, potassium, and sodium between samples of the gel.

Siltstone Involvement in ASR Activity

Figure 35 shows a 20X image of a chert fine aggregate particle on a fresh saw-cut surface of Core 4. Core 4 was taken on State Route 175 at a "No-Distress" location. The chert particle has undergone alkali-silica reaction (ASR) activity and some of the ASR gel has been deposited in an air void adjacent to the particle. In this example the chert particle is still intact and shows a thin darkened rim at its point of contact with the cement paste. There is no cracking associated with the ASR activity in the chert particle or the adjacent cement paste.

Figure 36 shows a 10X image of a siltstone fine aggregate particle on an as-cored surface of Core 8. Core 8 was taken on State Route 176 at a "No-Distress" location. The siltstone particle has undergone alkali-silica reaction (ASR) activity and some of the ASR gel has been deposited in an air void adjacent to the particle. In this example the siltstone particle shows a small number of very fine cracks and shows a darkened rim, but it is still intact.

As shown in Table A-6 (Appendix A), although siltstone particles are the second most abundant constituent of the sands in the ODOT slag aggregate cores, only a small minority show evidence of ASR activity. In those instances where siltstone particles are cracked, there is a single fracture through the particle. This is in contrast to chert particles, which, when cracked typically show multiple cracks.

Chert Involvement in ASR Activity

Chert is the 5 to 7th most abundant phase in the sand fraction of the pavement cores (Table A-6). The chert particles are typically of the hard, porcelaneous type, but softer particles are also present.

Figure 37 shows two examples of chert fine aggregate particles that have undergone mildly destructive alkali-silica reaction activity. These examples are in cores taken on State Route 175 @ Concord at a "Distress" location (Core 5) and a "No-Distress" area (Core 6). In both examples the chert particles have multiple cracks, some of which project into the adjacent cementitious matrix. In the top photograph in Figure 37 (Core 5) the cementitious matrix in contact with the chert particle has darkened due to the infiltration of ASR gel (indicated by yellow dots). In the bottom photograph (Core 6) a crack that may have originated in the chert particle passes through the cementitious phase and on through two siltstone fine aggregate particles. Although there is a common association of ASR gel with siltstone fine aggregate particles in the ODOT pavement cores examined in our study, in those instances where cracking is present in the particles, there typically is a single, not multiple, cracks.

At least a few chert particles having the features shown in Figure 37 are present in all eight of the ODOT pavement cores that we examined.

Other Evidence of ASR Activity (Gel Exudate)

Following the final lapping step in the petrographic examination the concrete sample is allowed to air dry for a brief period prior to a detailed examination under the microscope. If there is ASR activity in the concrete it is not unusual for some ASR gel (which is water soluble) to exit the concrete in the evaporating water phase and deposit as an exudate on the lapped surface. This phenomenon was a common occurrence in the core concretes examined here. Examples are shown in Figure 38, which shows a lapped surface of Core 5 taken from State Route 175 @ Concord at a "Distress" location. The white exudate stands proud of the lapped surface and abuts slag coarse aggregate particles. In the examples of Figure 38 the area covered by the exudate overlies both chert and siltstone fine aggregate particles. It is clear in this example and in all of the others examined here that the ASR activity is associated with the fine aggregate particles (chert and siltstones) and not the slag particles. In the bottom photograph of Figure 38 the primary source of the ASR gel may be the tan chert particle (C) which is cracked. The exudate deposit here runs linearly along a line (a crack) that passes into a cluster of quartz fine aggregate particles. Given the close proximity of the crack to the slag particle, the question arises as to whether the initial crack may have been due to internal sulfate attack.

The distribution of the exudate in Core 5 (as shown in Figure 38) is shown in Figure 39. In the top photograph of Figure 39 the exudate sites have been marked with red dots. The exudate sites, which are common, but not abundant, are present throughout the length of the core; a feature that was observed in other ODOT pavement cores showing ASR activity as revealed by the deposition of gel exudate on lapped surfaces.

The ASR gel exudate distribution pattern shown by the example in Figure 39 confirms that there has been ASR activity at these sites. As viewed in two dimensions of the lapped surfaces the source of the exudate is not always obvious. Well over half of the exudate sites are at locations where there is no cracking distress in any of the fine aggregate particles in the immediate vicinity. Even in those instances where chert aggregate particles are cracked themselves (such as those shown in Figure 37), the cracks do not represent a significant or extensive form of damage. Such cracks are often quite tight and may be less than 1inch (25 mm) long (as viewed on the lapped surfaces).

ASR and Internal Sulfate Attack Occurring Together

Pre-existing sub-surface horizontal fractures could be seen on a number of the as-received cores, within the top 3 in. thickness or so below the wearing surface. An example is shown in Figure 20 for Core 3 (taken from SR 175 at a "Distress" location). As described previously, we opened up some of these horizontal fractures by inserting a small chisel into the crack and lightly tapping with a small hammer until full separation occurred across the width of the core. The bottom photograph in Figure 20 shows one of these newly-exposed pre-existing horizontal fracture surfaces. Much of the fracture surface is covered with white secondary deposits. The colored dots on the photograph identify the sites of four types and/or condition of aggregate particles. One of theses sites is slag coarse aggregate particles (un-cracked), which were shown to be involved in cracking in the cementitious matrix due to internal sulfate attack. Other sites include (1) chert fine aggregate particles involved in ASR activity, and (2) siltstone fine aggregate particles involved in ASR activity. The reacted siltstone particles outnumber the reacted chert particles in the exposed fracture surface (see Figure 20).

A 7X view of the fracture surface shown in Figure 20 is shown in the top photograph of Figure 40. In this latter field of view five aggregate particles are identified by number (1 through 5). Particle 1 is a slag coarse aggregate that has pulled out of the matrix (see Figures 21 and 22). Particle 2 is a fractured and rimmed fine aggregate chert particle, which shows evidence of ASR activity. Particles 3, 4, and 5 are fractured siltstone fine aggregate particles, which also show evidence of ASR activity. A detailed SEM/EDX study was made of Siltstone Particle #3 and Chert Particle #2, which is described in the following text and figures.

SEM/EDX Examination and Analysis of Siltstone Particle #3

A 32 X view of Particle 3 is shown in the bottom photograph of Figure 40. The particle is fractured and the fracture surface is partially covered with white secondary deposits. The cementitious phase abuting the particle is also covered with white secondary deposits, which show a map cracking pattern. The entire siltstone particle along with portions of the adjacent cementitious phase was lifted off the fracture surface and mounted for study in the SEM examination.

Figure 41 shows the SEM image and the EDX spectrum (30X) of Particle #3. As will be shown, this low magnification shot reflects elemental chemistry contributions from all phases within the field of study including (1) constituents of the siltstone particle not covered with secondary deposits, (2) ASR gel, (3) ettringite, and (4) hydrated portland cement.

<u>Figure 42 shows the SEM image and the EDX spectrum (30X) of the framed area adjacent to Siltstone Particle #3</u>. The similarity of the spectra in Figures 41 and 42 indicate that there is very little if any contribution of the constituents of the siltstone particle itself to the elemental analysis.

<u>Figure 43 shows the SEM image and the EDX spectrum (30X) of the framed area that directly overlies the fracture surface in the interior of Siltstone Particle #3</u>. The fracture surface here is covered with ASR gel reaction product.

<u>Figures 44 and 45 show the SEM image taken at 1000X of the northwest tip of Particle #3 as shown in Figures 41, 42, and 43.</u> The region of the field of view is within the cementitious phase adjacent to the siltstone fine aggregate particle. The image shows a number of loose and agglomerated ettringite fibers and smooth, glassy bits of non-crystalline material, which is ASR gel. Figure 44 is a spot analysis of an ettringite fiber. Figure 45 is a small area analysis of the ASR gel.

<u>SEM/EDX Examination and Analysis of Chert Particle #2</u>

A 7 X view of Chert Particle #2 is shown in the top photograph of Figure 40. The particle is fractured and it lies in close proximity to Siltstone Particle #3 and to the Slag Coarse Aggregate Particle #1. The slag particle pulled out of the matrix; it is not fractured. A small piece excavated from the chert particle fracture surface was used in the SEM examination; this piece is shown in the 35 X SEM image in Figure 46. The EDX spectrum (also at 35X) shows only ASR gel, which covers the fracture surface of the particle.

<u>The Contribution of ASR Activity to the Cracking in the Pavement Cores</u>

In the “Distress” cores taken from the two State Route 175 sites (Cores 3 and 5) and from the State Route 176 site (Core 7) the most advanced and troublesome cracking is the sub-surface horizontal cracking that occurs within the top 3 in. thickness of the cores. Examples of this cracking are shown for Cores 5 and 7 in Figures 8 and 9. The most advanced fractures in this category are wide enough to be seen with the unaided eye and as viewed in two dimensions on the lapped surfaces cover the full width of the cores. This is the form of cracking that is the basis of the unique type of distress associated with these slag aggregate PCC pavements as shown in Figure 3.

Earlier in the present report we stated our opinion of the factors involved in the origin and progression of this cracking. Our interpretation of the petrographic observations and measurements on the eight cores examined here are the basis of this scenario, which is repeated (and elaborated on) here.

1. Expansive stresses resulting from internal sulfate attack create sub-surface horizontal cracks within the cementitious matrix phase of the core concretes. In the early life of the pavements this activity is confined to the top 3in. (8 cm) or so of the pavement slabs (although the topmost ¾ in. (19 mm) layer may not be affected.

2. As illustrated by the red arrows in Figure 16, the "direction" of the strains created by the internal expansive stresses is upward toward the free surface, which is the wearing surface of the pavement slabs (i.e. along the path of least resistance). In the process, the cementitious matrix phase is "lifted-off and away from" some of the slag aggregate particles, creating a separation at the paste/aggregate bond line (Figures 8, 9, 10, 11, 12, 14, 15, and 16).

3. The internal sub-surface expansive stresses create a condition of tensile strains in the immediate wearing surface layer as shown by the double yellow arrows in Figure 16. This condition results in the formation of tensile cracks (vertical cracks) in the immediate wearing surface of the pavement slabs (Figures 13, 14, and 15).

4. The horizontal cracks originating along the cement paste/slag aggregate boundaries subsequently pass into the adjacent cementitious phase. The presence of these cracks provides access routes for water movement into the cementitious phase. At some point alkali-silica reaction (ASR) activity is initiated in those areas where both potentially reactive particles (such as chert) and high moisture levels are present.

5. With increasing service time both the horizontal and the vertical cracks in the pavements widen and propagate, resulting ultimately in spalling (material loss). This condition is most prevalent in the concrete adjacent to joints and transverse cracks, where access to moisture is high, and repetitive traffic loads are most eccentric.

This distress scenario acknowledges an involvement of alkali-silica reaction (ASR) activity as a contributing factor to the sub-surface horizontal cracking, but places it in a secondary role. Recent findings of other petrographers who examined slag aggregate concretes in Michigan tend to support this opinion (Stehly, 2006). Eighteen slag aggregate cores were part of a twenty three core population that was examined in this 2006 study and the extent of ASR activity associated with chert fine aggregate particles was rated as follows,

- Degree of ASR = <u>Negligible</u> = 3 Cores (13 %)
- Degree of ASR = <u>Minor to Negligible</u> = 3 Cores (13 %)
- Degree of ASR = <u>Minor</u> = 8 Cores (35 %)

- Degree of ASR = Minor to Moderate = 2 Cores (9 %)
- Degree of ASR = Moderate = 5 Cores (22 %)
- Degree of ASR = Moderate to Severe = 2 Cores (9 %)

The "Moderate to Severe" rating category used here was reserved for,

> *"the observation of extensive, continuous, mostly horizontal micro and macro-cracking emanating from or proceeding through many chert particles, producing bulk expansion, and coupled with large deposits of silica gel product"*

Five of the cores in this 2006 study contained a carbonate coarse aggregate. These core concretes also showed evidence of ASR activity, including one with a "negligible" rating, three with a "minor" rating, and one with a "moderate" rating.

Prior to summarizing the findings and conclusions of the present study the next Section of the report provides a brief discussion of the results obtained in our examination of three slag aggregate ODOT pavement concretes evaluated in our 2009 - 2010 study (Lankard, 2010)

SLAG AGGREGATE CONCRETES EVALUATED IN OUR 2009 – 2010 FORENSIC STUDY

Twenty ODOT PCC pavements showing an acceptable level of performance were evaluated in this study (Lankard, 2010), including 3 that contain slag as the coarse aggregate. These pavement sites are,

- Jefferson County – State Route 22 (Constructed in 1990 - Average Performance Ranking)
- Jefferson County – State Route 7 (Constructed in 1990 – Excellent Performance Ranking.
- Cuyahoga County – State Route 176 (Constructed in 1994 – Average Performance Ranking

The eight slag aggregate cores examined in the present investigation were taken from ODOT pavements that showed "early" distress issues. In contrast, the slag aggregate cores examined in the Forensic Study (Lankard 2010) were taken in pavements that performed satisfactorily. The State Route 176 Site examined in the Forensic Study is the same pavement from which cores were taken for the present study. In the former case (satisfactory performance) the cores were taken from mainline slabs and in the latter case (distress) the cores were taken from a shoulder slab.

Relevant properties of the slag aggregate concretes examined in the Forensic Study are summarized in Table A-10. The slag sources are (1) LTV Steel in Cleveland for the Cuyahoga County pavement, and (2) Weirton Steel, Weirton WV for the Jefferson County pavements. The compressive strengths of the concretes range from 6260 psi to 7340 psi (43 to 51 MPa). The Jefferson County pavements are straight portland cement mixes, while the Cuyahoga County pavement contains portland cement and fly ash. The estimated water to cementitious material ratios (w/cm) are satisfactory, ranging from 0.42 to 0.46. Although all three pavement concretes are air entrained, the total air content in the Cuyahoga County pavement concrete is low at 1.9 percent.

At the time the ratings were made the Jefferson County SR 7 pavement was given an “Excellent” rating and the SR 22 pavement was given an “Average” rating. Despite having a satisfactory performance rating, the three slag aggregate pavement concretes show some distress. Currently however, the condition of the SR 22 pavement is better than that of the SR 7 pavement. The distress in both pavements is primarily related to transverse cracking and associated spalling. The Jefferson County pavements apparently do not show the pattern or map cracking that is unique to the Michigan slag aggregate pavements and the ODOT slag aggregate pavements examined in the present study.

The Cuyahoga County SR 176 shoulder concrete examined in the present investigation does however, show this unique form of distress.

Jefferson County Slag Aggregate Cores

Lapped top to bottom section views of the Jefferson County cores perpendicular to the plane of the wearing surface are shown in Figures 47 and 48. The cracks in the four Jefferson cores are marked with a black marking pen in the figures. As viewed in two dimensions on the lapped surfaces the features of the primary form of cracking distress are,

- The crack fracture planes are roughly parallel to the plane of the joint crack and the transverse crack.
- The cracks are closely spaced and are clustered in the region of the joint crack and the transverse crack.
- The cracks pass around and through slag coarse aggregate particles.
- Although the concretes are air entrained (5.2 and 6.1 %), the majority of air voids are completely filled with secondary deposits of ettringite.

Figure 49 shows enlarged (7X) lapped surface views of the two joint cores. The wearing surface is at the top in the photographs. The epoxy (yellow dots in top photograph) is the adhesive used to reassemble the two halves of the as-received cores. The joint crack that formed early in the life of the concrete passes around most of the slag aggregate particles. The nature of the other cracks strongly indicates that they were subsequently formed as a result of freeze/thaw cycling of the concrete while in a state of critical moisture saturation. The red arrows point to a few of the numerous entrained air voids that are filled with ettringite deposits. The moisture level of the concrete is expected to be highest in the region of top to bottom joint cracks and transverse cracks.

As discussed previously the unique cracking distress observed in other slag aggregate concrete pavements in Michigan and Ohio can be diagnosed by the presence of destructive sub-surface horizontal cracks and vertical cracks through near-surface slag aggregate particles. Neither of these diagnostic microstructural features were observed in the two Jefferson County SR-22 pavement cores. The vertical cracks were not seen in the Jefferson County SR-7 cores. However, as shown in the top photograph of Figure 47 there are two sub-surface horizontal cracks; one at depth of 2 in. (5 cm) and one at a depth of 5 in. (13 cm). These horizontal cracks do pass around, rather than through adjacent slag aggregate particles. However, given the large loss of support along the joint crack plane, it is probable that these horizontal cracks are a result of traffic-induces stresses within this poorly supported region.

It can be said with some confidence that the slag aggregate cores examined from the 19 year old Jefferson County pavements do not show the crack patterns that we have identified in the p nts p

Cuyahoga County Slag Aggregate Cores

Two of the cores taken from State Route 176 in Cuyahoga County for the Forensic Study include one over a transverse joint (labeled CUY-176-10-S [JT}), and one taken over a mid-slab crack, which is labeled (CUY-176-10-S [CR]). These cores were taken near Mile Marker 10 in the Southbound mainline lane. This pavement was given an "Average" performance rating. Photographs of these cores are shown in Figure 50.

The bottom photograph in Figure 50 is a view of the core taken through a transverse joint in the condition in which it was received at our laboratory. The core shows some spalling along the top portion of the joint crack, and shows a single horizontal crack about 5 in. (13 cm) below the wearing surface.

The top photograph in Figure 50 is a lapped section view of the core taken through the mid-slab crack. There are some sub-surface horizontal cracks, which are marked with a black marking pen. The cracks were marked on this core in December, 2009. We examined the lapped surface of the cores again in May, 2010, five months later, during which time they were stored in plastic bags. It is with reasonable certainty that we can claim that new cracks formed during this storage period as shown in Figures 51 and 52.

The two photographs in Figures 51and 52 show the same location on the core (5 in. (13 cm) below the wearing surface at three levels of magnification (7X, 25X, and 32 X). The wearing surface is at the top in the photographs. The photographs show two slag aggregate particles, which have been labeled S1 and S2. The paths of tight cracks in the concrete are tracked with arrows in the photographs. The cracks are filled with a white secondary deposit, which is ettringite.

The yellow arrows trace a crack that has developed along the paste/aggregate boundary of Slag Particle S1. Viewing from right to left in the bottom photograph of Figure 52, the crack associated with Slag Particle S1 passes through several siltstone fine aggregate particles and a small slag aggregate particle. The microstructural features shown here strongly support a conclusion that the crack originated along the paste/aggregate boundary and propagated into the surrounding paste and fine aggregates.

There are similar cracks associated with slag aggregate particle S2 as shown in the bottom photograph of Figure 51 and the top photograph of Figure 52. The red and blue arrows trace the path of these cracks, which also pass into the adjacent cementitious matrix and through a siltstone fine aggregate particle.

The microstructural features described for Figures 51 and 52 support the conclusion, expressed previously, that the sub-surface horizontal cracking is initiated as the result of internal sulfate attack, with the "new" sulfates coming from the slag aggregate particles. It is this sub-surface horizontal cracking that is the primary troublesome and unique distress mechanism in slag aggregate concretes.

SUMMARY AND CONCLUSIONS

The present report addresses the issue of materials-related distress in portland cement concrete (PCC) pavements in the Ohio Department of Transportation (ODOT) system that contain blast furnace slag coarse aggregates. In our examination of this problem, we conducted petrographic examinations and other tests on eight cores taken from four slag aggregate ODOT pavement sites in Cuyahoga County, Ohio.

At each of the four pavement sites one core was taken from a location in a distressed area on or near a joint (termed the "Distress" cores). A second core was taken for each site at a nearby location (within 4 ft. [1.2 m]) that did not show any distress (termed the "No Distress" cores). The distress referred to in this selection criterion refers to cracking and/or spalling that is manifest on the wearing surface of the pavements. For convenience, the eight cores examined here are labeled 1 through 8, with the even numbers representing the "No Distress" cores, and the odd numbers representing the "Distress" cores.

Previous Studies of the Problem

Previous and on-going studies of this issue in Michigan (FHWA, 2009) have led to the conclusion that,

> *"The role of air cooled blast furnace slag aggregates in materials-related distress in Michigan pavements has not yet been fully resolved".*

In the work done to date by other researchers (cited in [FHWA 2009]) at least three potential sources of distress have been cited to explain the unique distress observed in Michigan pavements prepared with concretes containing air-cooled blast furnace slag aggregates, including,

1. Alkali-silica reaction activity (ASR), affecting ASR-prone rocks and minerals in the fine aggregate phase of the concrete.

2. Internal sulfate attack, with the precursor source of sulfate being the sulfides (mainly calcium sulfide) residing in the slag aggregate particles.

3. Freeze/thaw damage resulting from malfunctioning of the entrained air void system due to in-filling of the voids with secondary deposits (ettringite).

All three of these potential sources of distress were shown to be operative in the ODOT slag aggregate pavement concretes that we examined. The relative contribution of each of the distress mechanisms to the observed forms of distress was assessed.

The "Unique" Form of Distress in Slag Aggregate Concrete Pavements (Map Cracking)

Examples of the cracking distress in these concrete pavements as expressed on the wearing surface of the pavements are shown in Figure 3. Most often the cracks are most numerous at locations near transverse control joints and initially show primarily a longitudinal orientation. In the early stages of the distress the cracks are relatively tight and there may be little or no spalling (as shown in the bottom photograph of Figure 3). In more advanced stages of the distress a "map-cracking" pattern can develop, along with associated spalling as shown in the top photograph of Figure 3.

The pattern of the cracking that can be seen in the wearing surface of the "Distress" cores taken from three of the four pavement sites fits the description of the "map-cracking" label (Figures 5, 6, and 7). These sites include,

- Two locations on State Route 175 in Cuyahoga County, Ohio (Cores 3, 4, 5, and 6).
- One location on State Route 176 in Cuyahoga County, Ohio (Cores 7 and 8).

The cracking distress in these cores is attributed primarily to the effects of (1) internal sulfate attack, which is the dominant distress mechanism, and to (2) alkali-silica reaction (ASR) activity, which is a secondary contributor.

The fourth ODOT slag aggregate pavement site is on State Route 91 in Cuyahoga County, Ohio (Cores 1 and 2). At this site the "Distress" core was taken through a transverse control joint in a spalled area. At this coring location approximately 90 percent of the original wearing surface is missing (has spalled, as shown in Figure 4). It is not possible to know if the wearing surface on this core exhibited the map-cracking pattern. However, it was subsequently shown that the mode of failure in the State Route 91 concrete is not the same as that of the other three pavement sites. The distress in this concrete is primarily a result of the effects of freezing and thawing of the concrete while in a state of critical moisture saturation.

Attention is first given in this Summary and Conclusion Section of the report to the ODOT slag aggregate cores that exhibit the type of cracking that is unique to slag aggregate concrete pavements in Michigan and Ohio; namely the distress that is referred to as “map-cracking”. Discussions of the cracking in the State Route 91 pavement will refer to the distress as “freeze/thaw cracking”.

The Nature and Origin of Map-Cracking Distress in the ODOT Slag Aggregate Concretes

The petrographic evidence generated in the present study provides strong evidence to support a conclusion that this cracking distress is caused by internal stresses created in the concrete by both (1) internal sulfate attack, and (2) alkali-silica reaction (ASR) activity associated with chert and siltstone fine aggregate particles. The latent source of the sulfates is the slag aggregate particles. The chemical interactions accompanying the release of sulfates into the concrete also create an environment that enhances the potential for ASR activity.

The nature and origin of the map-cracking form of distress in slag aggregate concretes are illustrated in Figure 16, and one of the photographs from this Figure is reproduced below. This is a section view (perpendicular to the plane of the wearing surface) of the top 3 in. (8 cm) of slag aggregate Core 7.

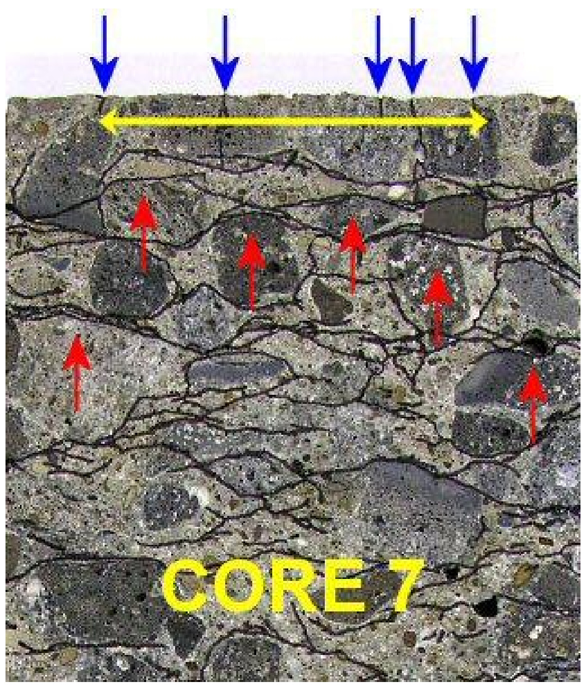

As viewed in two dimensions on a lapped surface of the concrete there are two forms of cracking that are diagnostic of the unique form of distress in slag aggregate concrete pavements. They include (1) shallow vertical cracks, which can be seen on the wearing surface of the pavement, and (2) sub-surface horizontal cracks. The internal sulfate attack reactions produce expansive stresses within the body of the pavement concrete. These expansive stresses create fractures in the concrete that are parallel to the plane of the wearing surface of the pavement slab. These fractures are referred to in our report as "sub-surface horizontal cracks" and in the above figure they have been marked with a black marking pen.

In service it is expected that the strains associated with these stresses will be greatest in the direction perpendicular to the nearest free surface (as shown by the red arrows in the figure). In this case the nearest free surface is the wearing surface of the pavement slab. This scenario results in the creation of tensile stresses in the immediate wearing surface layer as shown by the double yellow arrow in the figure. The result is the creation of shallow cracks, in which the fracture planes are oriented perpendicular to the plane of the wearing surface. These cracks are referred to in our report as "vertical cracks". Many of these cracks pass through near-surface slag aggregate particles.

Internal Sulfate Attack

The term "internal sulfate attack" refers to potentially destructive reactions that occur within the cementitious phase of portland cement concretes in service. In this form of distress a "new" source of sulfates is introduced into the hardened concrete, which react with existing forms of calcium aluminate phases to form additional ettringite. Historically the "new" source of sulfates has been from groundwaters that intrude the concrete, and more recently in the phenomenon known as delayed ettringite formation (DEF) in heat-cured concretes. In the present case, the "new" source of sulfates is provided by the slag aggregates. The petrographic evidence for the involvement of internal sulfate attack in the creation of cracking distress in the ODOT slag aggregate pavement concretes examined here is discussed in detail in our report.

As shown in the Figure on Page 51, (and in Figures 8, 9, 10, 11, 15, and 16), the dominant condition of the sub-surface horizontal fractures in the cores examined here is a separation of the cementitious matrix from the slag aggregate particles at and near the cement paste/aggregate bond line. The cracks are commonly filled with ettringite. Cement paste in the vicinity of the slag aggregate particles typically contain ettringite as in-fill in entrained air voids, and as ettringite within the paste itself. In advanced states of the cracking the cracks pass into the matrix phase of the concrete. The cracks may pass through some of the softer and weaker fine aggregate particles, such as shale, siltstones, and some cherts. They typically pass around the harder and stronger fine aggregate particles, such as quartz.

The conditions necessary for destructive internal sulfate reactions to initiate and progress in slag aggregate pavements in service are,

1. There must be cycles of wetting and drying to provide a mechanism for leaching the sulfides from the slag aggregate particles and subsequently moving the sulfides throughout the body of the concrete.

2. The concrete must experience some degree of drying so that the atmosphere can provide oxygen to the concrete, which is required to oxidize the sulfides leached from the slag aggregates.

3. There must be sufficient moisture available to initiate and sustain the reaction of the "new" sulfates with calcium aluminate phases in the concrete.

The three conditions listed above are best met by the pavement concrete at and near transverse control joints (and subsequently at and near transverse cracks in the pavement slabs). It is in these regions of the pavement slabs where the cracking distress is most prevalent. It can also be reasoned that the conditions are also favorable along the edges of pavement shoulders, where the slabs are in contact with soil or asphalt concrete.

Why Don't All Slag Aggregate Pavements Show Map-Cracking Distress?

If the three environmental conditions listed above were all that is required for slag aggregate pavement concretes to show the unique cracking distress, it is expected that all such pavements would exhibit this behavior. Experience over the years has established that this is not the case. Other factors potentially affecting this unique form of distress are discussed below.

Time of Exposure

One possible explanation is that it is simply a matter of increased time of exposure before the problem is manifest in those situations where the listed conditions are not prevalent. For example, of the four ODOT slag aggregate pavement cores examined from "No-Distress" areas two (Cores 2 and 4) do not currently exhibit any of the diagnostic vertical or sub-surface horizontal cracking. However, Cores 6 and 8 show a low amount of both types of cracks (Figure 12 and Table A-9). Cores 6 and 8 were taken in sound pavement areas and it is expected that all three of the listed environmental conditions would not be as operative.

Slag Chemical and Physical Properties

Another possible explanation is variability in the chemistry and mineralogy of the slag aggregate that is used in a given pavement. The ease of leaching of the sulfides from the slag particles likely varies from slag source to slag source. Two of the ODOT slag aggregate pavements evaluated in our Forensic Study (Lankard, 2010) had shown satisfactory performance for 19 years without showing any evidence of the diagnostic map-cracking distress (Jefferson County, Ohio). The source of the slag in both pavement projects was Weirton Steel, in Weirton, West Virginia.

A third ODOT slag aggregate concrete from the Forensic Study came from State Route 176 in Cuyahoga County, Ohio. One of these cores (CUY-176-10-S (CR) did show a small number of the sub-surface horizontal cracks at the time of our examination (December, 2009). As discussed in the present report, this core showed evidence of latent expansion and cracking when re-examined in May, 2010. This is the same pavement project from which Cores 7 and 8 were taken for evaluation in the present study. The source of the slag was LTV Steel in Cleveland.

The source of the slag aggregate in most of the Michigan pavements cited in the FHWA report (FHWA, 2009) is a steel plant in Detroit.

One of the recommendations for future research suggested by the authors of the 2009 FHWA project is for a "study comparing the chemical, mineralogical, and physical characteristics of all major sources of air cooled blast furnace slags used as coarse aggregate in modern concrete pavements."

However, even if it can be determined which of the physical, chemical, and mineralogical factors of the slag control the cracking problem, it would be difficult to implement a procedure that could separate the "good" from the "bad" particles. And, not only is there a plant-to-plant variability, but also a within-plant variability in these factors.

Portland Cement Source and Type

It is well known that there is a correlation between the susceptibility of concrete to sulfate attack and the tri-calcium aluminate (C_3A) content of the portland cement in the concrete. It is reasonable to assume that at least some of the slag aggregate concrete that performed satisfactorily in the past had a low C_3A content.

Supplementary Cementitious Materials (SCM)

It is well known that some supplementary cementitious materials (fly ash, silica fume, and slag cement) can improve the sulfate resistance of portland cement concretes. However, the beneficial effect is variable and must be evaluated on a case-by-case basis. The ODOT slag aggregate concrete taken from the State Route 176 pavement in Cuyahoga County contained Class C fly ash as one of the cementitious ingredients. In any event, it is reasonable to assume that at least some of the slag aggregate concrete that performed satisfactorily in the past contained some level of a beneficial SCM.

Alkali-Silica Reaction (ASR) Activity

Researchers studying the delayed ettringite (DEF) phenomenon over the years have observed concomitant ASR activity in most cases (Hime, 2000). This most frequently involved siliceous rocks in the fine aggregate phase and often involved sands that previously did not have a record of destructive ASR activity. This situation prevails in our current study of the ODOT slag aggregate cores from the Cuyahoga County, Ohio pavements. Some level of ASR activity was positively indentified in all of the cores, including the four cores taken from a "No-Distress" area.

As discussed in detail in the present report, we have concluded from the petrographic evidence that ASR activity has played a secondary role in the unique form of map-cracking distress,(which is the problem issue for these slag aggregate concretes).

Cracking Distress Due to Freeze/Thaw Cycling

It is a commonly accepted view that the in-filling of entrained air voids with a secondary deposit can have an adverse effect on the durability of concretes exposed to freeze/thaw conditions. This can occur inasmuch as the intended function of the air voids can be compromised when their void space is filled. This situation has occurred in Core 1, which was taken *through* a transverse control joint in a "Distress" location on State Route 91. This is the only one of the eight cores evaluated in the present study that was taken through a control joint.

A cone-shaped region of material has spalled from the top of the joint area in Core 1 and there is a significant amount of cracking adjacent to the spall (shown in Figure 19). These cracks are parallel to the sides of the existing spall (and to each other), and most of the cracks pass through, rather than around the slag aggregate particles. Most of the entrained air voids in this portion of the core are completely in-filled with ettringite. The petrographic evidence supports a conclusion that the cone-shaped cracking and spalling in Core 1 is due in large part to freeze/thaw cycling of the concrete following the loss of functionality of the air void system due to the in-filling.

This type of cracking distress was not observed in the other seven cores examined in the present study. This finding highlights the importance of the accessibility of water to the concrete in the field. Surface water can accumulate along joint lines and intrude into the joint crack. The higher moisture content of the concrete in this portion of the pavement (1) leads to a condition of critical moisture saturation, and (2) will increase the thermal conductivity of the concrete here, leading to more opportunities for freezing temperatures to reach lower levels in the slab.

1. It is noted that the two cores taken from State Route 91 in Cuyahoga County (Cores 1 and 2) do not show the diagnostic map-cracking features of the other six cores. The slag source for the SR 91 pavement is the same for the SR 175 pavements (Allegra SL, Cleveland). The absence of map-cracking distress in the SR 91 pavement could be due to (1) different age of the slag aggregate source, (2) fewer years of exposure, (3) different cement source, and (4) the SR 91 pavement is younger (2002) than the SR 175 pavement (1999).

RECOMMENDATIONS

Air cooled blast furnace slags are useful as aggregates in portland cements concretes for a number of reasons. They are relatively inexpensive, they are hard and sound, and their use provides an outlet for what otherwise would be a discarded waste product. Despite this, their continued use does require that the type of distress associated with some of these concretes in the field be controlled.

Currently it is not known which chemical and physical properties of blast furnace slag aggregates control their involvement in potentially destructive materials-related distress in portland cement concretes for pavement applications. Even if this correlation could be identified, it does not appear that it would be practical or economical to cull out the undesirable product. Given this situation the issue must be addressed through other avenues. These can include (1) an informed choice of cementitious ingredients to limit the effects of internal sulfate attack, and, (2) providing limits on moisture accessibility to the concrete in the field.

Selection of Cementitious Ingredients

1. Select a portland cement with a low C_3A content. Choose an ASTM C 150 Type II cement if available.

2. Use a supplementary cementitious material that has a proven record of improving the sulfate resistance of portland cement concretes.

Limiting Water Ingress Along Control Joints

The map-cracking form of distress and the freeze/thaw-related distress associated with the ODOT slag aggregate concretes evaluated here are most prevalent in the concrete comprising the pavement control joints and immediately adjacent to the control joints. A major factor in this situation is the increased accessibility of water and air to the concrete at these locations. Any steps that could be taken to provide a better joint seal should be considered.

One such step is suggested by results obtained on a 64 year old ODOT pavement evaluated in our Forensic Study (Lankard, 2010). This pavement, constructed in 1946, is on State Route 7 in Gallia County, Ohio. The control joint spacing on the project is 40 ft. (12 m), and many of the joints are originals. Significantly, the control joint seal material in place on the core that we examined was also still in place after 64 years of surface. A lapped surface view of this joint core is shown in Figure 53.

The control joint seal is a sanded bituminous material that was poured into the joint void. The requirement at the time called for the material to meet the requirements of Section M-5.6 F-1 of the General Specifications. The joint seal material was placed (presumably a hot mix) after the joint crack had opened. The red arrow in Figure 53 shows the depth to which the sealant reached in the joint crack.

It is recommended that consideration be given to the evaluation of joint sealant materials such as this one for slag aggregate concrete pavements to limit moisture egress along the joints.

Dr. David Lankard, President & Petrographer

REFERENCES

Belle Lowe, (1937), "The Formation of Ferrous Sulfide in Cooked Eggs", Experimental Cookery from the Chemical and Physical Standpoint, John Wiley and Sons, (Original 1937, see Web Sites).

FHWA Draft Interim Report (2009), "Use of Air-Cooled Blast Furnace Slag as Coarse Aggregate in Concrete Pavements", U.S. Department of Transportation, Federal Highway Administration, October, 2009.

Hammerling, D. et. al. (2000) "Ettringite: Not Just in Concrete", Proceedings of the 22nd International Conference on Cement Microscopy, Montreal, April 30 to May 4, 2000, pages 431-441.

Hime, W., Marusin, S., Jogovic, Z., Martinek, R., Cechner, R., and Backus, L., (2000), "Chemical and Petrographic Analyses and ASTM Test Procedures for the Study of Delayed Ettringite Formation", Cement, Concrete, and Aggregates, Volume 22, No. 2, December 2000, pp. 160-168.

Hime, W., and Erlin, B.,(2008), "Color, Color, Color", Concrete Construction Magazine, January 1, 2008, Two pages.

Lankard, D. (2010), "Forensic Investigation of AC and PCC Pavements with Extended Service Life: Volume 2, Petrographic Examination of PCC Core Samples at Lankard Materials Laboratory", Prepared in Cooperation with the Federal Highway Administration, The Ohio Department of Transportation, and the Ohio Research Institute for Transportation & the Environment, Ohio University, Athens, Ohio, April, 2010, 109 pages + 7 Appendices.

National Slag Association (www.tfhra/hnr/20/recycle/waste/bfsl.htm)

Slag Cement Association Newsletter, (2010), "Why Does Slag Cement Concrete Sometimes Temporarily Turn Green?" One page. www.slagcement.org .

Stehly, R. and Wolter, S., (2006), *Report of Concrete Testing of Michigan Concrete Pavements to the National Concrete Pavement Technology Center at Iowa State University,* American Petrographic Services, Inc., Job No. 10-04139, February 2, 2006, 5 pages.

Vaughan, D., and Craig, J., (1978), *Mineral Chemistry of Metal Sulfides*, Cambridge University Press, ISBN 0-521-21489-0.

Van Dam, T.J., Peterson, K.R., Sutter, L.L., and Housewright, M.E., (2003), "Deterioration in Concrete Pavements Constructed with Slag Coarse Aggregate", Transportation Research Record 1834, Paper No. 03-3400, pages 8-15.

APPENDIX A

TABLES

CORING DATA, PROJECT CONCRETE DATA, AND CORE DATA

LML REPORT 5536N

Table A-1. CORING DATA AND AS-RECEIVED CONDITION OF ODOT PAVEMENT CORES (LML PROJECT 5536N)

LML Core Number	Core I.D. Number	Core Length, In.	Coring Site	Date Pavement Placed	Coring Location	As-Received Condition
1	SR 91 DISTRESS	10	Station 100+50 in the northbound driving lane	2002	Core taken from a joint, approximately 1 ft from the longitudinal joint between the driving and passing lane	Full depth core was taken through a transverse control joint. Contains steel mesh layer at 7 in. to 8 in. depth below the wearing surface.
2	SR 91 NO DISTRESS	9 ½	Station 100+50 in the northbound driving lane	2002	Core taken from adjacent slab (re Core 1), 3 f from the same transverse joint and 3 ft from the same long joint	Full depth core received in one piece. Contains steel mesh layer at 5 in to 6 in depth below the wearing surface.
3	SR 175 DISTRESS	9 ¼	Station 269+80	1999	Core taken approximately 1 ft from a transverse joint and 1 ft from the longitudinal joint	Full depth core received in 3 pieces separated by a horizontal fracture ca. 1 in to 2 in. below the wearing surface. Short piece of steel mesh ca. 5 in. below wearing surface.
4	SR 175 NO DISTRESS	10 ¼	Station 269+80	1999	Core taken from adjacent slab (re Core 3), 3 ft from the same transverse joint and 3 ft from the same longitudinal joint.	Full depth core received in one piece. Contains steel mesh layer at ca. 6 in. depth below the wearing surface.

Note: Core diameter is 4 in. unless otherwise noted. All cores are from ODOT pavements in Cuyahoga County, Ohio.
All cores contain blast furnace slag as the coarse aggregate.

Table A-1 (cont'd). CORING DATA AND AS-RECEIVED CONDITION OF ODOT PAVEMENT CORES (LML PROJECT 5536N)

LML Core Number	Core I.D. Number	Core Length, In.	Coring Site	Date Pavement Placed	Coring Location	As-Received Condition
5	SR 175 @ CONCORD (DISTRESS)	10 ½	Station 270+80	1999	Core taken approximately 1 ft from a transverse joint and 1 ft from a longitudinal joint	Full depth core received in two pieces separated by a horizontal fracture ca. 2 in. below the wearing surface. No Steel.
6	SR 175 @ CONCORD (NO DISTRESS)	10 ¼	Station 270+80	1999	Core taken from an adjacent slab (re above) 3 ft from the same transverse joint and 3 ft from the same longitudinal joint	Full depth core received in one piece. Contains steel mesh layer at 6 in to 7 in. depth below the wearing surface.
7	CUY 176 (DISTRESS)	11 ½	Station 107	1994	Core taken approximately 1 ft from a transverse joint and 4 ft from a longitudinal joint in a shoulder slab	Full depth core received in one piece. No Steel
8	CUY 176 (NO DISTRESS)	11 ½	Station 107	1994	Core taken in the same shoulder slab as Core 7 approximately 6 ft from Core 7 in the same longitudinal line	Full depth core received in one piece. No Steel

Note: Core diameter is 4 in. unless otherwise noted. All cores are from ODOT pavements in Cuyahoga County, Ohio.
All cores contain blast furnace slag as the coarse aggregate.

Table A-2. Mix Design ODOT Class C Concrete (BF Slag Coarse Aggregate) Based on a Water-Cement Ratio of 0.50. Class C Concrete was used in the construction of the State Route 91 PCC pavement examined in the present study.

Concrete Constituent	lb of Constituent per Cubic Yard of Concrete	Specific Gravity (Density) of Constituent, lb/ft^3	Cubic feet of Constituent per Cubic Yard of Concrete
Cement	600	196.6	3.05
Fine Aggregate [(a)]	1330	163.5	8.14
Coarse Aggregate [(b)]	1340	143.5	9.34
Water (0.50)	300	62.4	4.81
Entrained Air[©]	(6 %)	-	1.62
Totals	3570	-	26.96

(a) Based on a fine aggregate specific gravity of 2.62

(b) Based on a slag coarse aggregate specific gravity of 2.30

(c) The target air content is 6 % .

Theoretical Unit Weight (w/cm = 0.5) = 3750/26.96 = 139.1 lb/ft^3 .

Theoretical Cement Paste Content = 7.86/26.96 = 29.2 %.

Water to Cementitious Material Ratio (w/cm) = 300/600 = 0.50

Table A-3. Mix Design ODOT Class C Option 1 Concrete (BF Slag Coarse Aggregate) Based on a Water to Cementitious Material Ratio of 0.46. Class C Option 1 Concrete was used in the construction of the State Route 176 PCC pavement examined in the present study.

Concrete Constituent	lb of Constituent per Cubic Yard of Concrete	Specific Gravity (Density) of Constituent, lb/ft^3	Cubic feet of Constituent per Cubic Yard of Concrete
Cement	510	196.6	2.59
Class C Fly Ash[(a)]	90	143.5	0.63
Fine Aggregate [(b)]	1350	164.1	8.23
Coarse Aggregate [(c)]	1390	147.3	9.44
Water (0.46)	275	62.4	4.41
Entrained Air©	(6 %)	-	1.62
Totals	3615	-	26.92

(a) Based on a fly ash specific gravity of 2.30

(b) Based on a fine aggregate specific gravity of 2.63

(c) Based on a slag coarse aggregate specific gravity of 2.36

(d) The target air content is 6 %.

Theoretical Unit Weight (w/cm = 0.46) = 3615/26.92 = 134.3 lb/ft^3 .

Theoretical Cement Paste Content = 7.63/26.92 = 28.3 %.

Water to Cementitious Material Ratio (w/cm) = 275/600 = 0.46

Table A-4. Mix Design ODOT Class Moderate Set/High Strength (BF Slag Coarse Aggregate) Based on a Water to Cementitious Material Ratio of 0.43. This Concrete was used in the construction of the Two State Route 175 PCC pavements examined in the present study.

Concrete Constituent	lb of Constituent per Cubic Yard of Concrete	Specific Gravity (Density) of Constituent, lb/ft^3	Cubic feet of Constituent per Cubic Yard of Concrete
Cement	800	196.6	4.07
Fine Aggregate [(a)]	1028	163.5	6.29
Coarse Aggregate [(b)]	1440	147.9	9.74
Water (0.43)	344	62.4	5.51
Entrained Air[©]	(6 %)	-	1.62
Totals	3612	-	27.23

(a) Based on a fine aggregate specific gravity of 2.62

(b) Based on a slag coarse aggregate specific gravity of 2.37

(c) The target air content is 6 %.

Theoretical Unit Weight (w/cm = 0.43) = 3612/27.23 = 132.6 lb/ft^3 .

Theoretical Cement Paste Content = 9.58/27.23 = 35.2 %.

Water to Cementitious Material Ratio (w/cm) = 344/800 = 0.43

Table A-5. Sources of the Concreting Materials used in the ODOT PCC pavements from which cores were taken for Examination in the Present Study.

ODOT Pavement Project	Portland Cement Source	Fine Aggregate Source[a]	Coarse (Slag) Aggregate Source	Fly Ash Source
SR 91	Essroc (Picton Ont	Lafarge/Shalersville or Jefferson/Streetboro	Allega SL (Cleveland)	None Used
SR 175	Essroc (Picton Ont)	Jefferson/Streetboro	Allegra SL (Cleveland)	None Used
SR 176	Essroc (Bessemer)	Lafarge/Shalesville	Lafarge (Cleveland)	Detroit (Bell River #1)

(a) The fine aggregate for all the projects is a natural sand.

Table A-6. FINE AGGREGATE CHARACTERIZATION DATA: (LML PROJECT 5536N)

LML Core Number	Pavement Coring Site	Maximum Sand Size, mm	Rock/Mineral Type									
			Quartz	Siltstone	Sand-stone	Limestone	Igneous	Chert	Shale	Feldspar	Iron Oxides	Other
2	SR 91	4.5	1	2	3	4	9	7	6	5	8	10
4	SR 175	4.5	1	2	4	3	5	6	10	7	8	9
6	SR 175 @ Concord	4.5	1	2	4	3	6	7	8	5	9	10
8	SR 176	4.5	1	2	4	3	7	5	9	8	6	10

Table A-7. FINE AGGREGATE CHARACTERIZATION DATA: (LML PROJECT 5536)

LML Core Number	Core Identification Number	Maximum Sand Size, mm	Rock/Mineral Type									
			Quartz	Siltstone	Sand-stone	Limestone	Igneous	Chert	Shale	Feldspar	Iron Oxides	Other
1	GAL-7 (CR)	5	1	2	4	5	10	3	9	8	7	6
3	ATH-682 (CR)	5	1	3	-	2	6	5	4	7	9	8, 10
5	ATH-33 (CR)	3.5	1	3	-	2	4	5	-	8	6	7
7	GRE-35 (CR)	3	1	3	5	2	4	7	6	9	10	8, 11
9	HAM-126 (CR)	5	1	6	7	2	4	3	5	8	10	9, 11-13
11	ALL-30 (CR)	3	1	10	9	3	4	6	2	7	-	5,8
13	JEF-22 (CR)	4.5	1	2	4	3	6	5	7	8	9	10-11
16	JEF-7 (JT)	4	1	2	4	3	6	5	9	7	8	10-12
17	TUS-39 (CR)	5	1	2	4	3	6	5	9	7	8	10-12
19	CUY-82 (CR)	4	1	2	4	3	5	-	6	7	9	8, 10

21	CUY-176-10-S (CR)	4.5	1	2	3	4	6	9	7	8	5	10

Table A-7 (Cont'd). FINE AGGREGATE CHARACTERIZATION DATA: (LML PROJECT 5536)

LML Core Number	Core Identification Number	Maximum Sand Size, mm	Rock/Mineral Type									
			Quartz	Siltstone	Sand-stone	Limestone	Igneous	Chert	Shale	Feldspar	Iron Oxides	Other
23	CUY-176-11-S (CR)	4	1	2	3	4	5	6	7	10	8	9, 11-12
25	CUY-176-12-S (CR)	4.5	1	2	3	4	5	7	6	9	8	10-11
29	CUY-322 (CR)	3	1	2	3	4	9	8	6	5	7	10
32	CUY-252 (CR)	5	1	3	4	2	5	9	8	7	6	10-11
33	SUM-76-15-W (CR)	4.5	1	2	4	3	6	5	9	7	8	-
37	SUM-76-15-E (CR)	4.5	1	2	3	4	6	5	9	7	8	10-12
39	MOT-35 (CR)	4.5	1	3	6	2	4	5	7	8	10	9
41	MOT-202 (CR)	4.5	1	3	7	2	6	5	4	8	9	10
43	LOG-33 (JT)	4	1	2	6	3	5	7	4	-	8	9

Table A-8. AIR VOID SYSTEM AND CEMENT PASTE CONTENT DATA: LML PROJECT 5536N)

LML Core Number	Core Identification Number	ASTM C 457 Measurement Parameters				Specific Surface Area, in^2/in^3	Air-Void Spacing Factor, in.	Total Air Void Content, %	Cement Paste Content, %
		Voids Per Inch	Traverse Length, in.	Traverse Area, in^2	Number of Stops				
2	SR 91	12.1	102.0	71.0	2040	703	0.0054	6.9	26.0
4	SR 175	21.0	101.7	71.0	2033	1197	0.0038	7.03	33.5
6	SR 175@ Concord	13.9	100.6	71.0	2012	1487	0.0040	3.73	33.1
8	SR 176	14.3	100.5	71.0	2009	835	0.0052	6.87	29.6

Table A-9. Chracterization of the Presence and Extent of Cracking Distress in the ODOT Slag Aggregate PCC pavement cores.

ODOT Pavement Project	Age of Concrete, years	Core Number	Distress Characterization		Estimated Extent of Horizontal Cracking[a]	Vertical Cracks Through Slag Particles[c]	ASR Identified?	Ettringite in Air Voids
			No Distress	Distress				
SR 91	8	1		√	(b)	(b)		Moderate throughout length, Heavy near joint
SR 91	8	2	√		None	No	Very Light	Only present in bottom 0.5 to 1 in. (Moderate).
SR 175	11	3		√	Heavy	Yes		Moderate throughout length of core
SR 175	11	4	√		None	No	Light Throughout	Only present in bottom 0.5 to 1 in. (Moderate)
SR 175 @ Concord	11	5		√	Heavy	Yes		Moderate throughout length of core
SR 175 @ Concord	11	6	√		Light	Yes	Light Throughout	Moderate except in top 2 in. of core
SR 176	16	7		√	Heavy	Yes		Light to Moderate throughout core length
SR 176	16	8	√		Light	Yes	Moderate Throughout	Light throughout the core length

(a) “Estimate” categories are Heavy, Moderate, Light, and None

(b) Core 1 was taken through a transverse control joint and there is a significant amount of cone-shaped spalling in the joint. However, there are no sub-surface horizontal cracks of the type present in the cores from State Routes 175 and 176. The cracks that are present (shown in Figure 19 do pass through some of the near surface slag aggregate particles.

(c) The reference here is to cracks in the pavement wearing surface with fracture planes oriented perpendicular to the plane of the wearing surface and which pass completely through near-surface slag coarse aggregate particles.

Table A-10. Property Data on Slag Aggregate PCC Pavement Cores Examined in the Forensic Study (Lankard, 2010).

ODOT Pavement Project	Age of Concrete, years	Core Numbers	Cementitious Constituents	Estimated w/cm	Total Air Void Content, %	Slag Aggregate Size, in.	Slag Aggregate Source	Evidence of Destructive Cem/Agg Reactions	Compressive Strength, psi
Jefferson County State Route 22	19	13 & 14	Portland Cement	0.42	5.2	1	#57 Slag LaFarge, Weirton, WV	No	7340
Jefferson County State Route 7	19	15 & 16	Portland Cement	0.46	6.1	¾	#57 Slag LaFarge, Weirton, WV	Very Limited	6830
Cuyahoga County State Route 176	15	21 & 22	Portland Cement and Fly Ash	0.44	1.9	1	LaFarge, LTV, Cleveland	No*	6260

APPENDIX B

REPORT FIGURES

LML REPORT 5536N

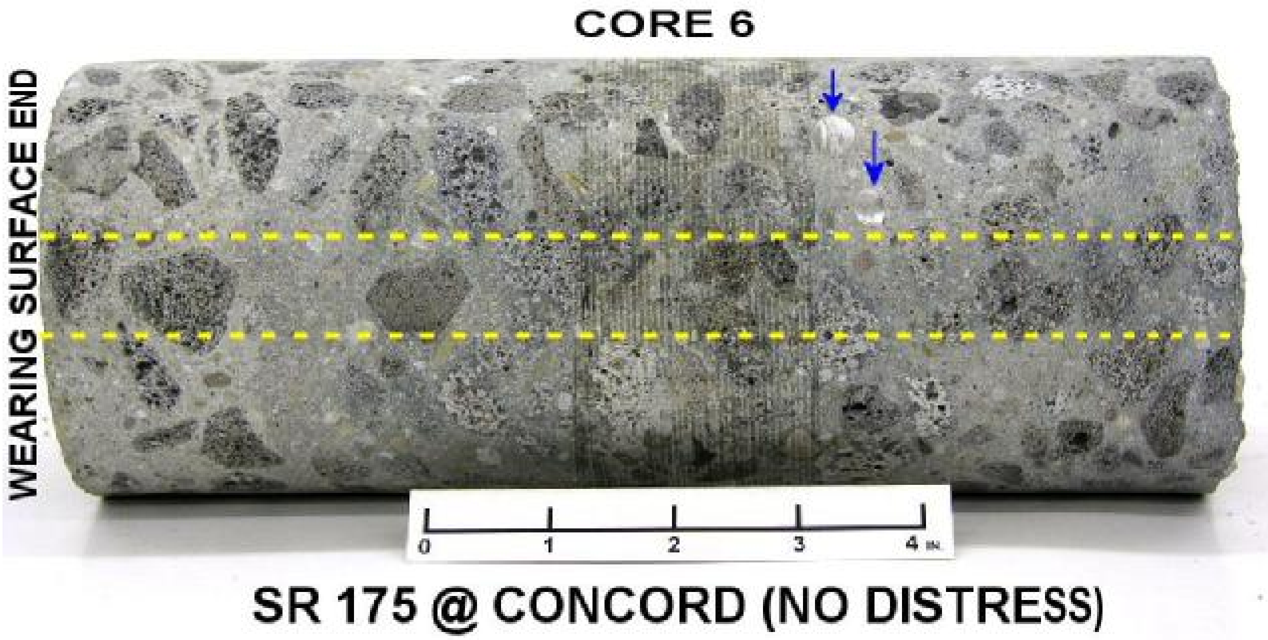

CORE 6 WEARING SURFACE

Figure 1. As-received condition of Core 6 taken from the "No Distress" location at the SR 175 @ Concord site. This 10 ¼ in. long core was received in one piece and no sub-surface horizontal cracks could be seen on the cored surfaces. The arrows in the bottom photograph point to a tight longitudinal crack in the textured wearing surface.

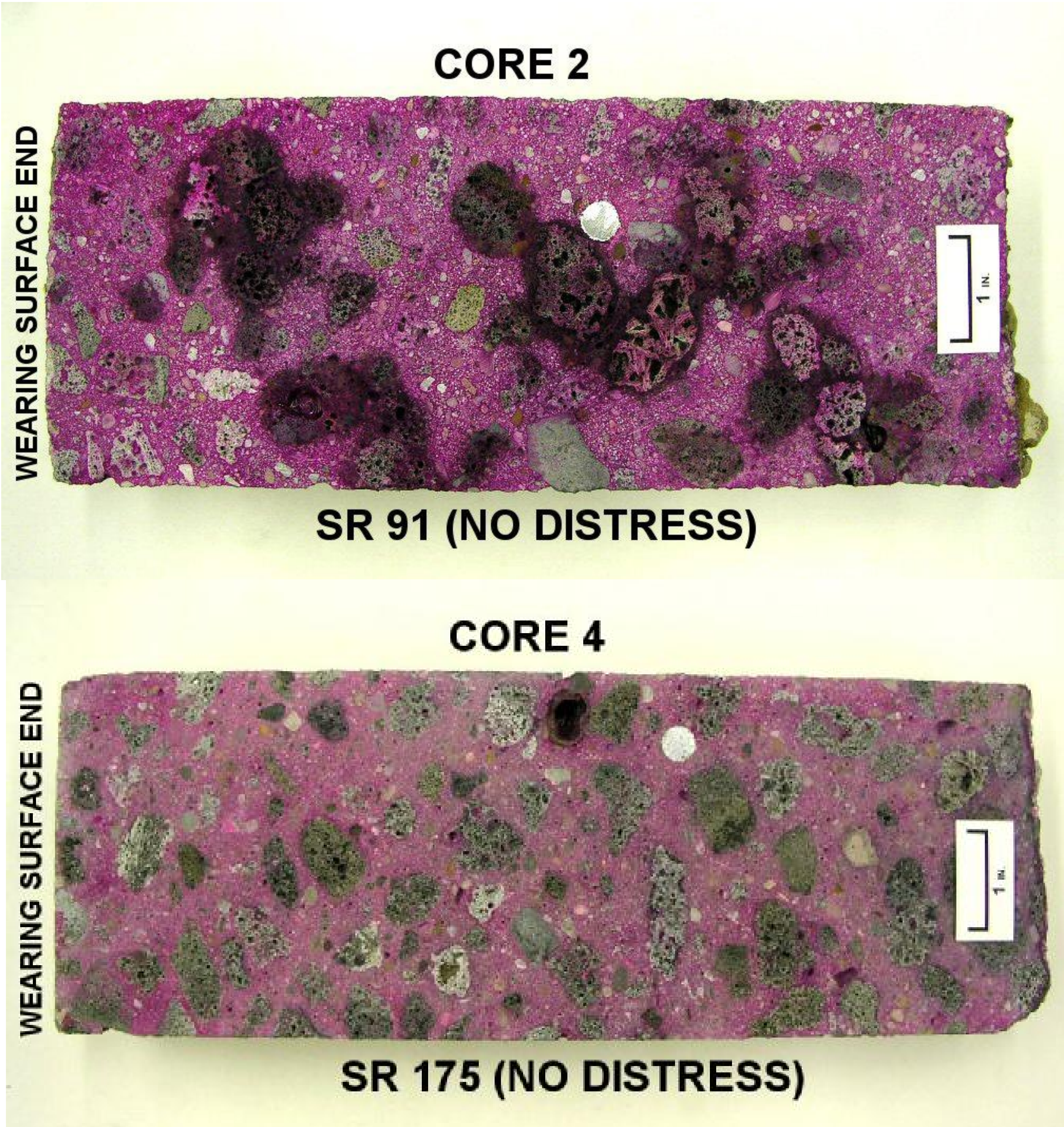

Figure 2. Saw-cut surfaces of Cores 2 and 4 following the application of the phenolphthalein pH indicating solution. No carbonation has occurred in the red colored areas (virtually the entire thickness of the cores).

Figure 3. Examples of the cracking and spalling distress that is uniquely associated with slag aggregate concrete pavements in Michigan and Ohio. The top photograph is an example of advanced deterioration of a transverse joint and map cracking on a tied slag aggregate concrete shoulder in Michigan (Van Dam, 2003). The bottom photograph is cracking distress adjacent to a transverse joint in a 15 year old Cuyahoga County (Ohio) pavement (SR 176) in 2009 (also shoulder panels).

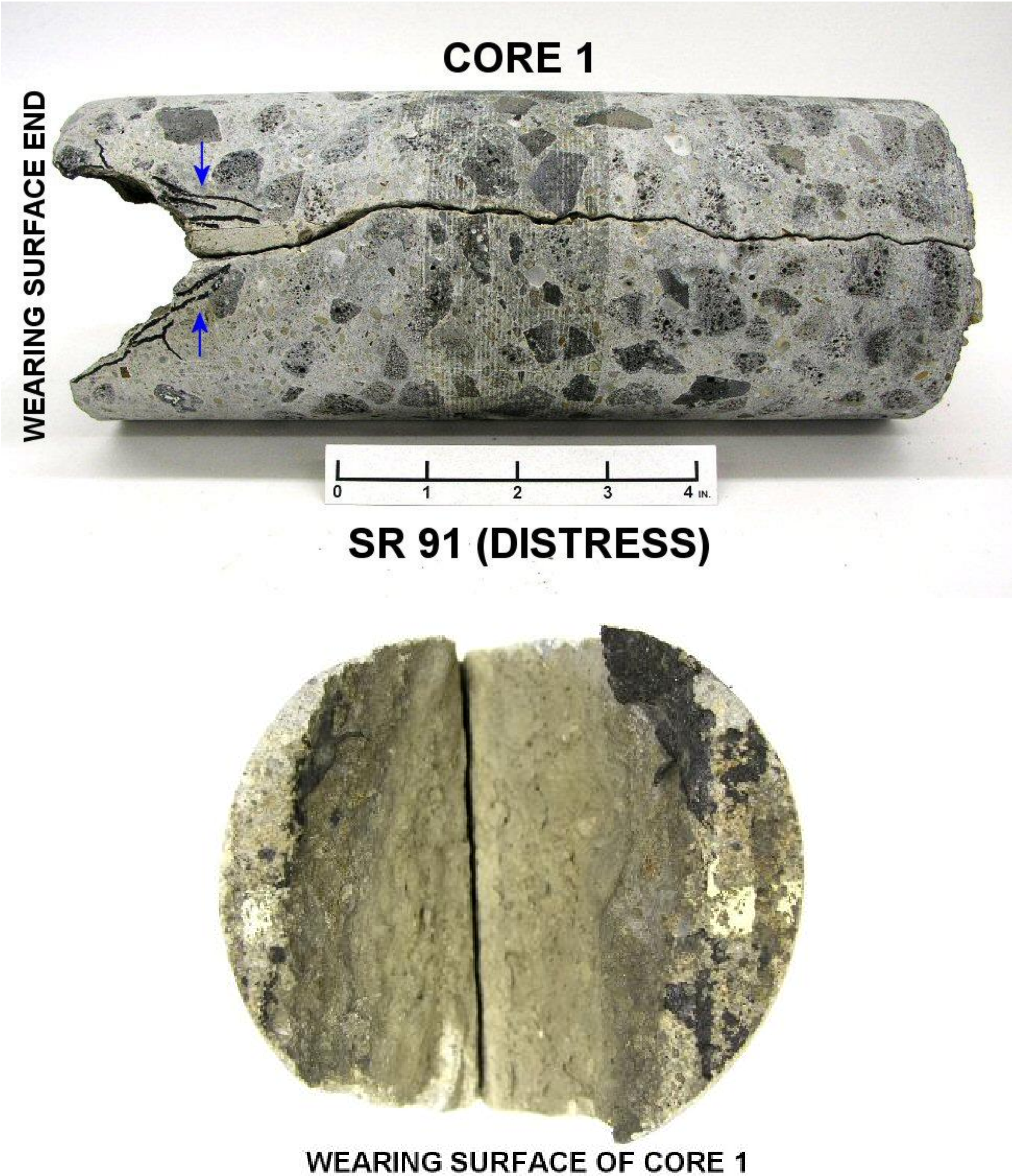

Figure 4. Core 1 taken at a "Distress" location on State Route 91 in Cuyahoga County, Ohio as-received at Lankard Materials Lab on March 3, 2010. This core was taken through a control joint in the pavement, where some spalling has occurred. The arrows point to cracks in the core that have been marked with a black marking pen. There is a $^{3}/_{16}$ in (5 mm) diameter mesh strand holding the two core pieces together.

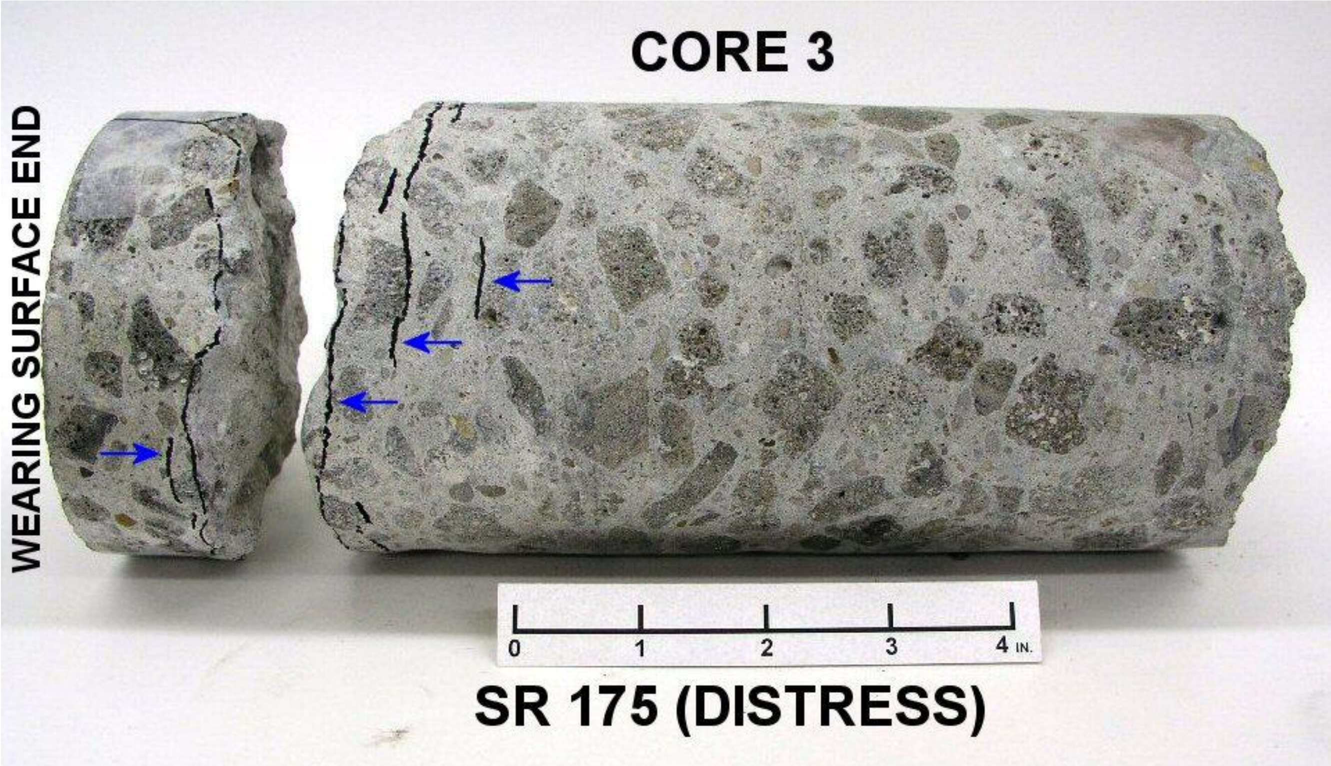

Figure 5. Core 3 taken at a "Distress" location on State Route 175 in Cuyahoga County, Ohio as-received at Lankard Materials Lab on March 3, 2010. This core was taken 1 ft. from a transverse control joint and 1 ft. from a longitudinal joint. Horizontal cracks in the core are marked with black marking pen in the top photograph. Cracks in the wearing surface are also marked with a black pen and the arrows point to a full core width crack along which the top portion of the core was separated into two pieces as-received.

WEARING SURFACE OF CORE 5

Figure 6. Core 5 taken at a "Distress" location on State Route 175 @ Concord in Cuyahoga County, Ohio as-received at Lankard Materials Lab on March 3, 2010. This core was taken 1 ft. from a transverse control joint and 1 ft. from a longitudinal joint. Horizontal cracks in the core are marked with black marking pen in the top photograph. Cracks in the wearing surface are also marked with a black pen. The arrow points to a full core width crack along which the core was separated into two pieces as-received.

Figure 7. Core 7 taken at a "Distress" location on State Route 176 in Cuyahoga County, Ohio as-received at Lankard Materials Lab on March 3, 2010. This core was taken 1 ft. from a transverse control joint and 4 ft. from a longitudinal joint in the same shoulder slab. Horizontal cracks in the core are marked with black marking pen in the top photograph (arrows). Cracks in the wearing surface are also marked with a black pen. This core was received in one piece.

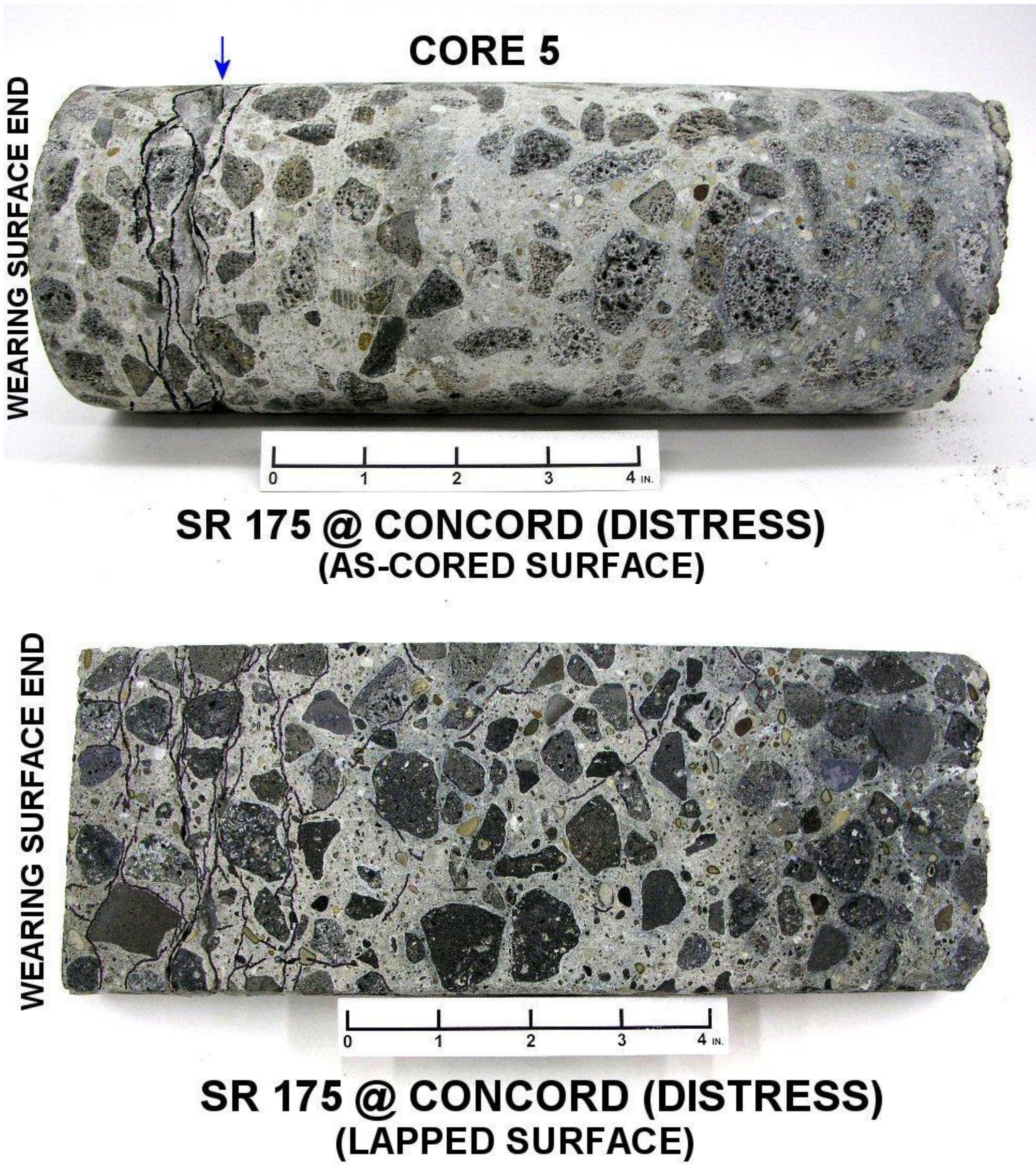

Figure 8. Two views (an as-cored surface and a lapped surface) of Core 5 taken from a "Distress" location on the SR 175 @ Concord pavement. The core was received in two pieces that were re-attached with an epoxy adhesive (at the site of the arrow). The lapping operation on the slab section of Core 5 (bottom photograph) revealed the presence of many more horizontal cracks in the core concrete than could be detected on the as-cored surfaces. Cracks that were detected in the microscopic examinations are marked with a black marking pen in both photographs.

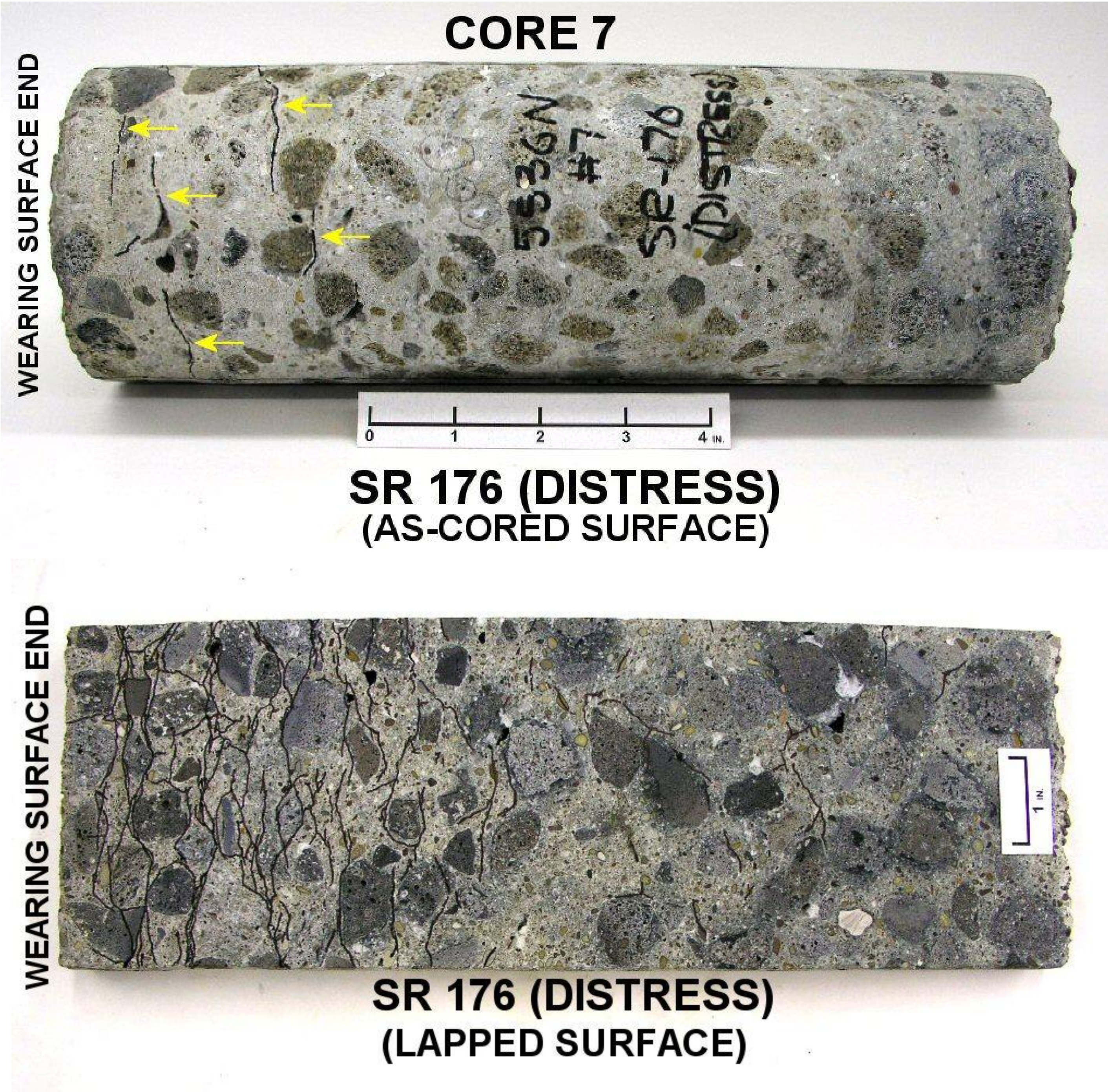

Figure 9. Two views (an as-cored surface and a lapped surface) of Core 7 taken from a "Distress" location on the SR 176 pavement. The lapping operation revealed the presence of many more horizontal cracks in the core concrete than could be detected on the as-cored surfaces. Cracks that were detected in the examinations are marked with a black marking pen.

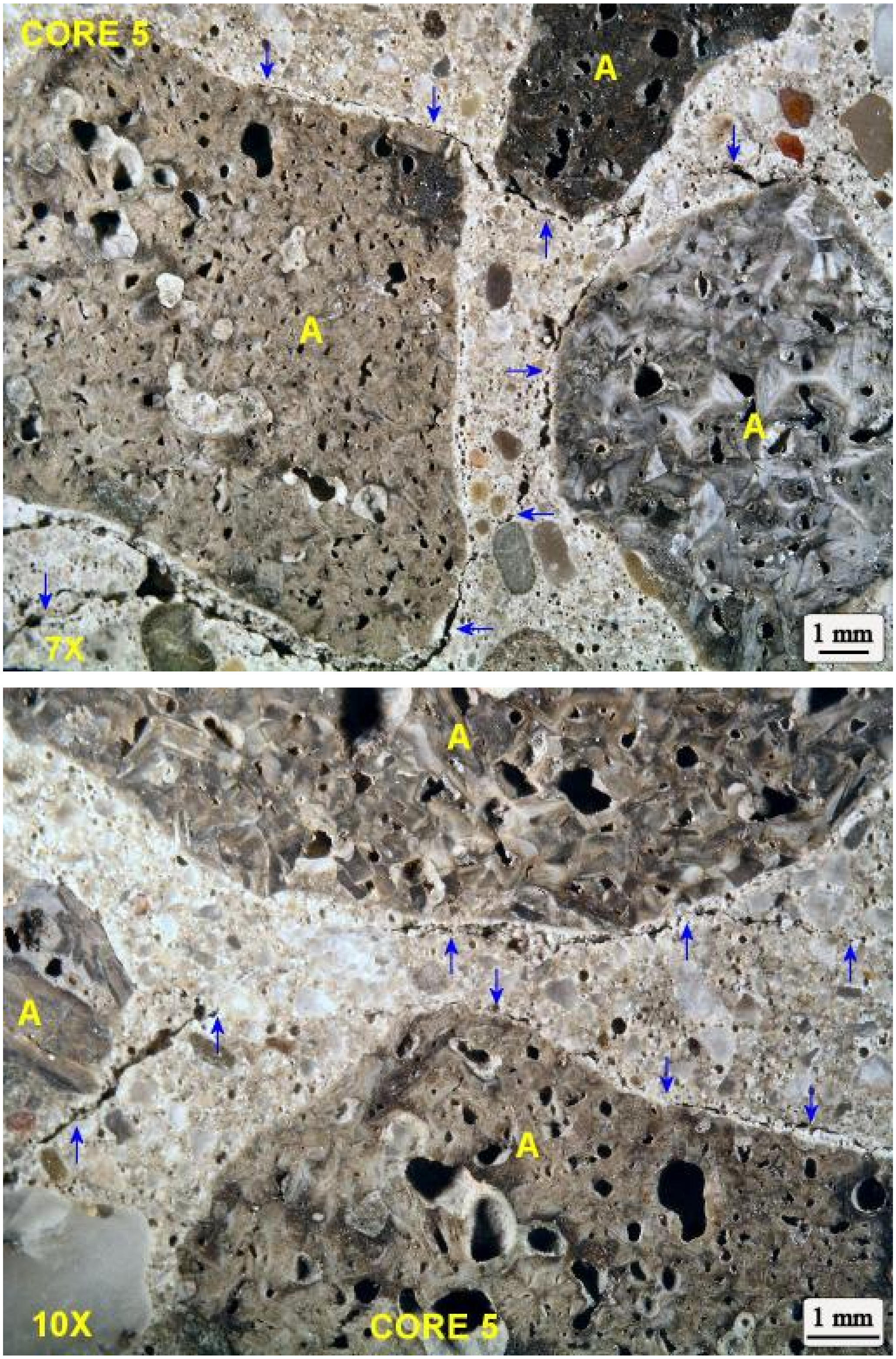

Figure 10. Lapped surface views of Core 5 at a distance of 1 in. below the plane of the wearing surface showing cracks (arrows) that pass around, rather than through slag coarse aggregate particles (A). This microstructural feature is common in the cores taken from the "Distress" locations adjacent to transverse control joints in the ODOT Cuyahoga County, Ohio pavements.

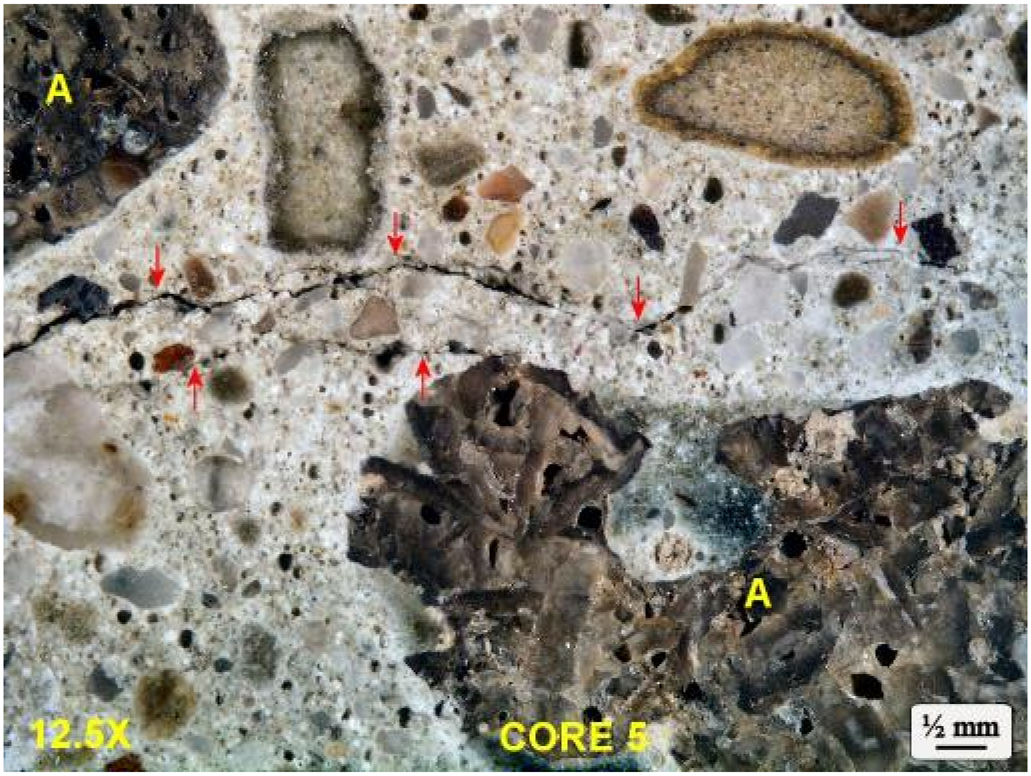

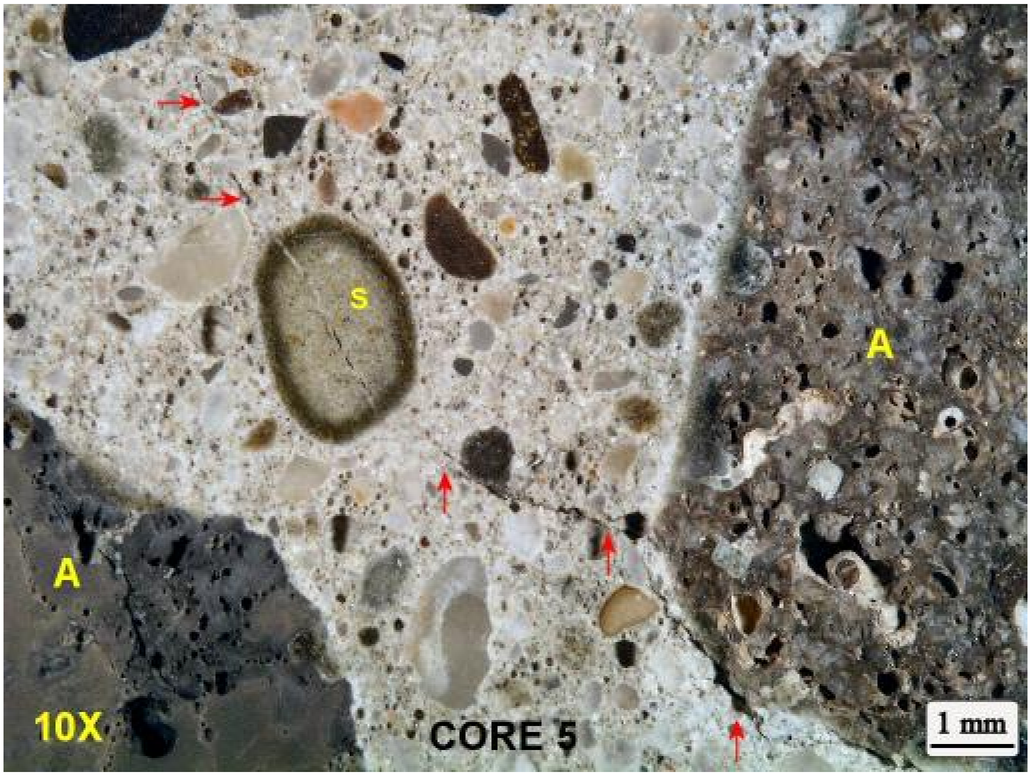

Figure 11. Enlarged lapped surface views showing horizontal cracking within the cementitious matrix in Core 5 . These cracks are within the top 3 in. of the core. The wearing surface is at the top in the photographs. The top photograph shows a crack passing around fine aggregate particles. The bottom photograph shows a crack that passes around a slag coarse aggregate particle (A), which intersects a siltstone fine aggregate particle (S).

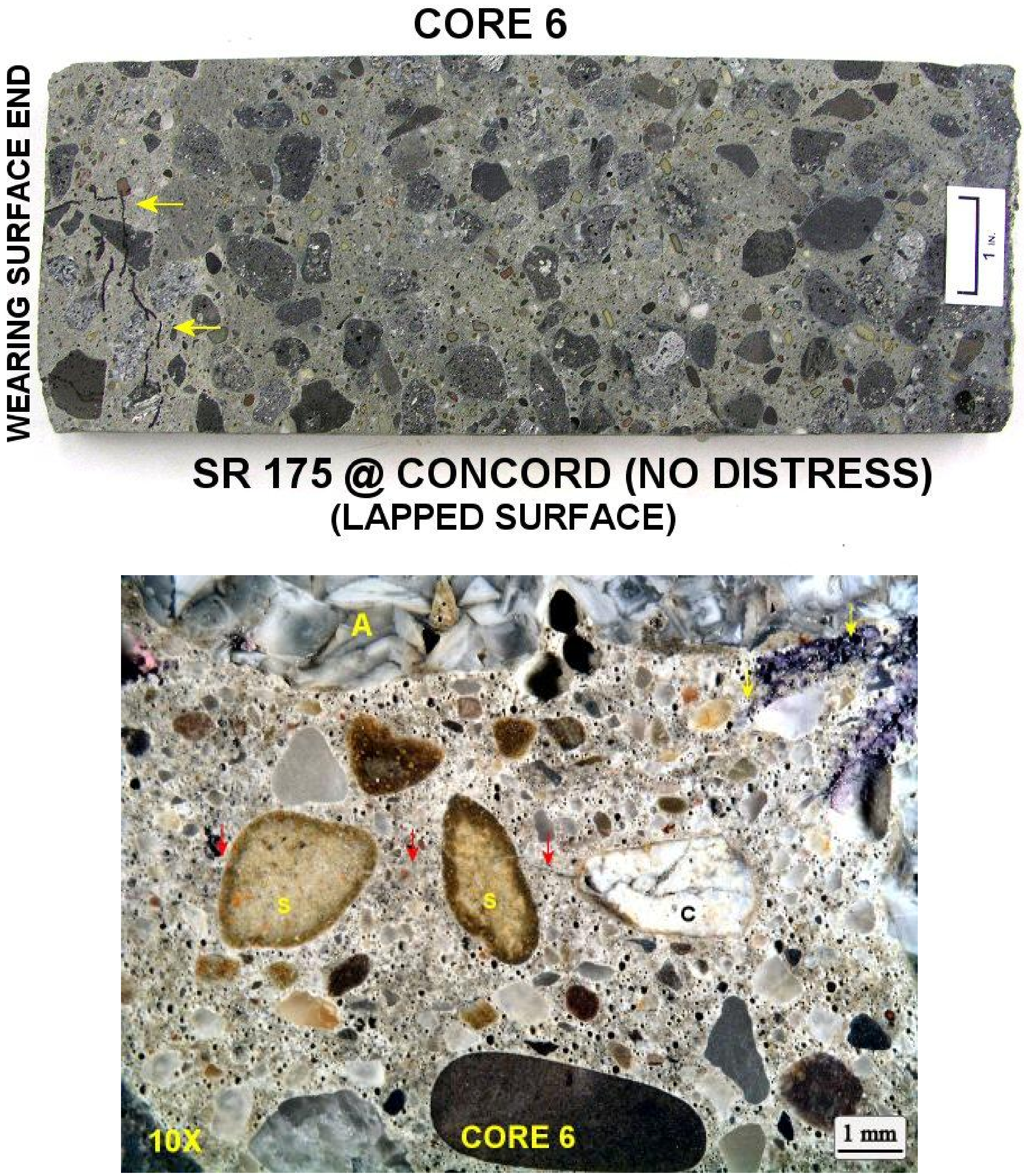

Figure 12. Two views of Core 6 taken from a "No Distress" area of the SR 175 @ Concord pavement. The top photograph is a lapped surface on which horizontal cracks in the top ¾ in. to 1 ¼ in. thickness of the core have been marked (arrows) with a black marking pen. The bottom photograph is an enlarged view (10X) of the lapped surface showing horizontal cracks passing around a slag coarse aggregate particle (A) (yellow arrows) and a horizontal crack passing through a chert (C) and siltstone (S) particles (red arrows).

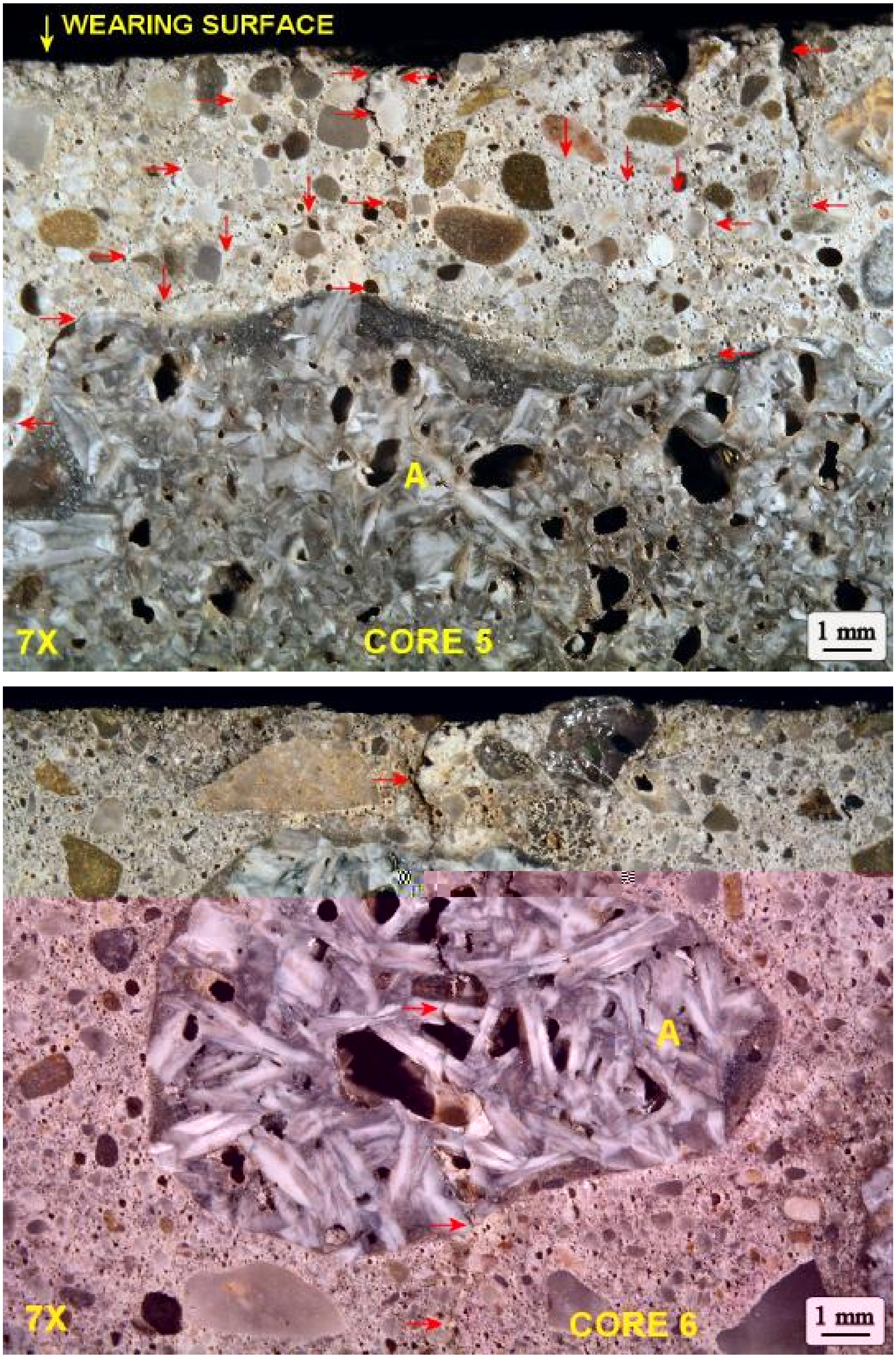

Figure 13. Enlarged (7X) lapped surface views perpendicular to the wearing surface of Core 5 (Distress core taken from SR 175 @ Concord) and Core 6 (No Distress core taken from SR 175 @ Concord). The red arrows point to the path of vertical cracks overlying near-surface slag coarse aggregate particles (A). The cracks pass around and through the aggregate particles (A) and through the matrix phase of the concretes.

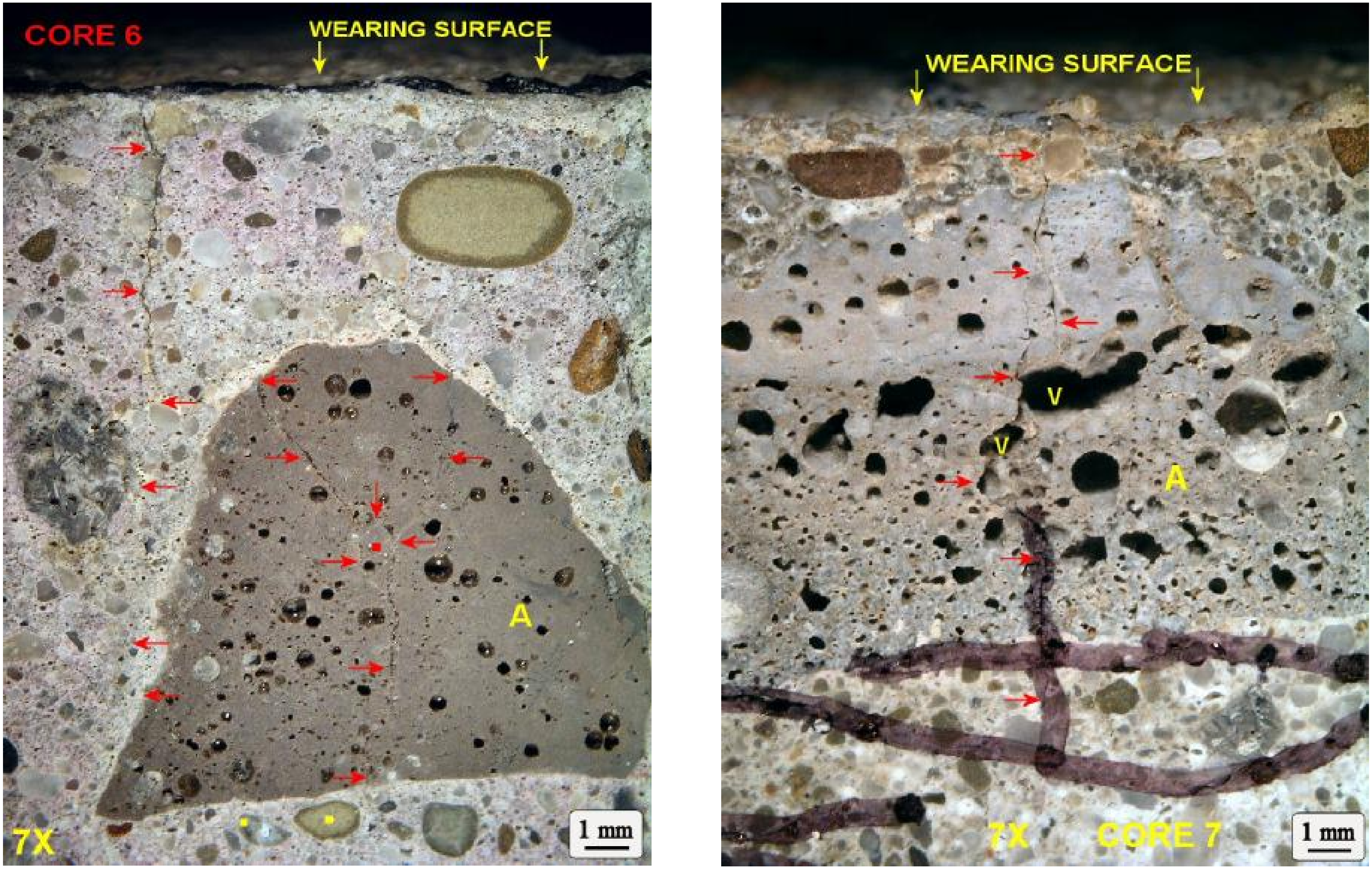

Figure 14. Enlarged (7X) lapped surface views perpendicular to the wearing surface of Core 6 (No-Distress core taken on SR 175 @ Concord) and Core 7 (Distress core taken on SR 176). The red arrows point to the path of vertical cracks that pass around and through near-surface slag coarse aggregate particles (A) and through the matrix phase of the concrete. The yellow dots on the Core 6 photograph are on fine aggregate particles that have a white exudate on their surface. Horizontal cracks in the Core 7 concrete are marked with a black marking pen. The "V" identifies a large void in the slag particle.

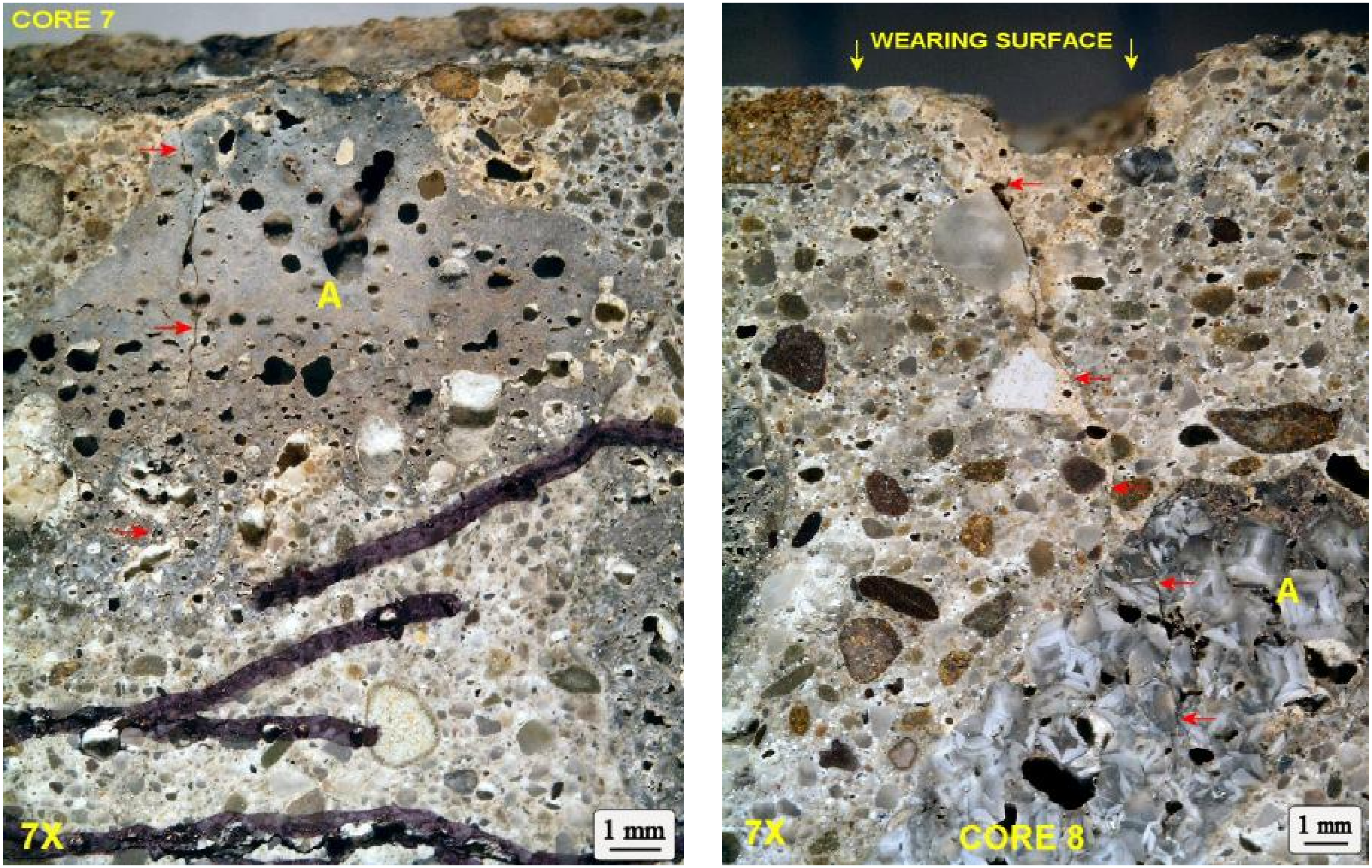

Figure 15. **Enlarged (7X) lapped surface views perpendicular to the wearing surface of Core 7 (Distress) and Core 8 (No Distress) taken from SR 176 Pavement Site. The red arrows point to the path of vertical cracks through near-surface slag coarse aggregate particles and through the matrix phase of the concretes. The black lines mark the location of sub-surface horizontal cracks in the concrete of Core 7.**

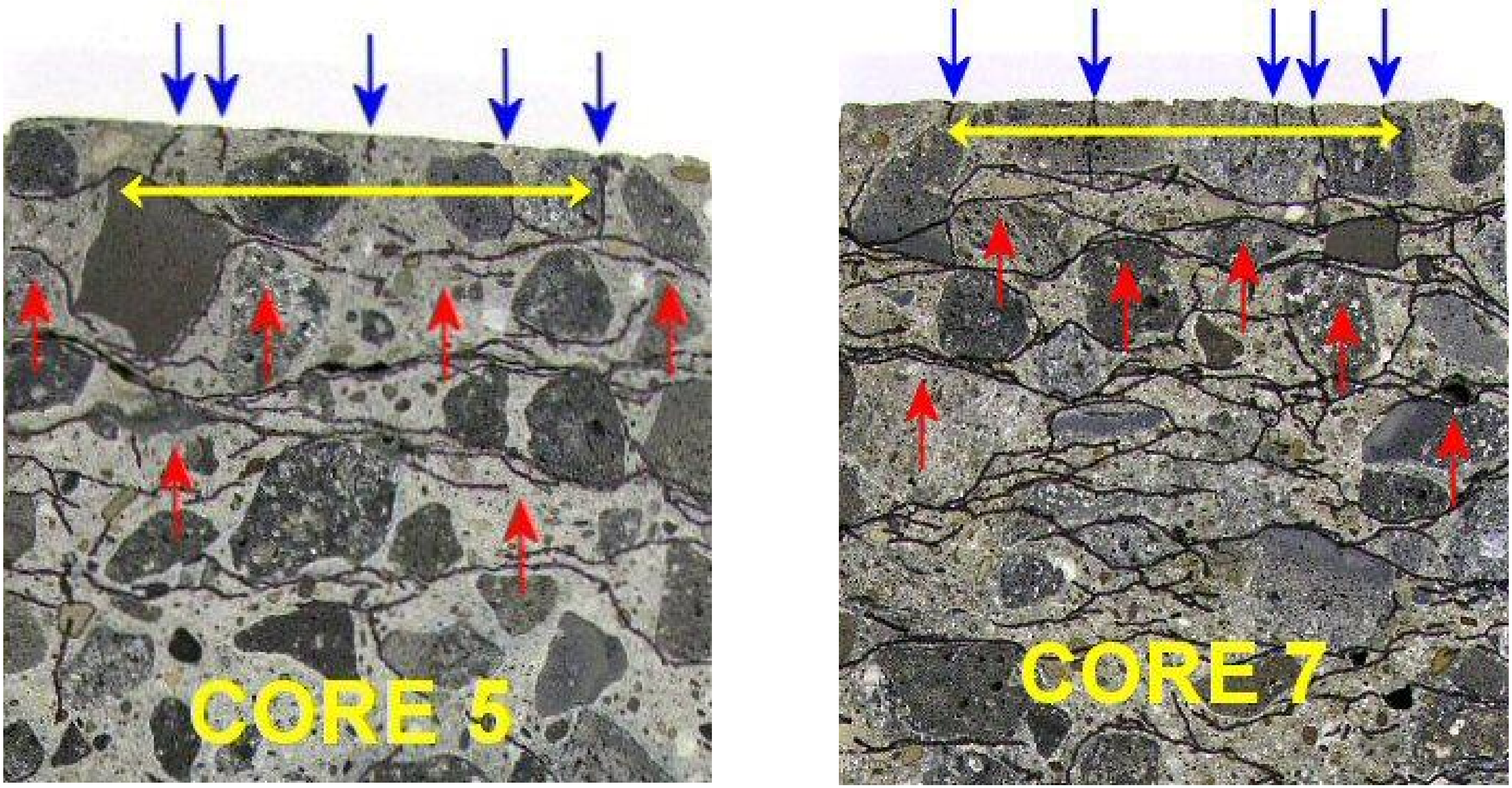

Figure 16. Lapped surface views of Core 5 (Distress Core from SR 175 @ Concord) and Core 7 (Distress Core from SR 176) showing the location of vertical cracks (blue arrows) that penetrate the plane of the wearing surface of the cores. All vertical and sub-surface horizontal cracks that could be detected in the microscopic examination are marked with a black marking pen. The magnification is around 0.9X.

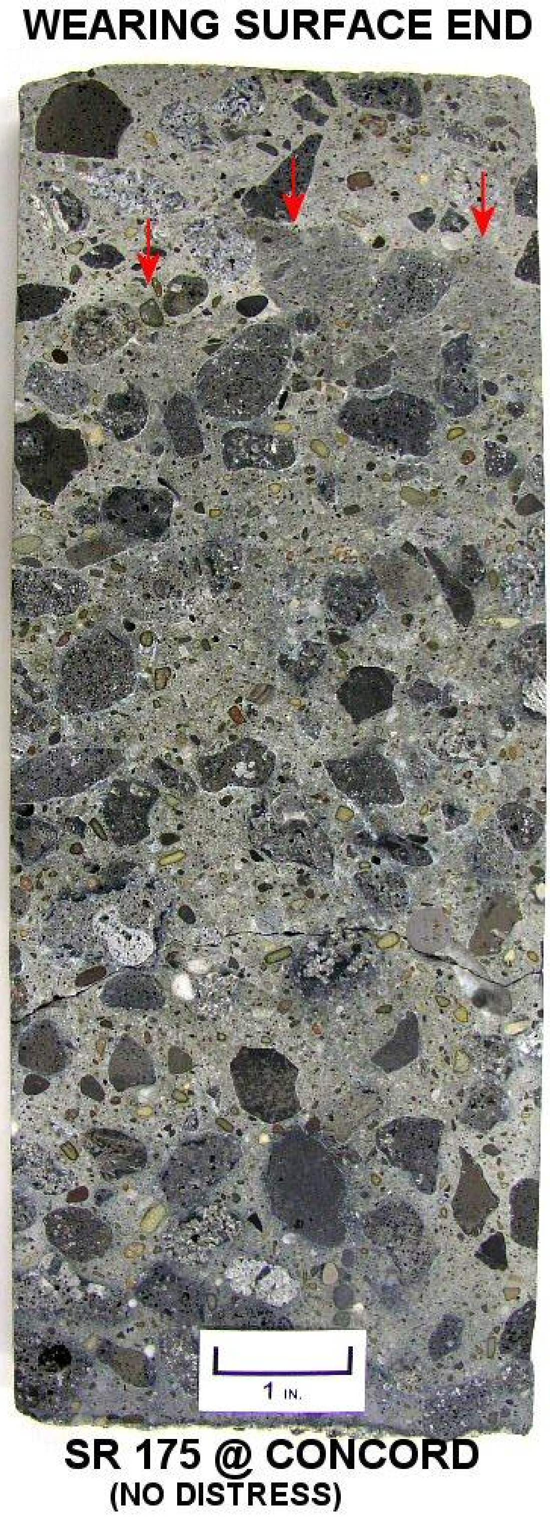

Figure 17. Lapped surface of Core 6 taken from a "No Distress" location on SR 175 @ Concord. The core is 10 ¼ in. long. On the freshly cut and lapped core the cementitious phase of the concrete below the arrows is green in color, while the portion of the core above the arrows is gray. The green coloration is due to the presence of sulfides derived from the slag aggregate that have not yet oxidized. Where the cementitious phase is gray (top 1 ½ to 2 in. [38 to 51 mm]) the sulfides have oxidized. The crack in the core occurred on handling after the lapping step.

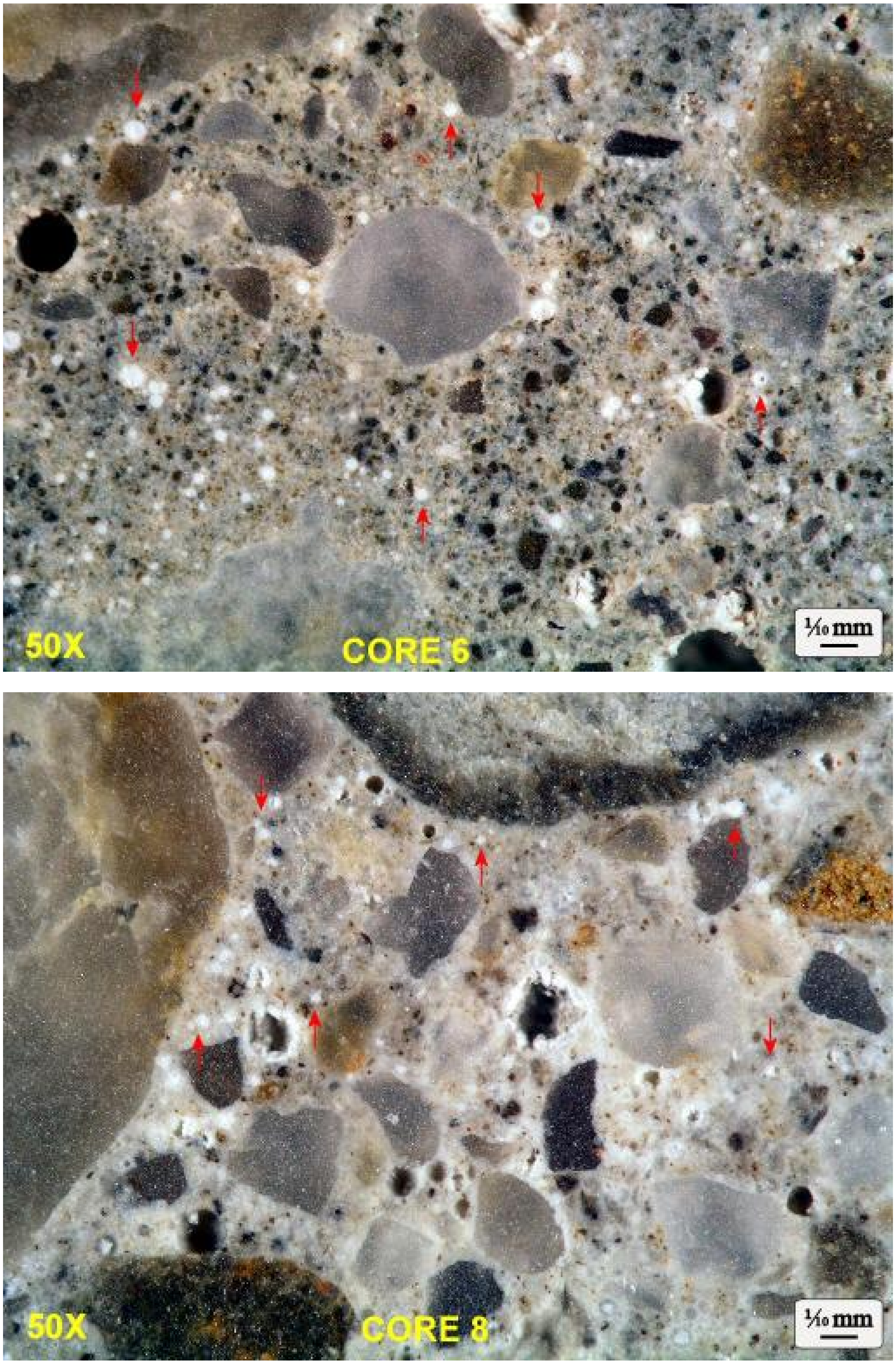

Figure 18. **Lapped surface views (50X) of Core 6 (taken from a No-Distress location on SR 175 @ Concord), and Core 8 (taken from a No-Distress location on SR 176), showing entrained air voids that have been fully or partially filled with ettringite (red arrows). The majority of voids less than 0.05 mm in diameter are completely filled. The view in the top photograph is 6 in. (15 cm) below the wearing surface. The view in the bottom photograph is 1 in. (25 mm) below the wearing surface.**

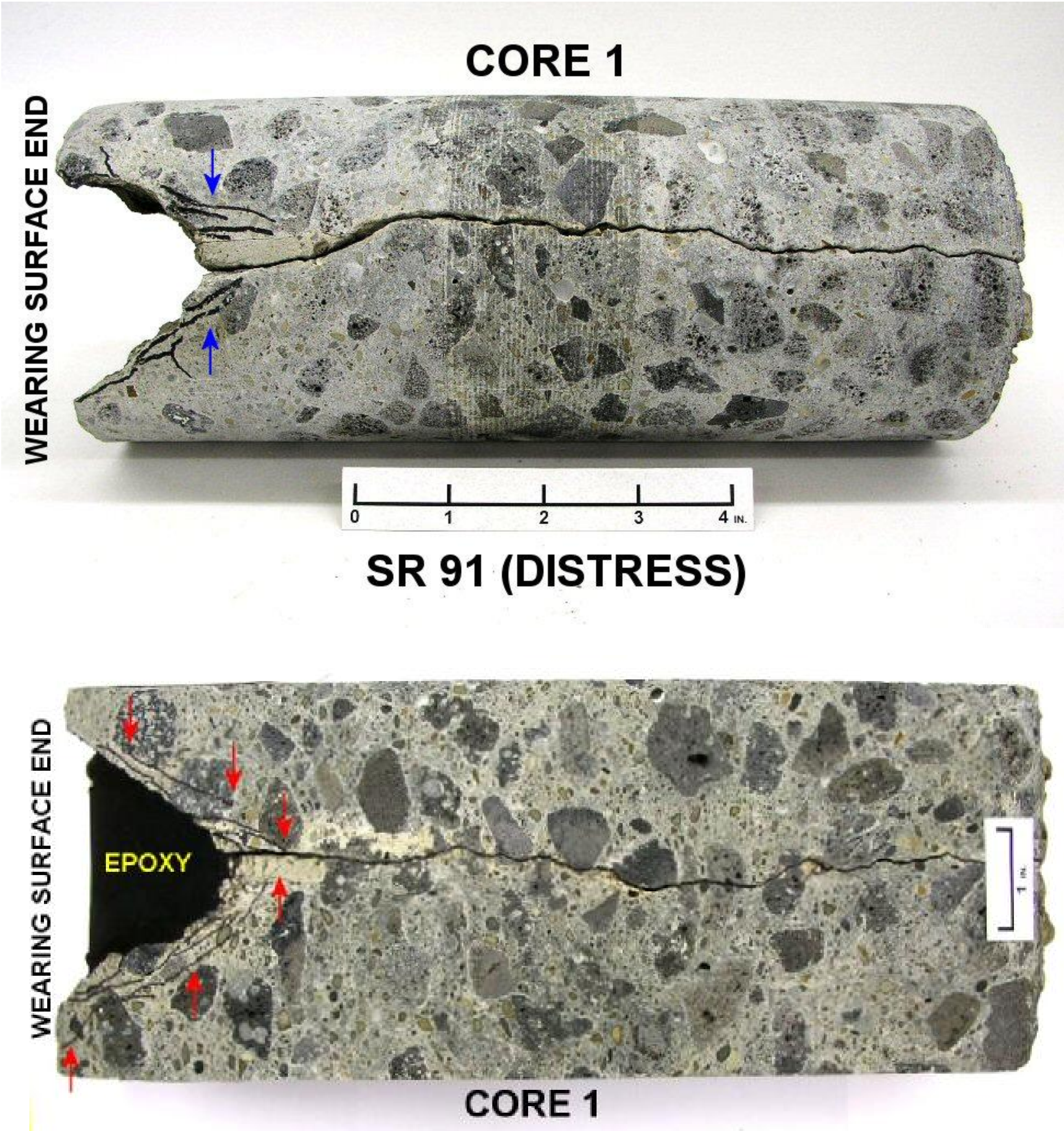

Figure 19 . Two views of Core 1 taken through a transverse control joint on State Route 91 at a "Distress" location. The top photograph shows the core in the as-received condition. The two core halves are held together by a steel mesh layer located 7 ½ in. (19 cm) below the wearing surface. The arrows point to cracks in the core that could be detected on the as-cored surfaces.). The bottom photograph is a view on a lapped surface of the core. Prior to saw-cutting and lapped the spall void and the crack fracture plane were filled with a low viscosity epoxy resin. Cracks in the concrete are marked with a black pen in both photographs.

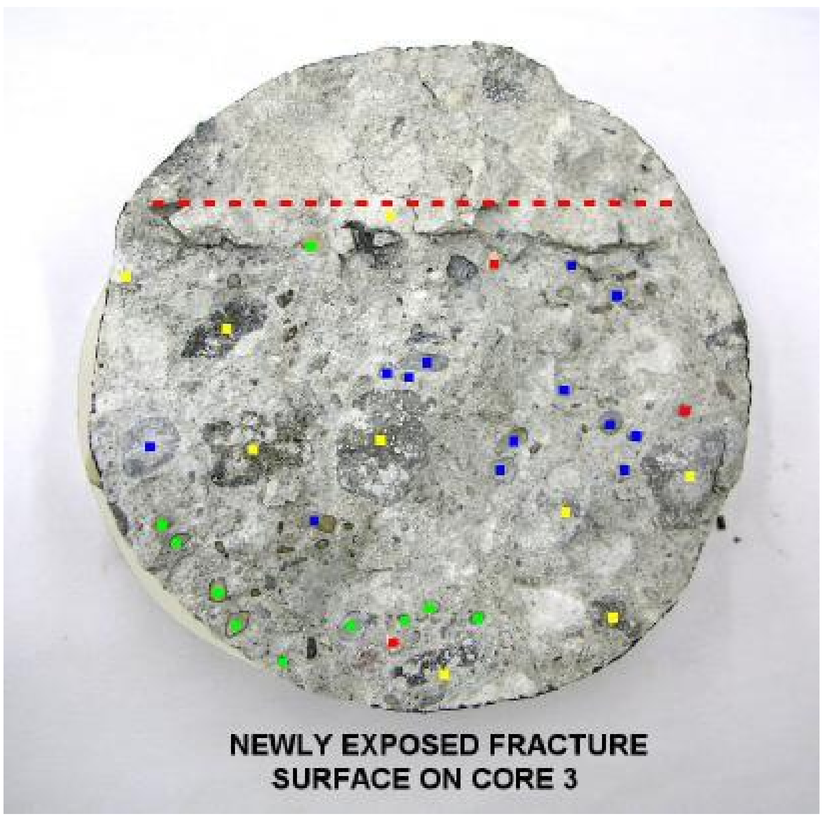

Figure 20. Two views of Core 3 taken from the "Distress" location on SR 175. In the top photograph sub-surface horizontal cracks in the core that could be detected on the as-cored surfaces are marked with a black marking pen. Subsequently, the not-yet-exposed fracture planes (blue arrows) were opened up by inserting the top of a small chisel and lightly tapping until the separation occurred. The bottom photograph shows a plan view of one of these newly-exposed pre-existing fractures surfaces. The colored dots are explained in the text of the report.

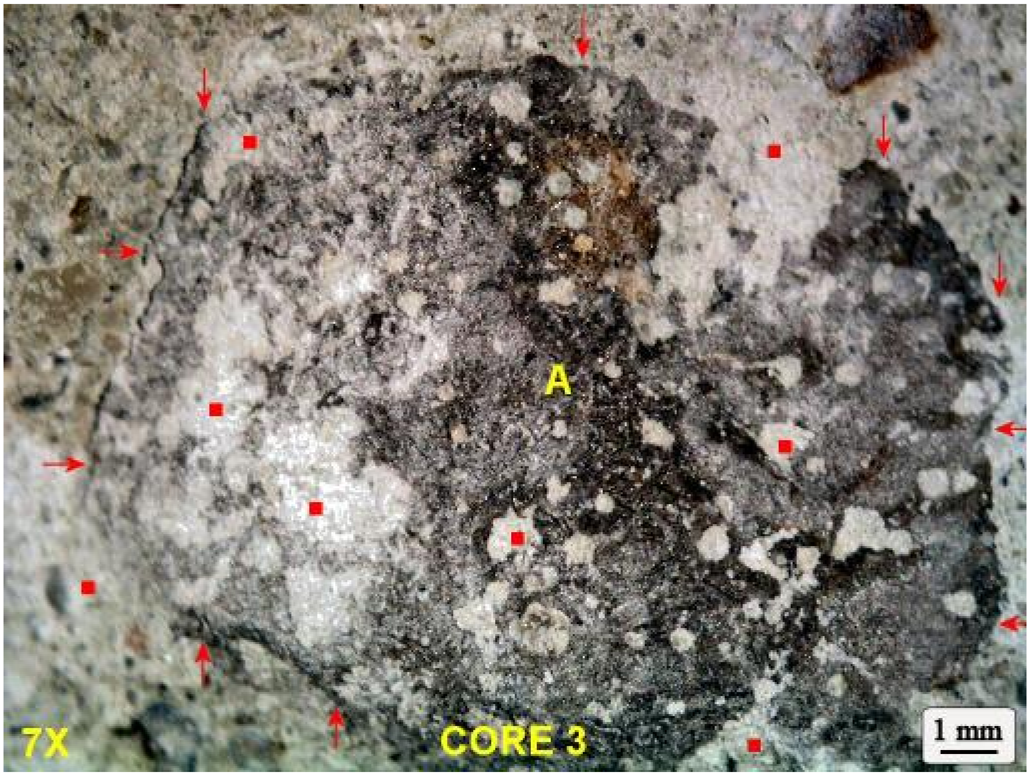

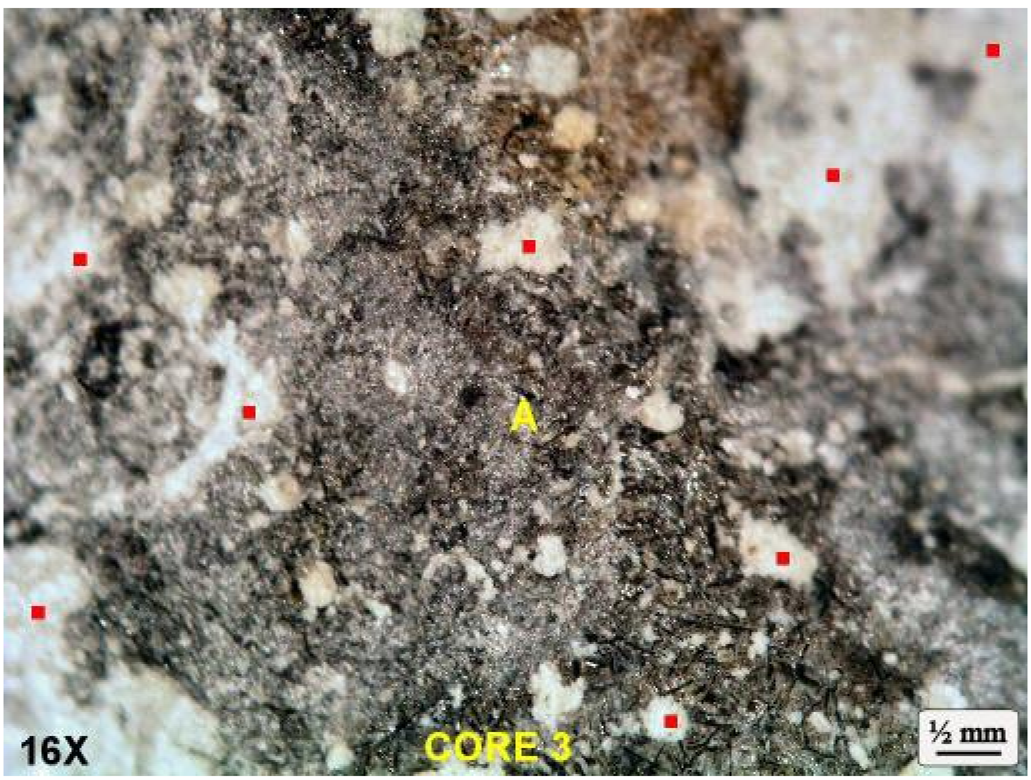

Figure 21. Enlarged views (7X and 16 X) of a newly-exposed, pre-existing horizontal fracture surface on Core 3 ("Distress" location – SR 175), showing a slag coarse aggregate particle (A) that has separated from the cementitious matrix of the concrete. The red arrows in the top photograph point to the cement paste/ aggregate boundary. The red dots are placed on remnants of the cement paste that remain adhered to the surface of the slag aggregate particle after it was pulled out of the matrix.

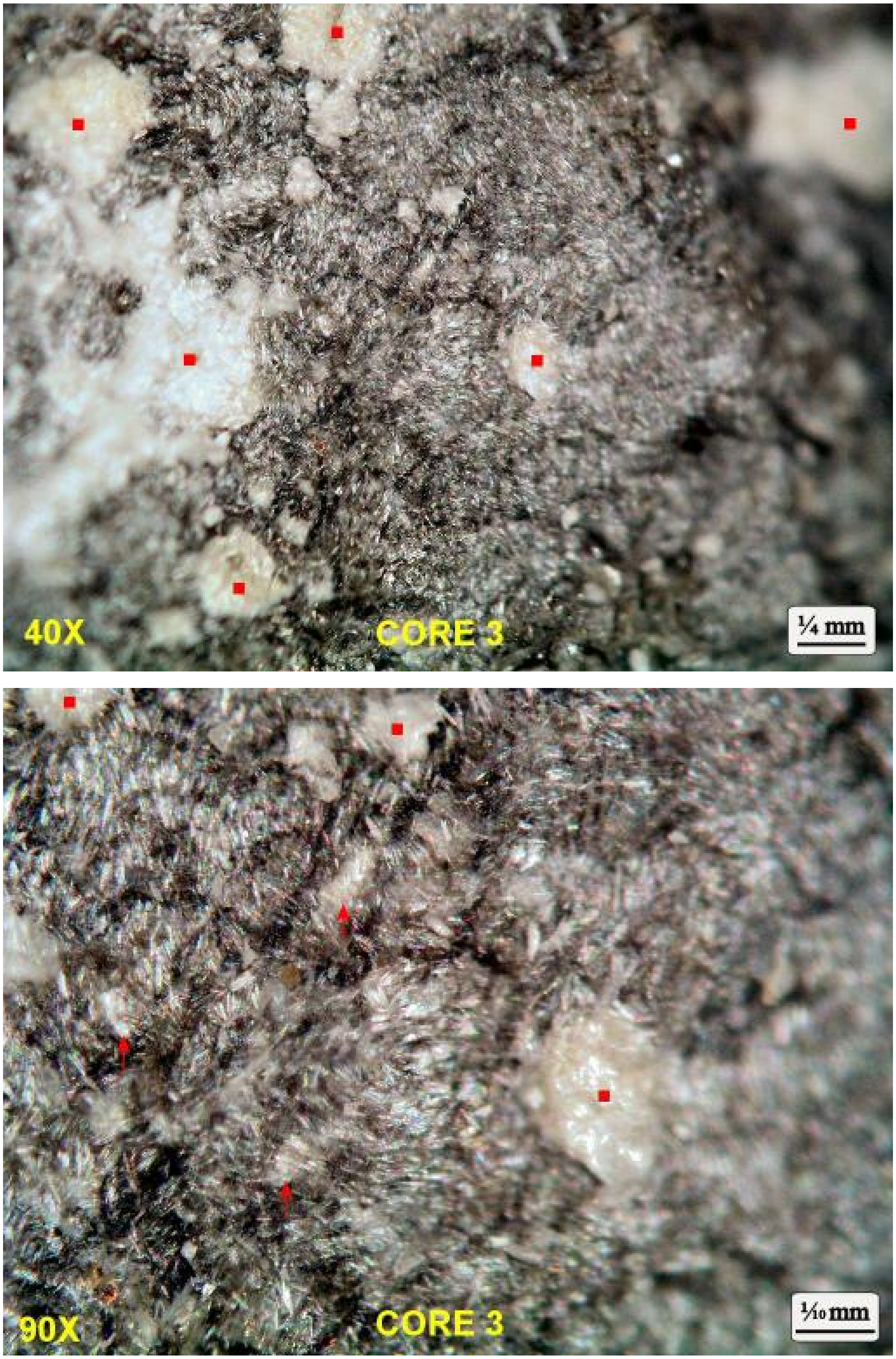

Figure 22. Enlarged views (40X and 90X) of the slag coarse aggregate particle shown in Figure 21 (from Core 3). The red dots are placed on remnants of the cement paste that remain adhered to the surface of the slag aggregate particle after it was pulled out of the matrix. The patches of cement paste contain interspersed acicular fibers, which are ettringite. The red arrows point to smaller regions of the cement paste. The entire surface of the slag aggregate particle is covered with a layer of acicular ettringite crystal laid down like jackstraws.

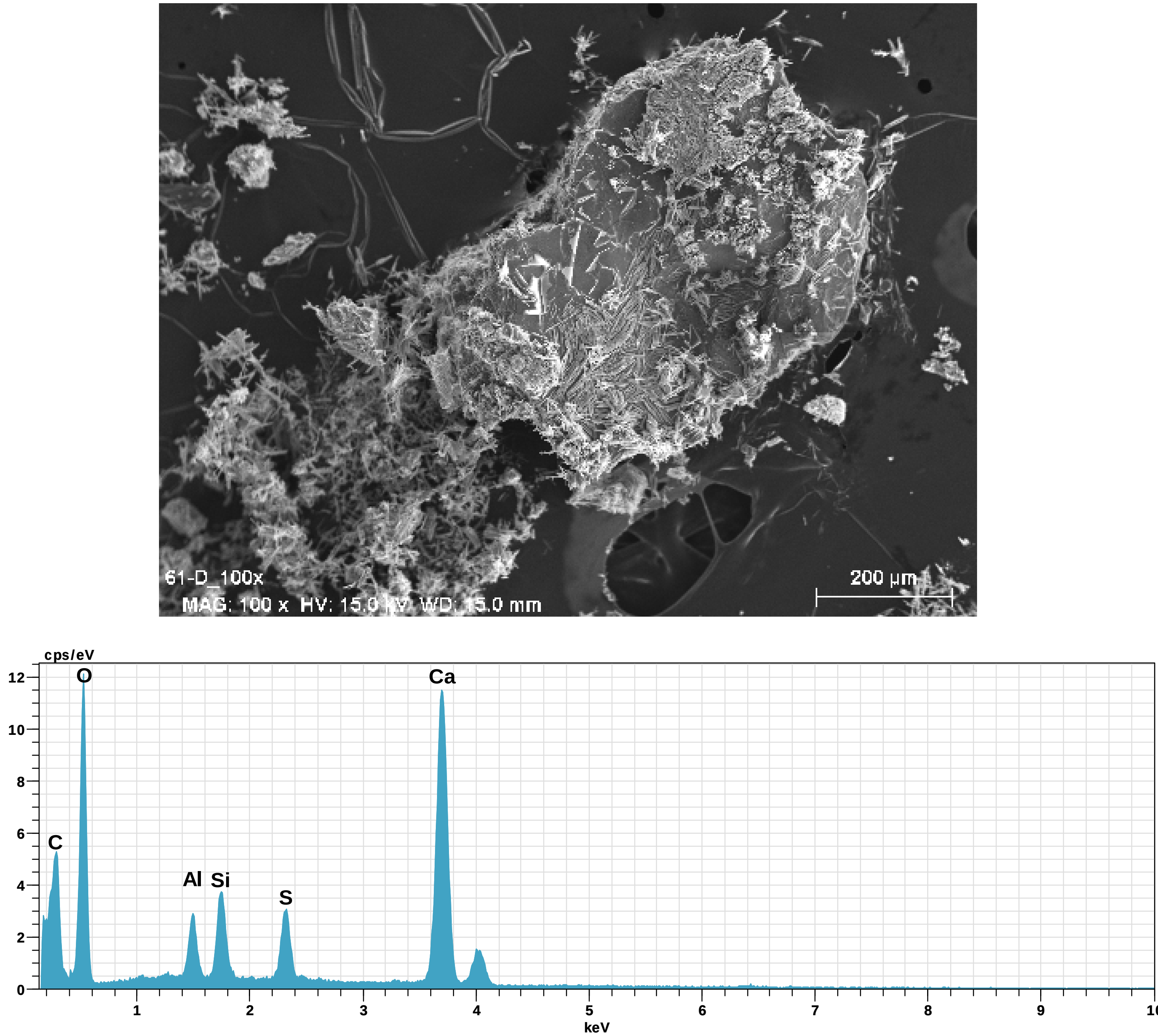

Figure 23. Scanning Electron Microscope (SEM) image and Energy Dispersive X-Ray Spectrography (EDX) spectrum (100X) of a sample of the material taken from the surface of the slag coarse aggregate particle shown in Figures 21 and 22. The material is a mixture of portland cement paste and ettringite.

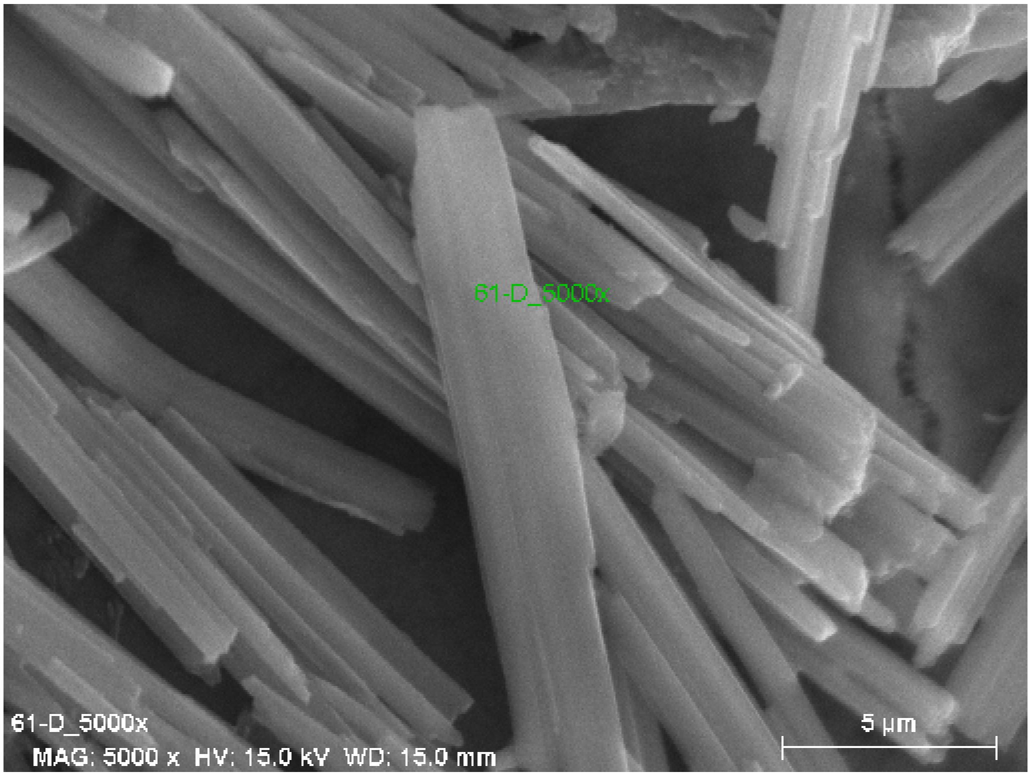

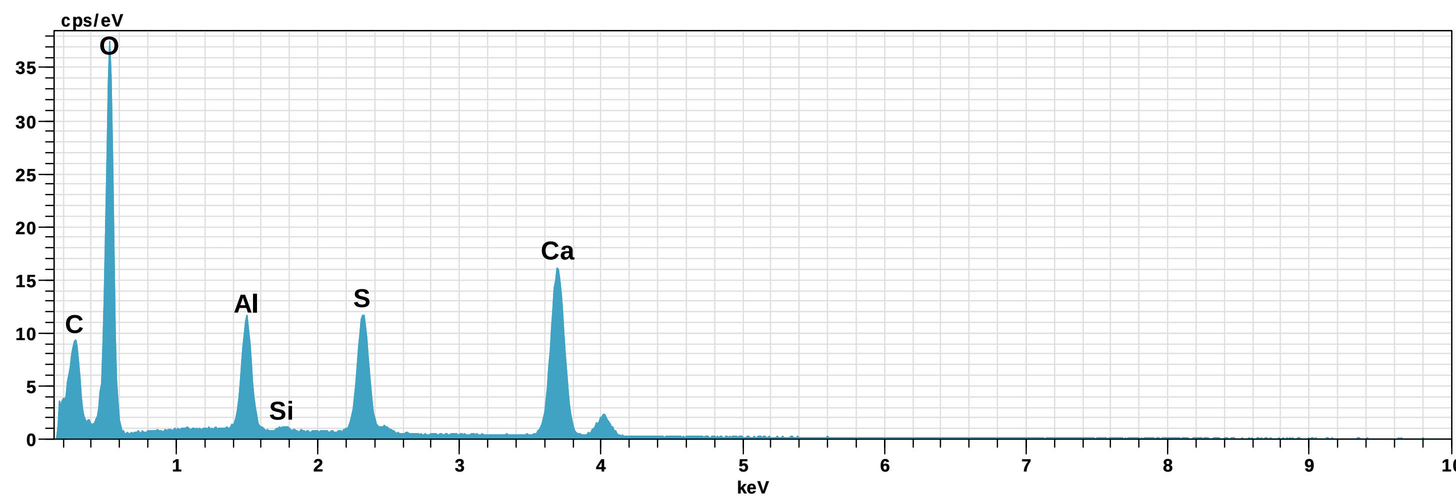

Figure 24. Scanning Electron Microscope (SEM) image and Energy Dispersive X-Ray Spectrography (EDX) spectrum (5000X) of a sample of the material taken from the surface of the slag coarse aggregate particle shown in Figures 21 and 22. The spot analysis on one of the acicular crystals shows that they are ettringite.

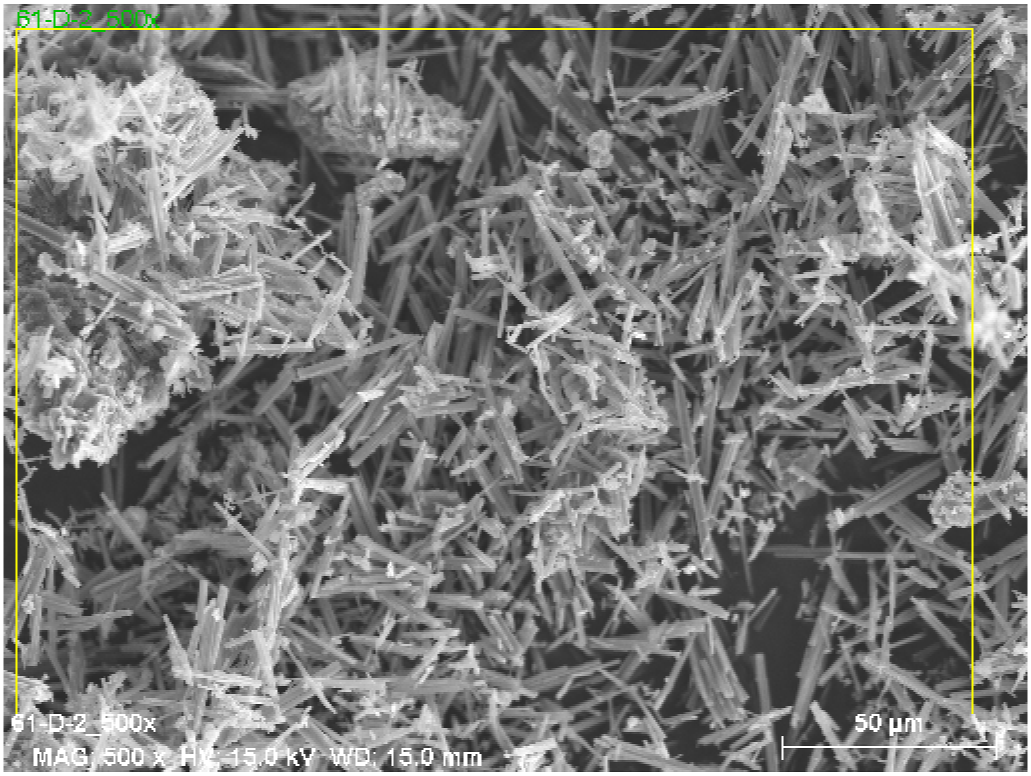

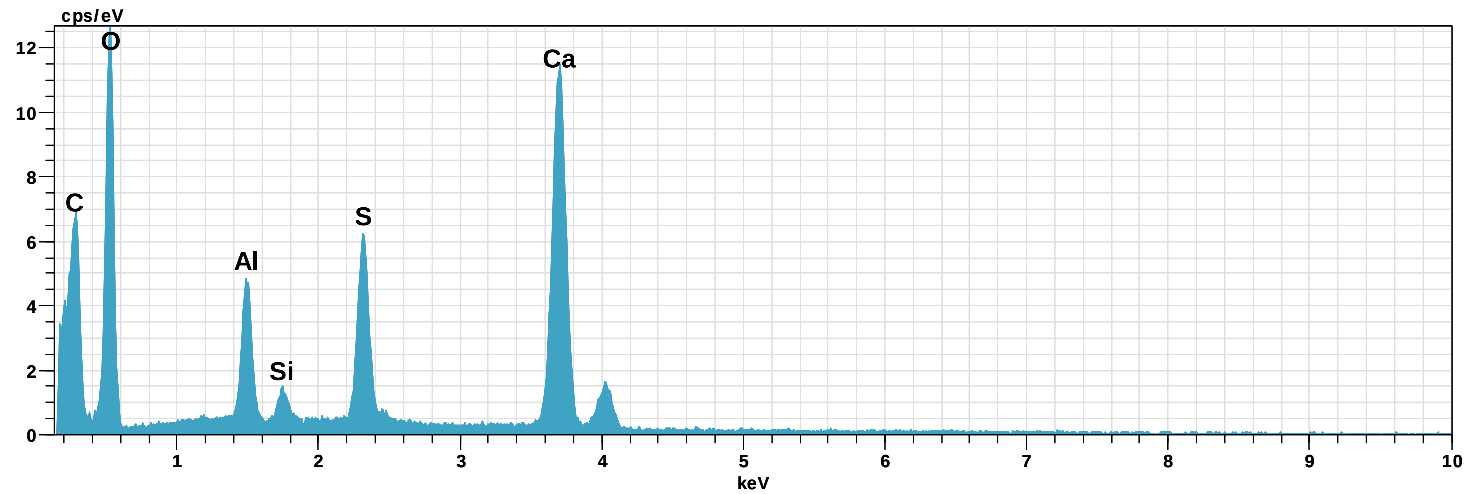

Figure 25. Scanning Electron Microscope (SEM) image and Energy Dispersive X-Ray Spectrography (EDX) spectrum (500X) of a sample of the material taken from the surface of the slag coarse aggregate particle shown in Figures 21 and 22. The individual acicular crystals are ettringite. The "clumped" material in the northwest corner of the photograph is a mixture of hydrated portland cement and ettringite.

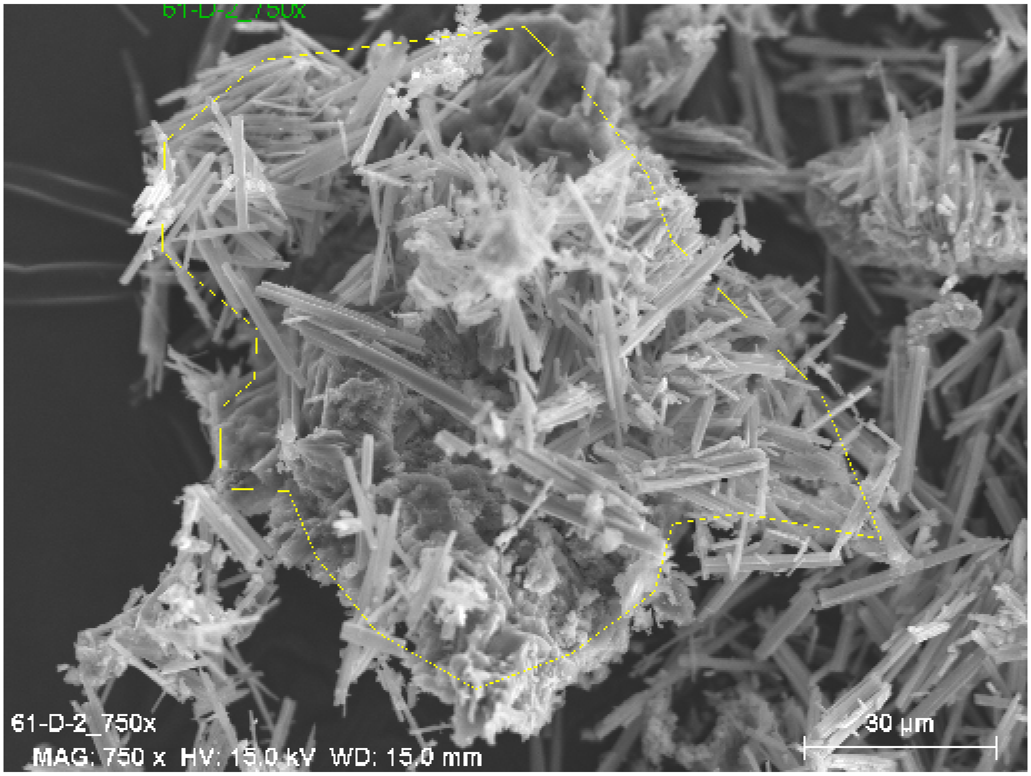

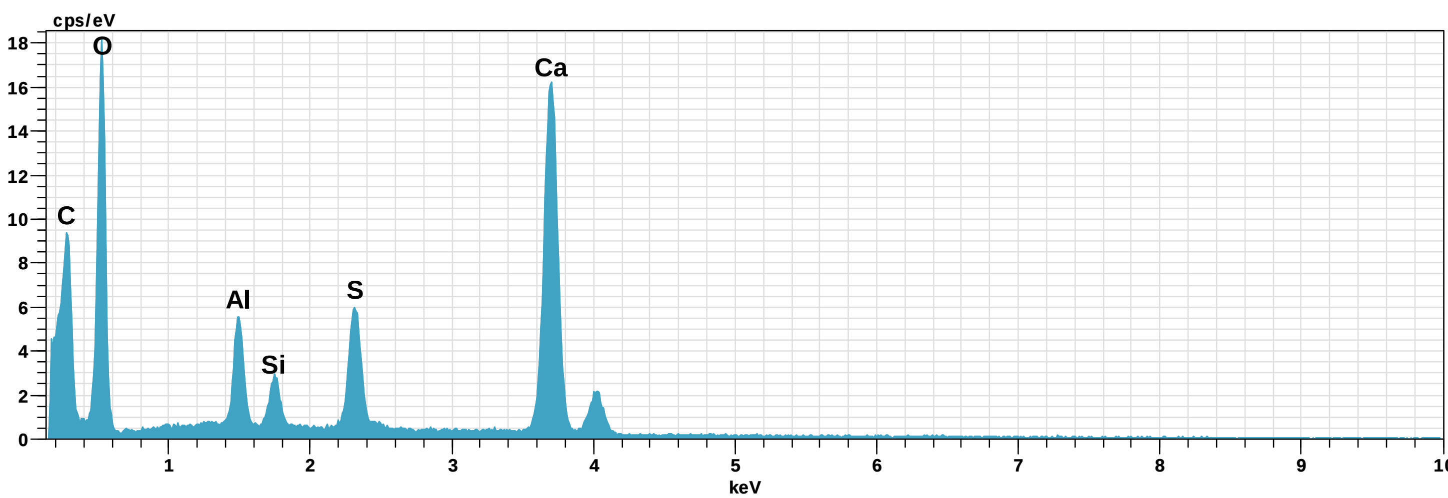

Figure 26. Scanning Electron Microscope (SEM) image and Energy Dispersive X-Ray Spectrography (EDX) spectrum (750X) of the "clumped" material in the northwest corner of the SEM image shown in Figure 25. The individual acicular crystals are ettringite. The matrix material holding the fiber bundle together is hydrated portland cement paste as shown in Figures 27 and 28.

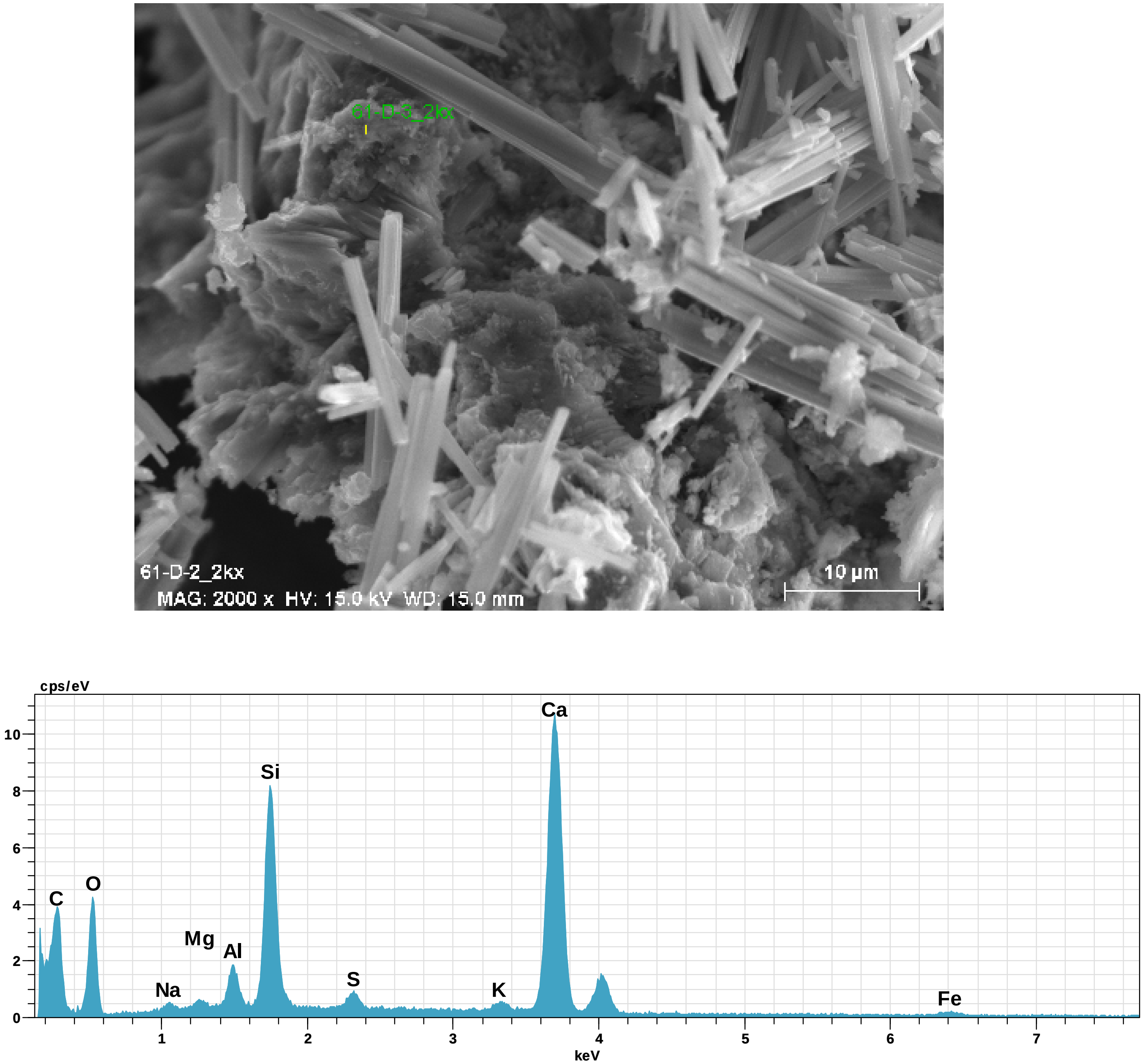

Figure 27. Scanning Electron Microscope (SEM) image and Energy Dispersive X-Ray Spectrography (EDX) spectrum at a magnification of 2000X of the "clumped" material in the northwest corner of the SEM image shown in Figure 25 and in Figure 26. The individual acicular crystals are ettringite. The matrix material holding the fiber bundle together is hydrated portland cement paste.

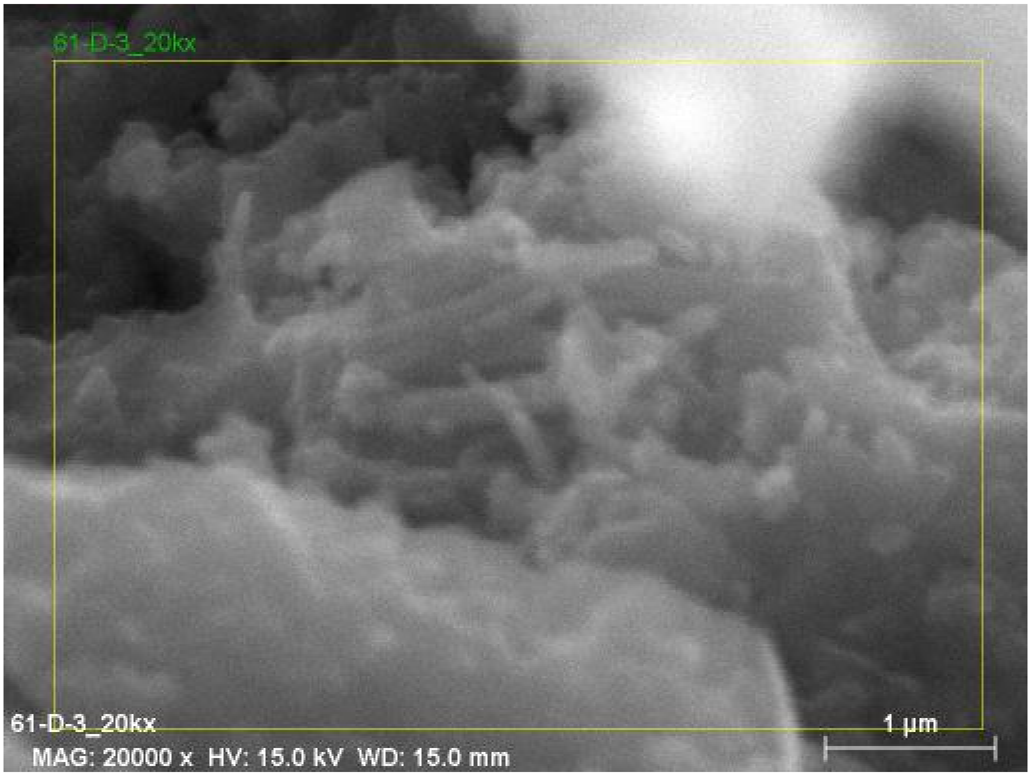

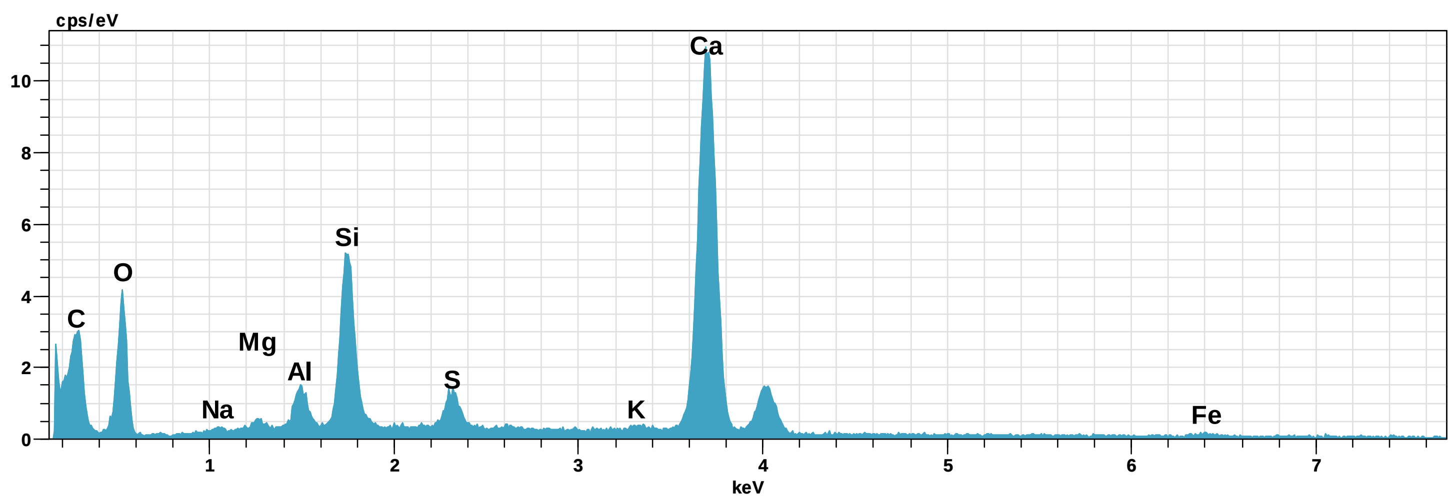

Figure 28. Scanning Electron Microscope (SEM) image and Energy Dispersive X-Ray Spectrography (EDX) spectrum at a magnification of 20,000X on the “matrix” phase of the “clumped” material in the northwest corner of the SEM image shown in Figure 25, 26, and 27. The EDS signature is primarily for hydrated portland cement. Acicular crystals bound up in the matrix are ettringite.

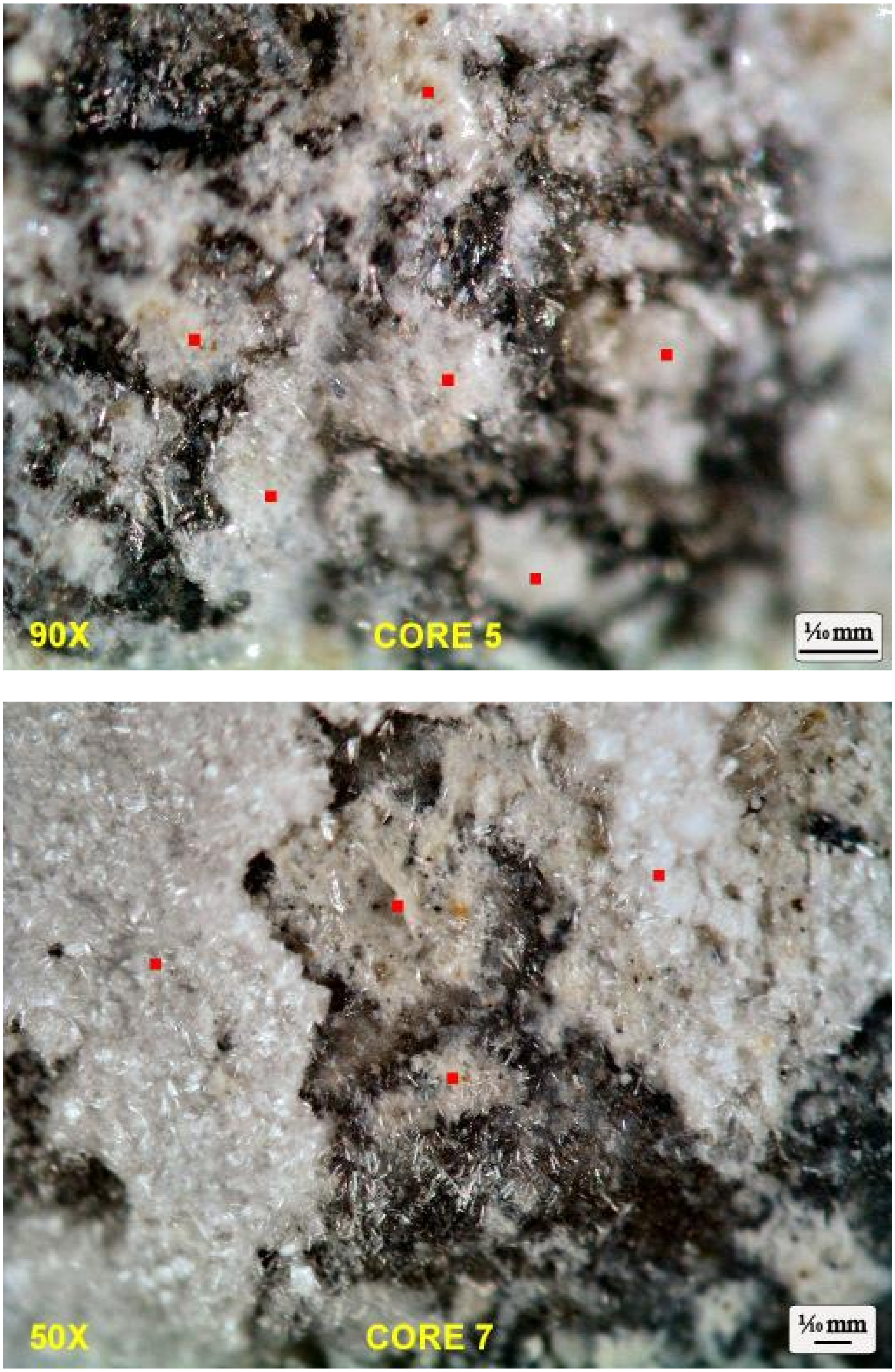

Figure 29. Enlarged views of slag coarse aggregate particles (dark areas) pulled from the cementitious matrix along a pre-existing sub-surface horizontal fracture surface in Core 5 (SR 175 @ Concord – "Distress location) and Core 7 (SR 176 – "Distress location), showing microstructural features associated with destructive internal sulfate attack in these pavement concretes. The red dots are placed on remnants of the cement paste that remained adhered to the slag particle after it was pulled from the matrix. The acicular crystals are ettringite fibers.

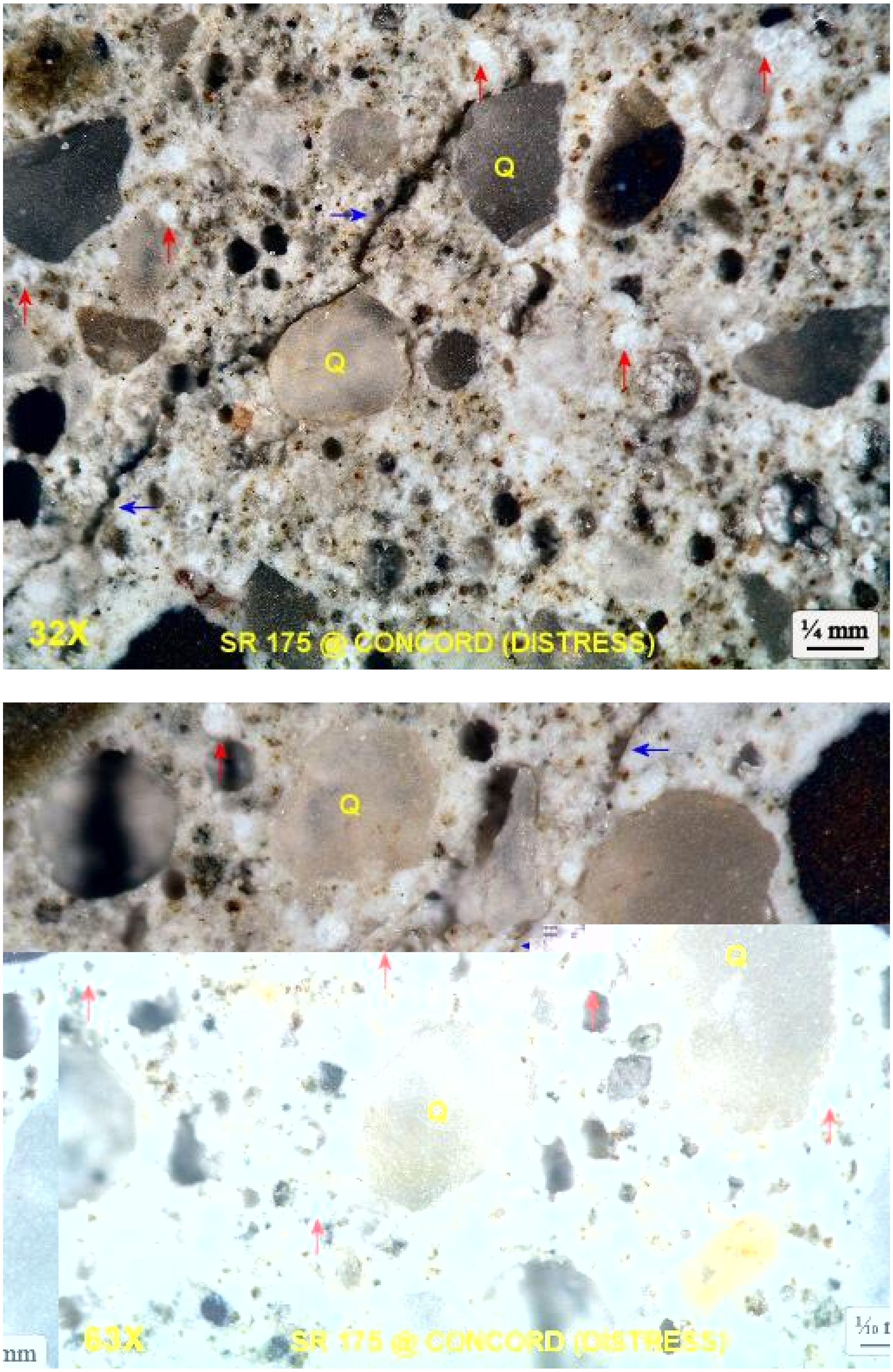

Figure 30. Two enlarged views of a lapped surface of Core 5 (SR 175 @ Concord (Distress) showing latent cracking in the concrete (blue arrows). The tight cracks are within the cementitious phase of the concrete and pass around quartz fine aggregate particles (Q). The red arrows point to a few of the numerous small diameter entrained air voids that are completely or partially filled with ettringite.

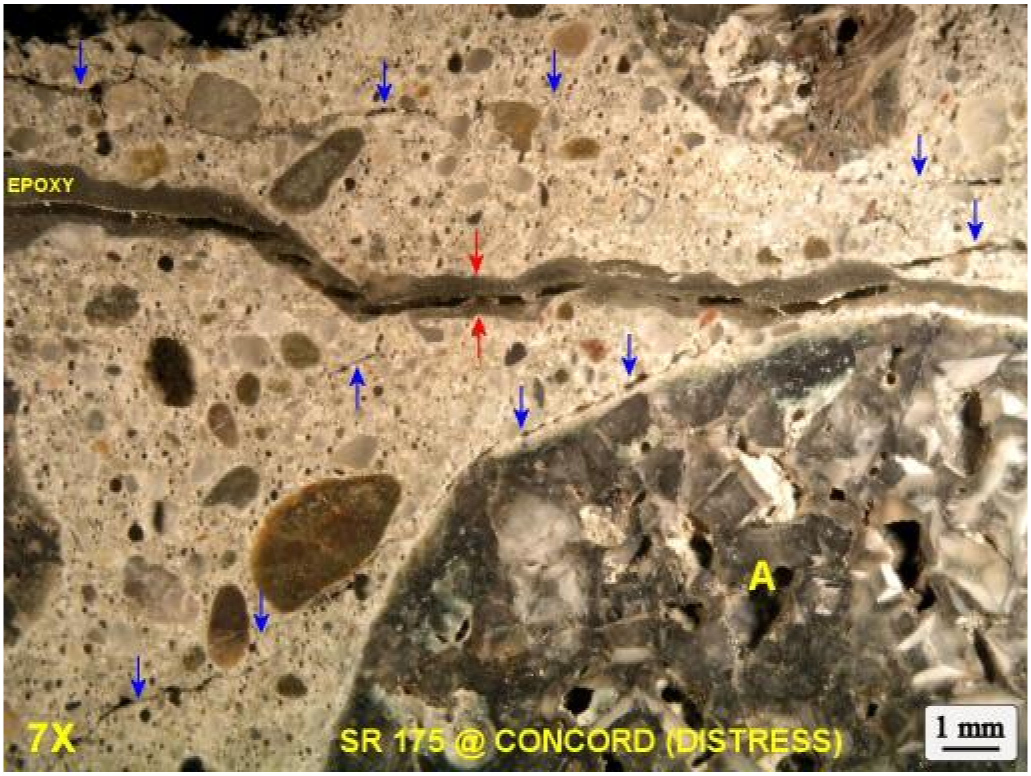

Figure 31. Two enlarged views of a lapped surface of Core 5 (SR 175 @ Concord (Distress) showing the condition of the epoxy adhesive following two weeks of storage of the concrete in a sealed plastic bag. The red arrows show the width of the epoxy seam (ca. 0.5 mm). The epoxy layer has been literally pulled apart resulting in tears within the epoxy layer (yellow dots). The blue arrows point to cracks within the cementitious matrix of the concrete. The green arrows point to a few of the numerous small air voids that have been in-filled with ettringite.

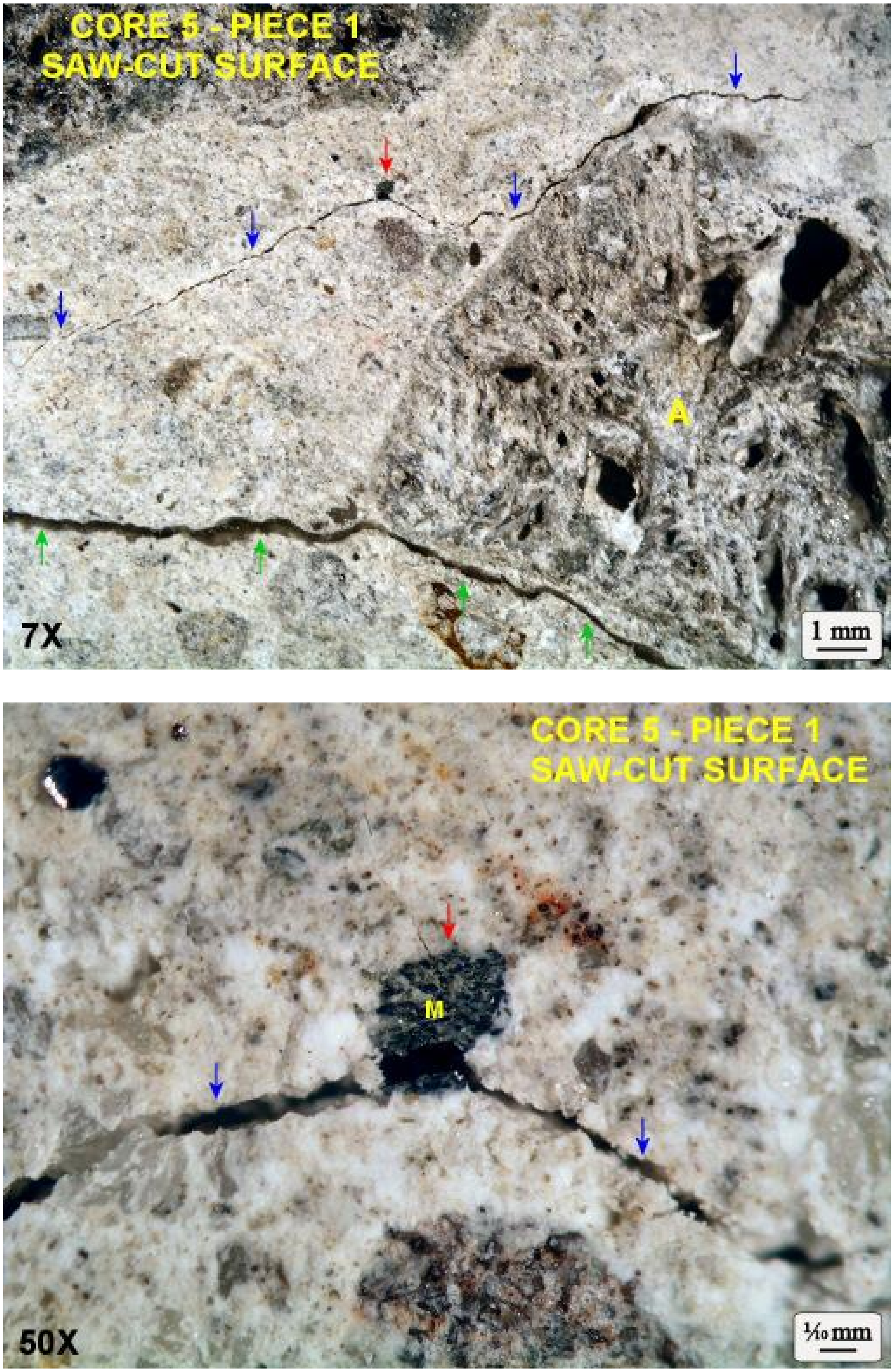

Figure 32. **Two enlarged views (7X and 50X) of a saw-cut surface of Piece 1 of Core 5 at a location about 2 in. below the wearing surface. The green arrows in the top photograph point to the pre-existing horizontal crack in Core 5 which is filled with epoxy. The blue arrows point to a crack that was formed in the Core Piece sometime during the 19 day period that it was stored in a sealed plastic bag. The red arrow points to a small mafic mineral fine aggregate particle in the crack fracture plane.**

Figure 33. Two enlarged views (16X) at the same location on the lapped surface of Piece 1 of Core 5 at two different times. The top photograph was taken on April 29, 2010 right after the completion of the lapping operation. The bottom photograph was taken on May 18, 2010 after the lapped core piece had been in a sealed plastic bag (for 19 days). The green arrows point to the pre-existing horizontal crack in Core 5 which is filled with epoxy. During the 19 day storage period the concrete expanded, which enlarged the width of the cracks and which created tears in the epoxy seam (yellow arrows).

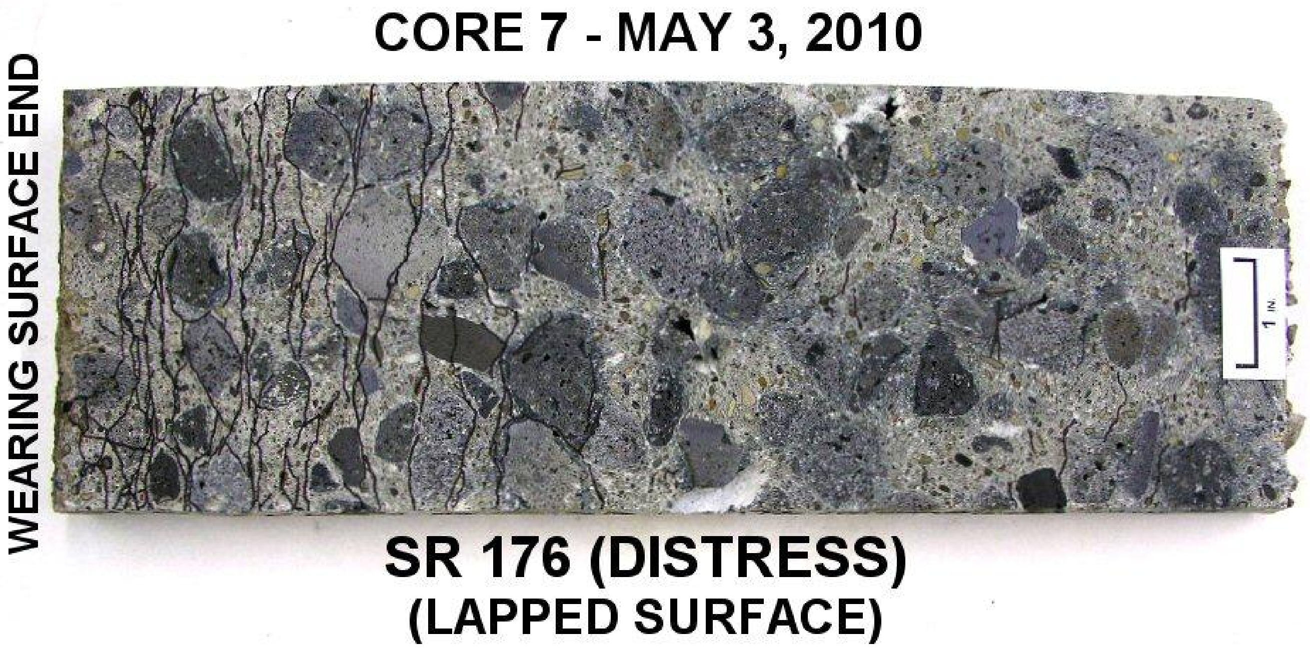

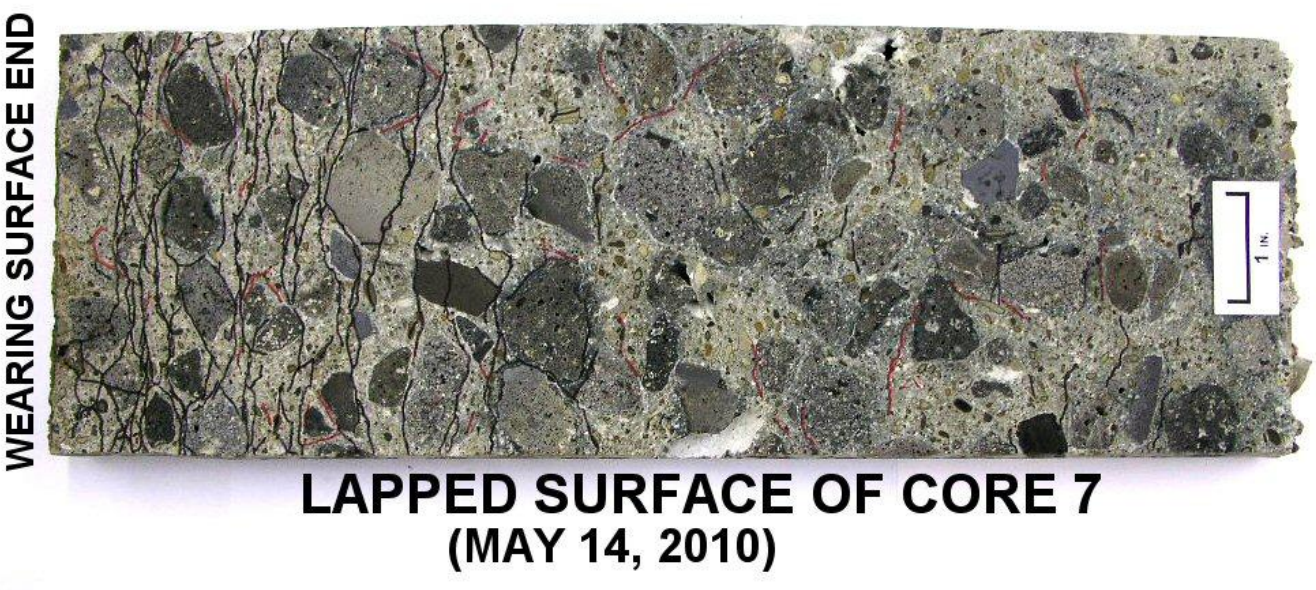

Figure 34. Two views of the same lapped surface of Piece 1 of Core 7 on two different dates. Sub-surface horizontal cracks that were present in the core piece right after lapping on May 3, 2010 are marked in black in the top photograph. New cracks that formed in the concrete during the 11 day storage period in a sealed plastic bag are marked in red in the bottom photograph.

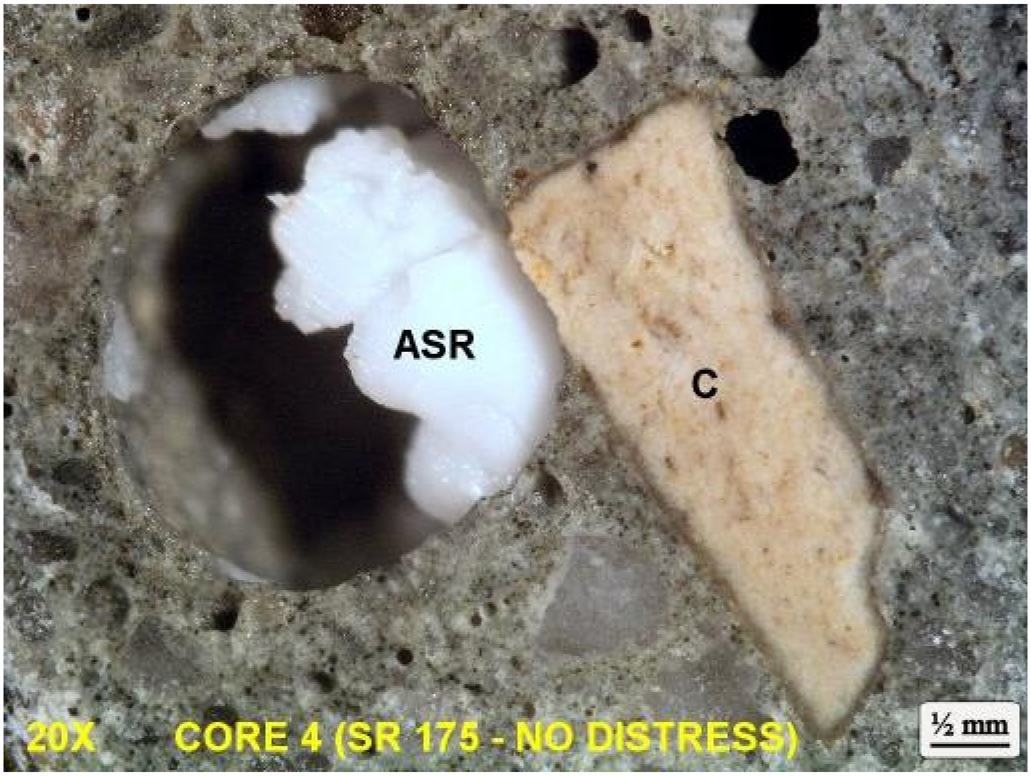

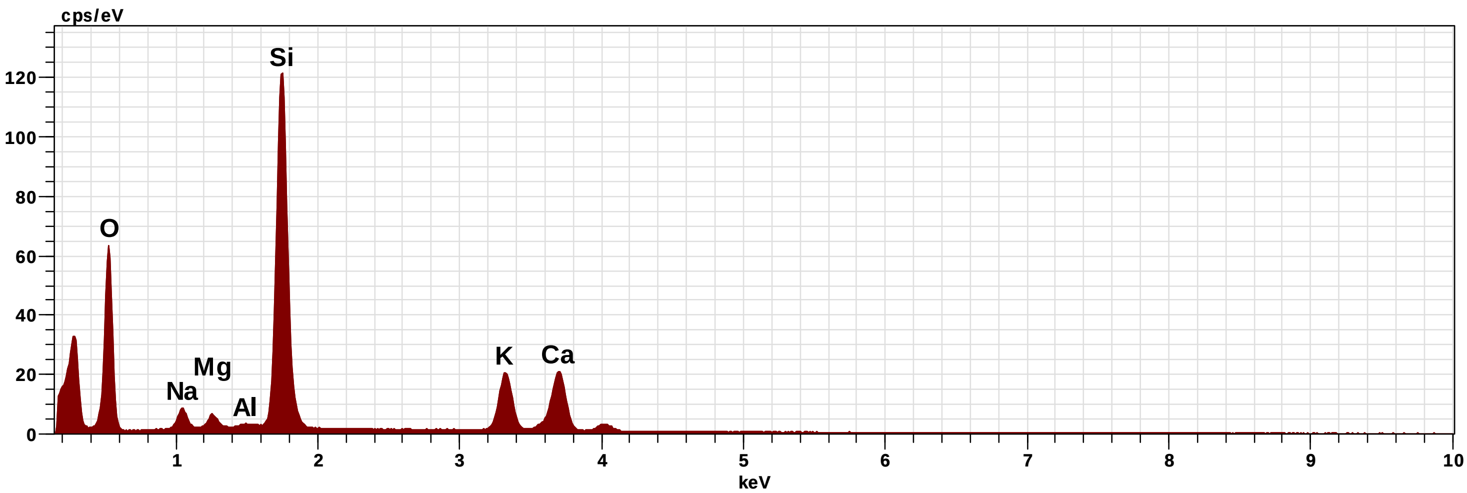

Figure 35. Enlarged view (20X) of a fresh saw-cut surface of Core 4 taken from State Route 175 at a "No-Distress" location. The chert fine aggregate particle (C) has undergone alkali-silica reaction activity and ASR gel has been deposited in an air void adjacent to the particle. The gel was excavated from the air void for the EDX elemental analysis, which was obtained at a magnification of 200X (Scan Number 58-B3).

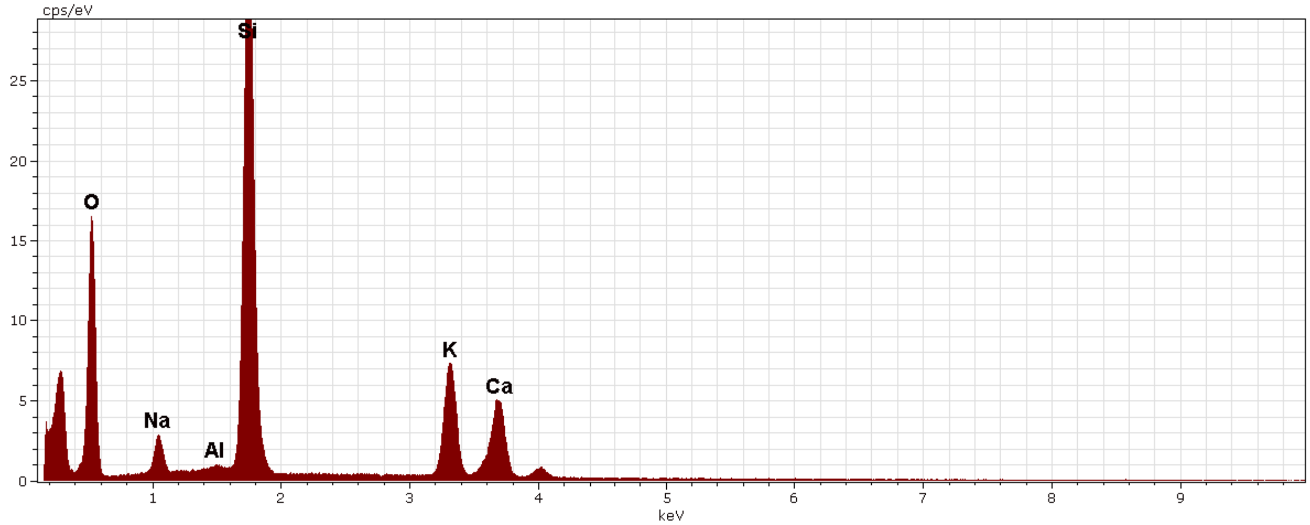

Figure 36. Enlarged view (10X) of an as-cored surface of Core 8 taken from State Route 176 at a "No-Distress" location. A siltstone fine aggregate particle (S) has undergone alkali-silica reaction activity and ASR gel (A) has been deposited in an air void adjacent to the particle. The gel was excavated from the air void for the EDX elemental analysis, which was obtained at a magnification of 1000X (Scan Number 59-C2).

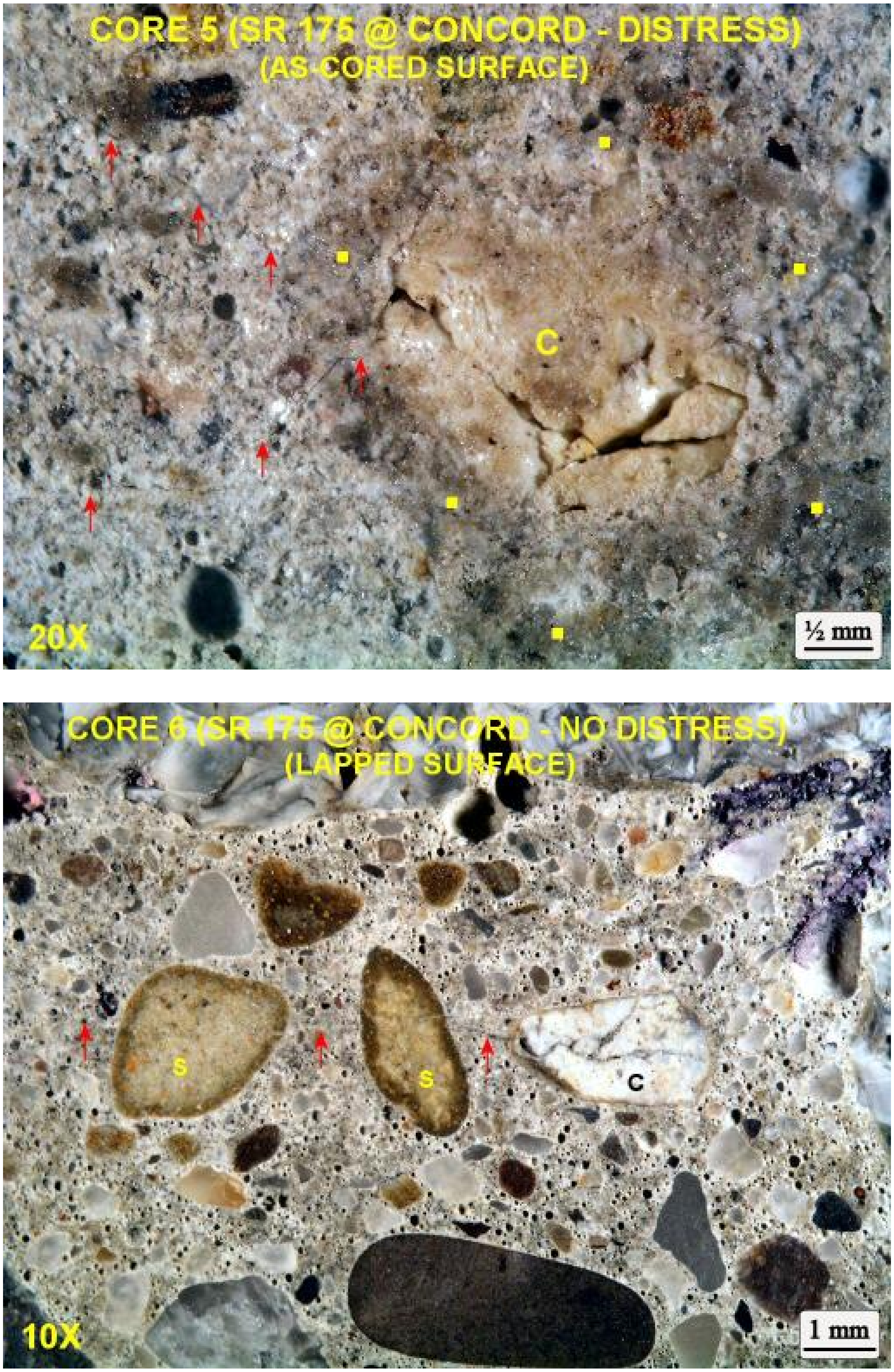

Figure 37. Enlarged views of chert fine aggregate particles (C) that have undergone alkali-silica reaction (ASR) activity in the pavement cores taken from State Route 175 @ Concord. In the top photograph the yellow dots are placed on areas of the cementitious matrix that is darkened due to infiltration of ASR gel. The red arrows in both photographs point to cracks in the cementitious matrix associated with the reaction activity. In the bottom photograph the crack originating in the chert particle passes through two siltstone fine aggregate particles (S).

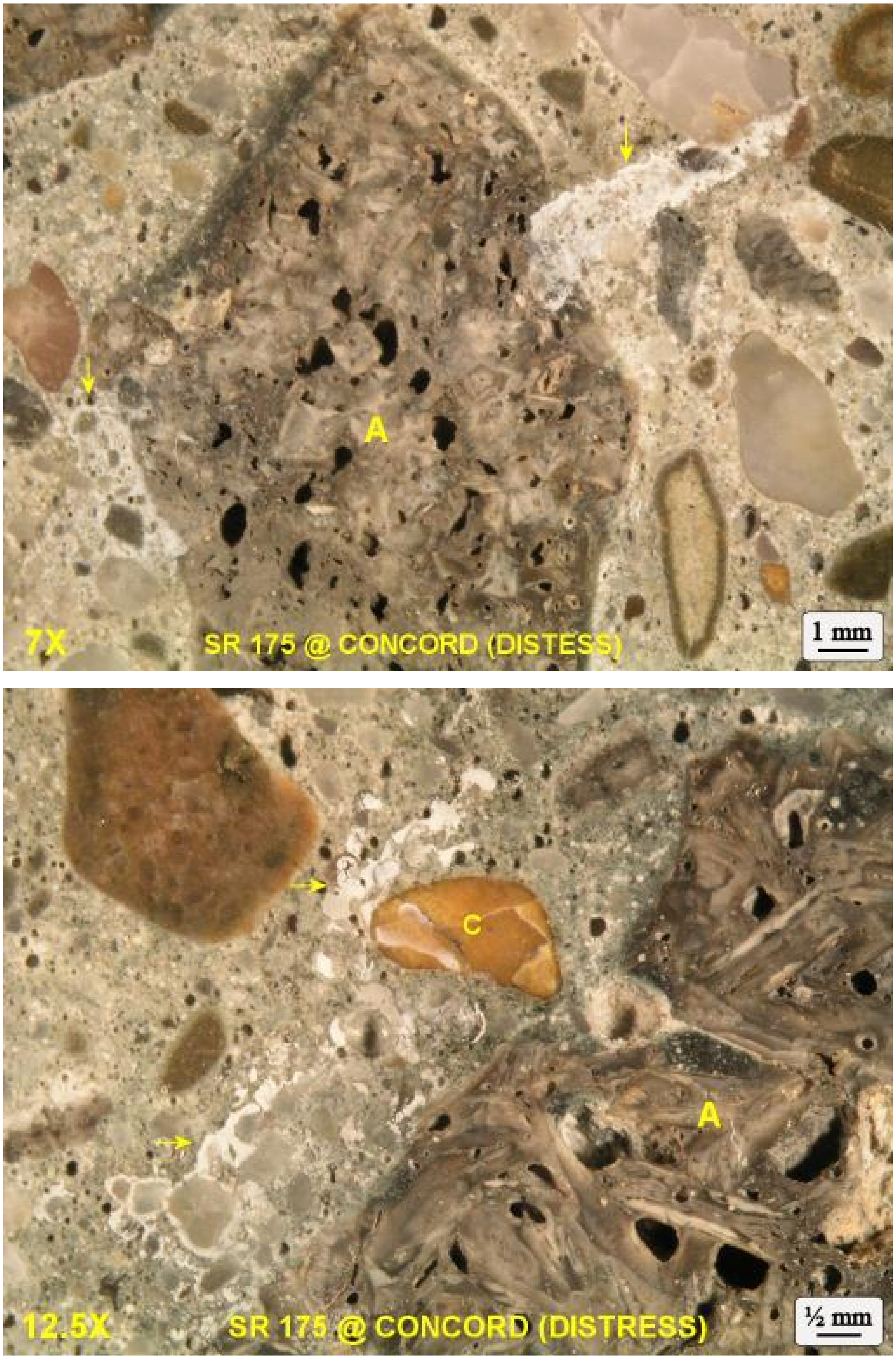

Figure 38. Lapped surfaces of Core 5 taken from SR 175 @ Concord (Distress) showing ASR gel exudate (arrows) deposited on the surfaces following a period of air drying. In the top photograph the exudate is adjacent to a slag coarse aggregate particle (A). In the bottom photograph the exudate is adjacent to a slag coarse aggregate particle (A) and a chert particle (C).

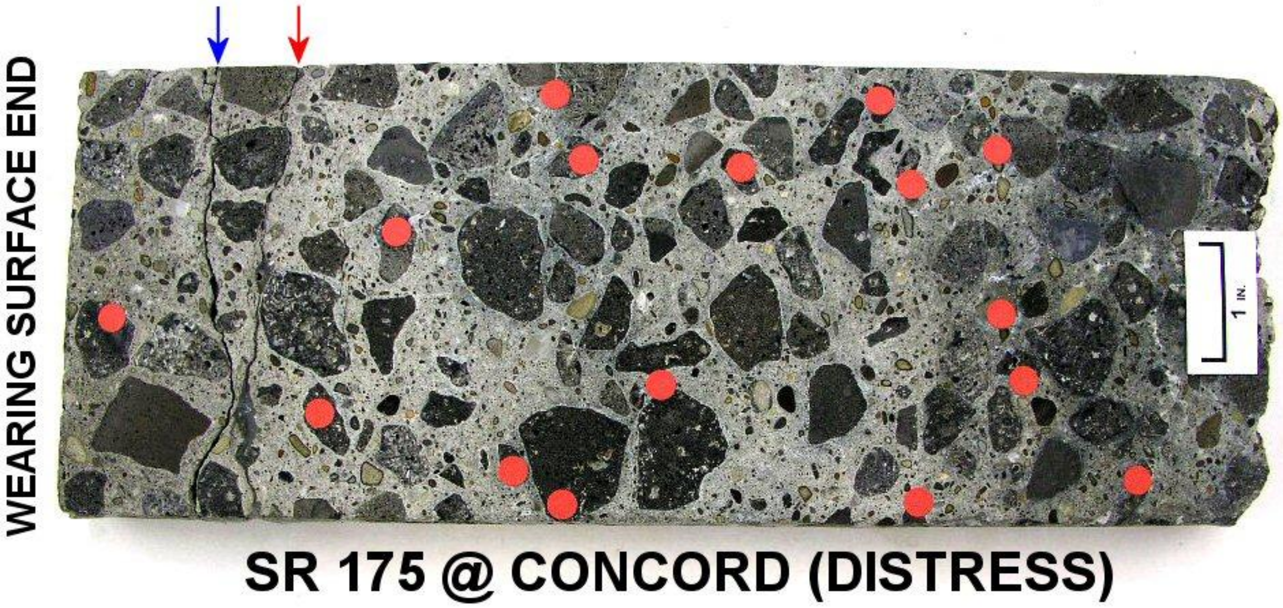

CORE 5

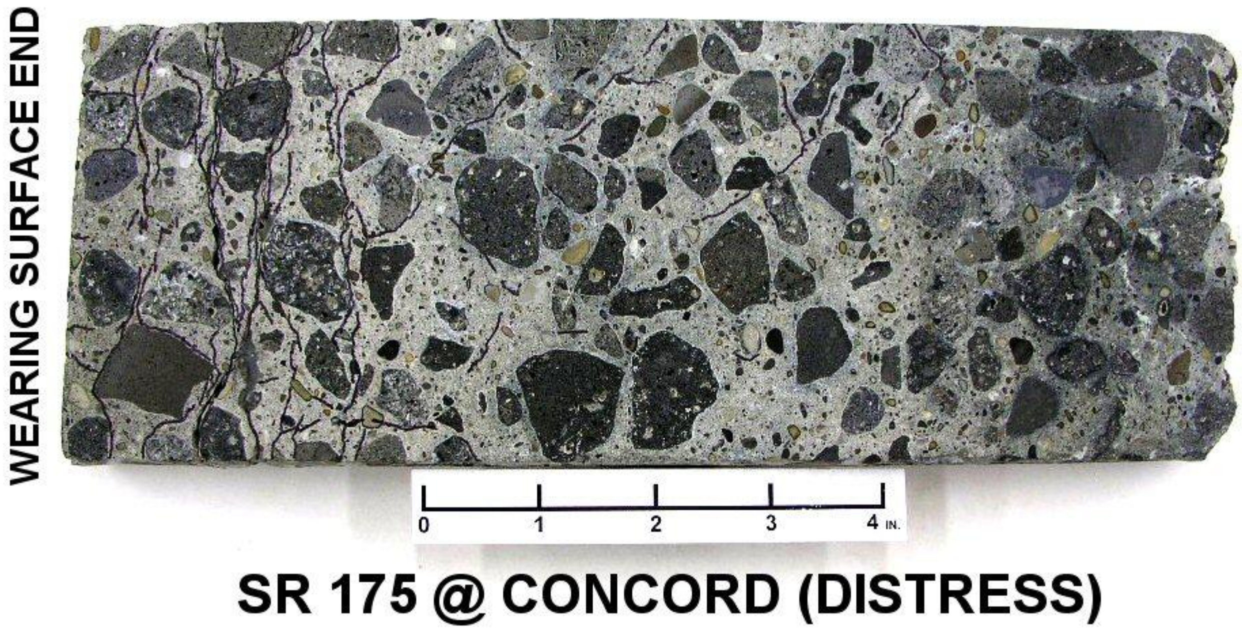

Figure 39. Two views of a lapped surface of Core 5: SR 175 @ Concord (Distress). The red dots in the top photograph are at sites where white patches of ASR gel exudate have been deposited on the surface during drying of the piece. The red arrow points to the full core width crack that was present in the as-received core. The blue arrow points to a full core width fracture that was formed at the end of the lapping operation in a pre-existing crack. The bottom photograph shows the lapped surface of the core slab following 2 weeks storage in a moist condition in a sealed plastic bag. Cracks in the core piece at this time are marked with a black marking pen.

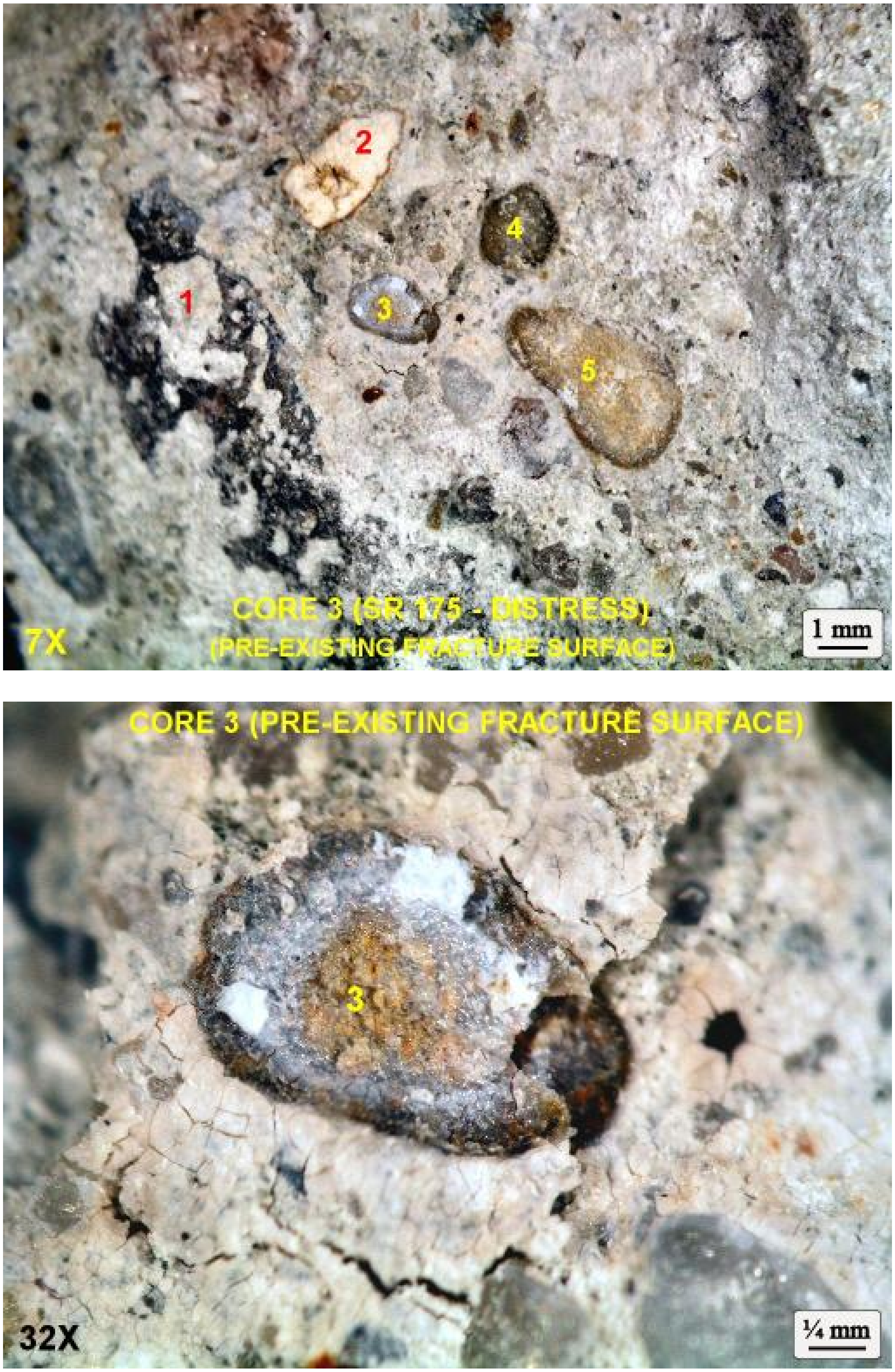

Figure 40. Two views of a pre-existing horizontal fracture surface (freshly exposed) in the top 2 in. thickness of Core 3. Core 3 was taken from SR 175 at a Distress location. Site 1 is a slag coarse aggregate particle. Site 2 is a chert fine aggregate particle. Sites 3, 4, and 5 are siltstone fine aggregate particles.

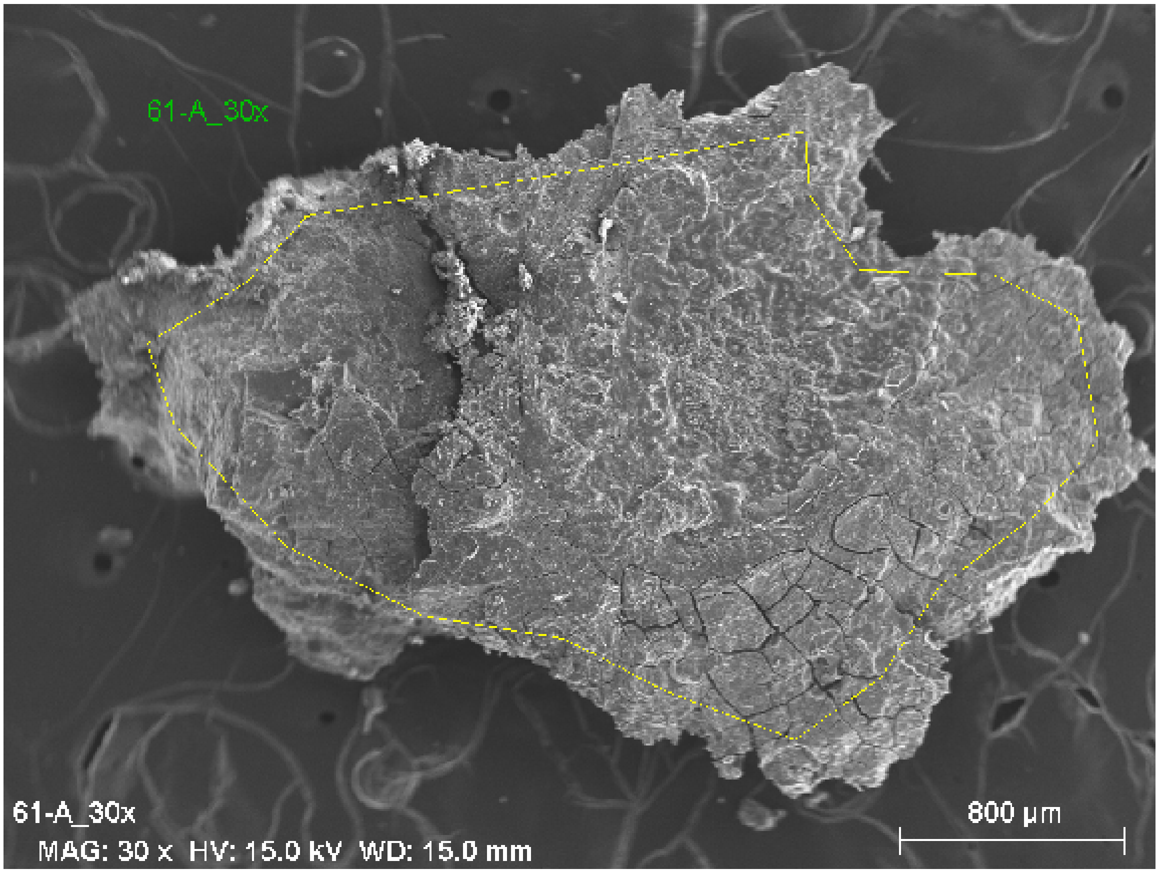

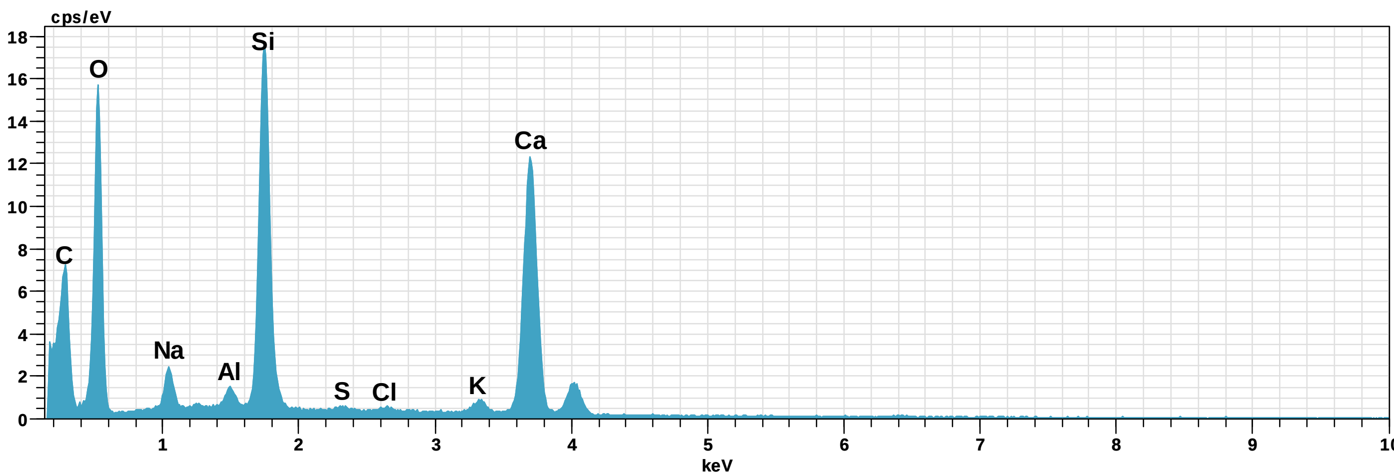

Figure 41. SEM image and EDS spectrum (30X) of Siltstone Particle #3 as shown in Figure 40. The particle was taken from a pre-existing fracture surface of Core 3 as shown in Figure 20. Core 3 was taken on State Route 175 at a "Distress" location. Contributions to the EDX spectrum include (1) constituents of the siltstone particle, (2) ASR gel, (3) ettringite, and (4) hydrated portland cement.

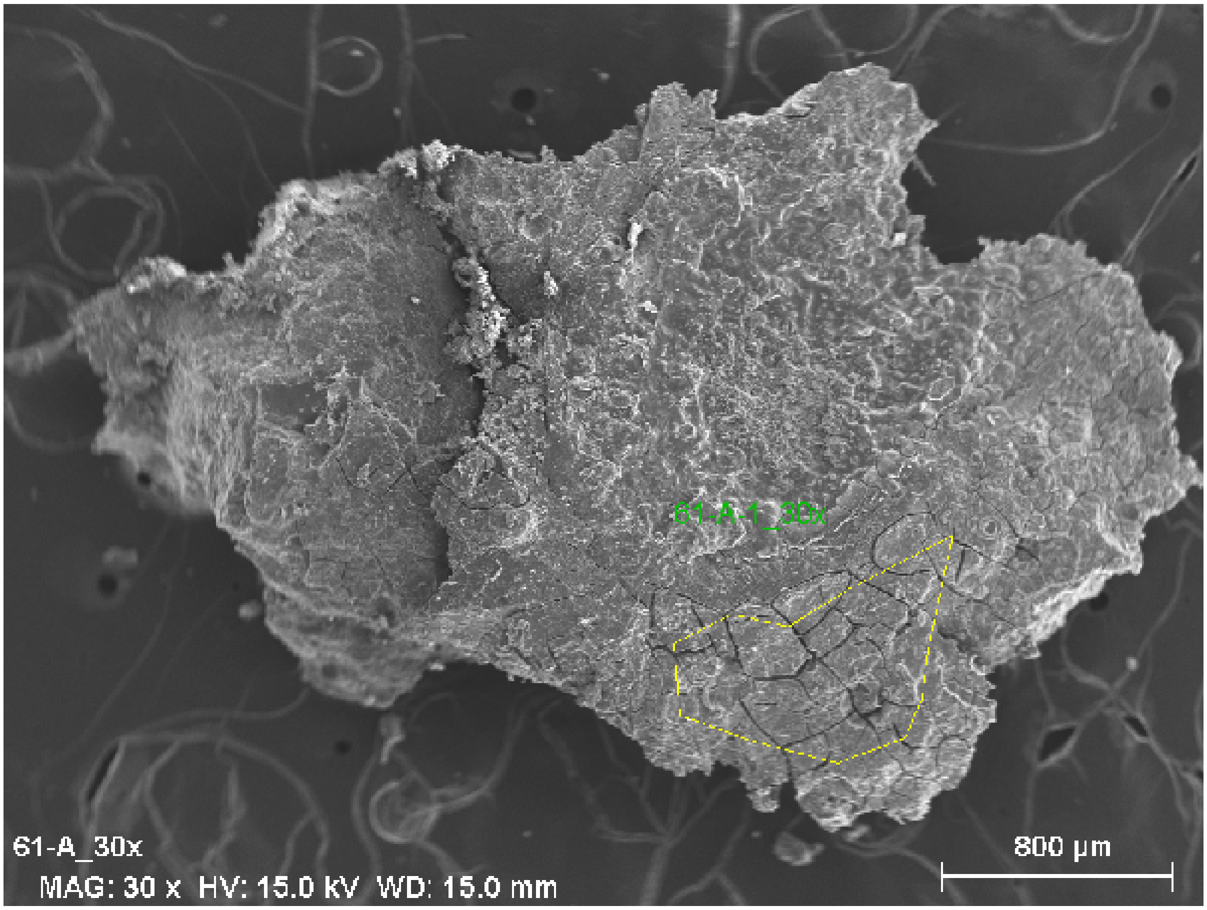

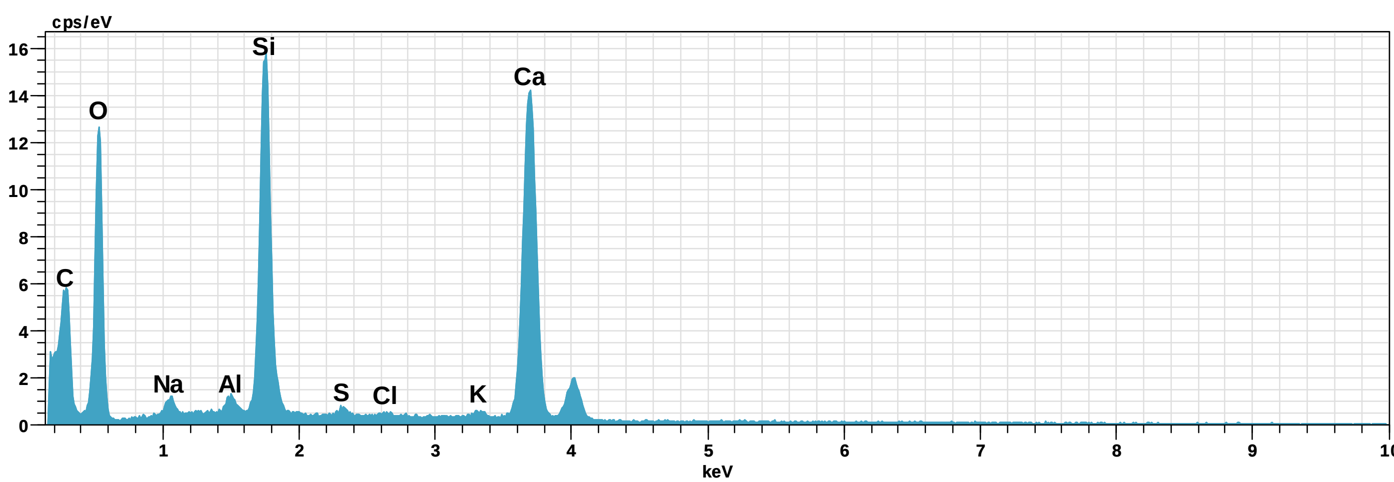

Figure 42. SEM image and EDS spectrum (30X) of the framed area shown in the above image, which is adjacent to Siltstone Particle #3. The spectrum is similar to that shown in Figure 41.

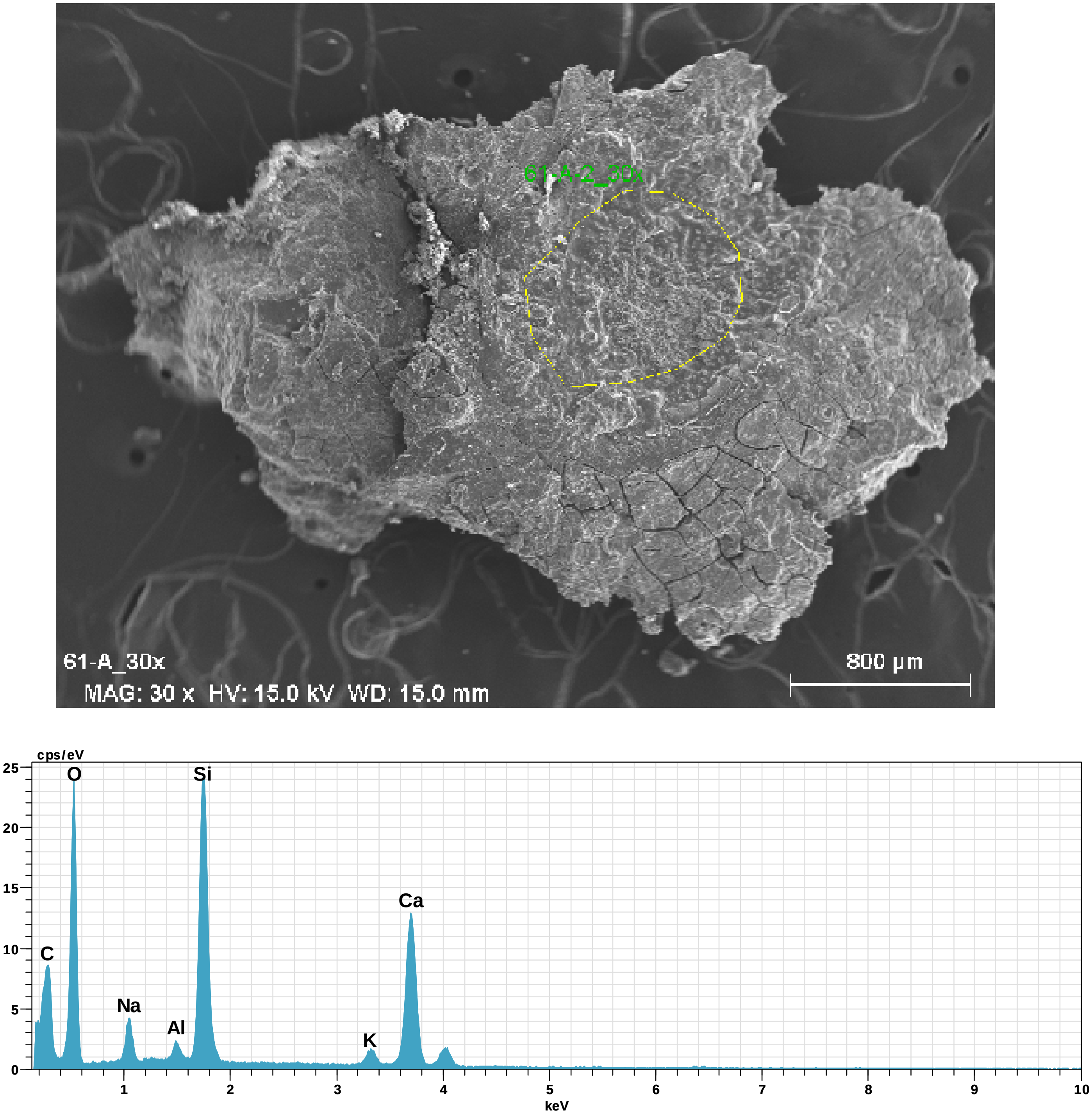

Figure 43. SEM image and EDS spectrum (30X) of the framed area shown in the above image, which is directly over the fracture surface of Siltstone Particle #3.

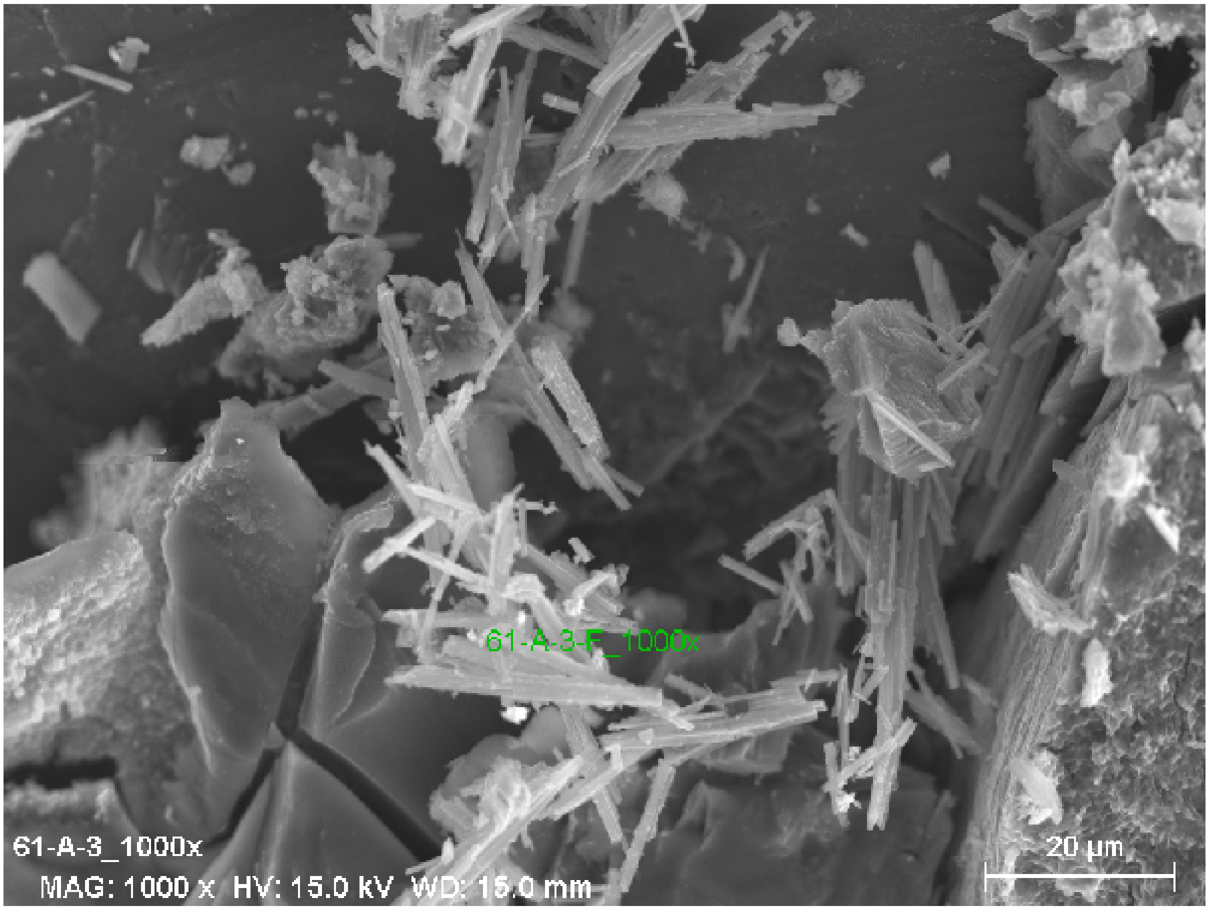

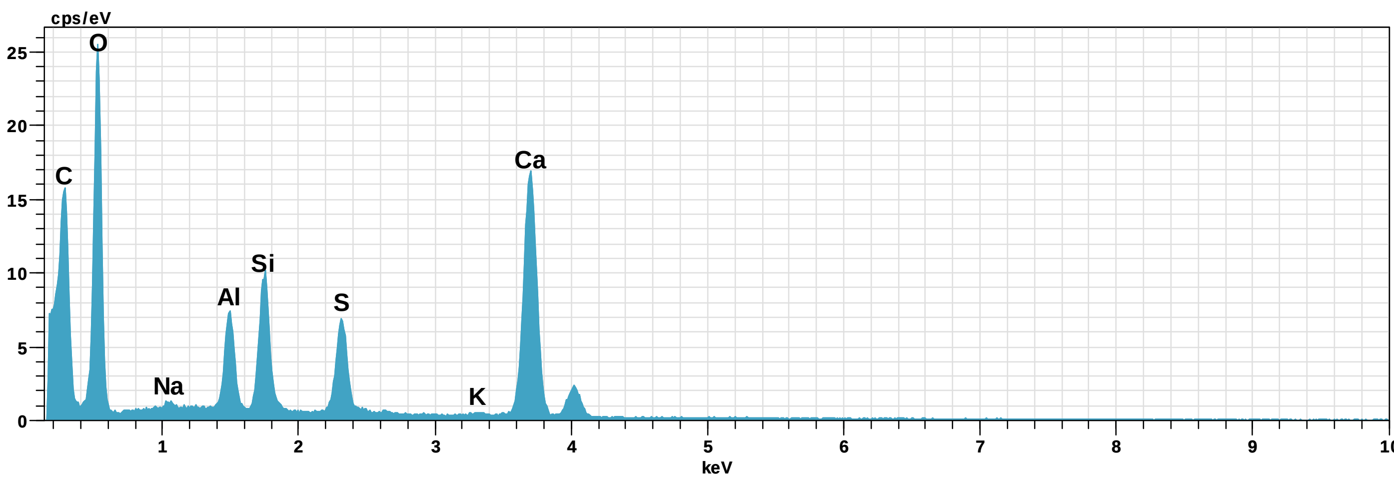

Figure 44. SEM image and EDS spectrum (1000X) of the northwest tip of the SEM study sample shown in Figures 41 through 43. This spectrum is a spot analysis at the site of the (+) on one of the ettringite fibers.

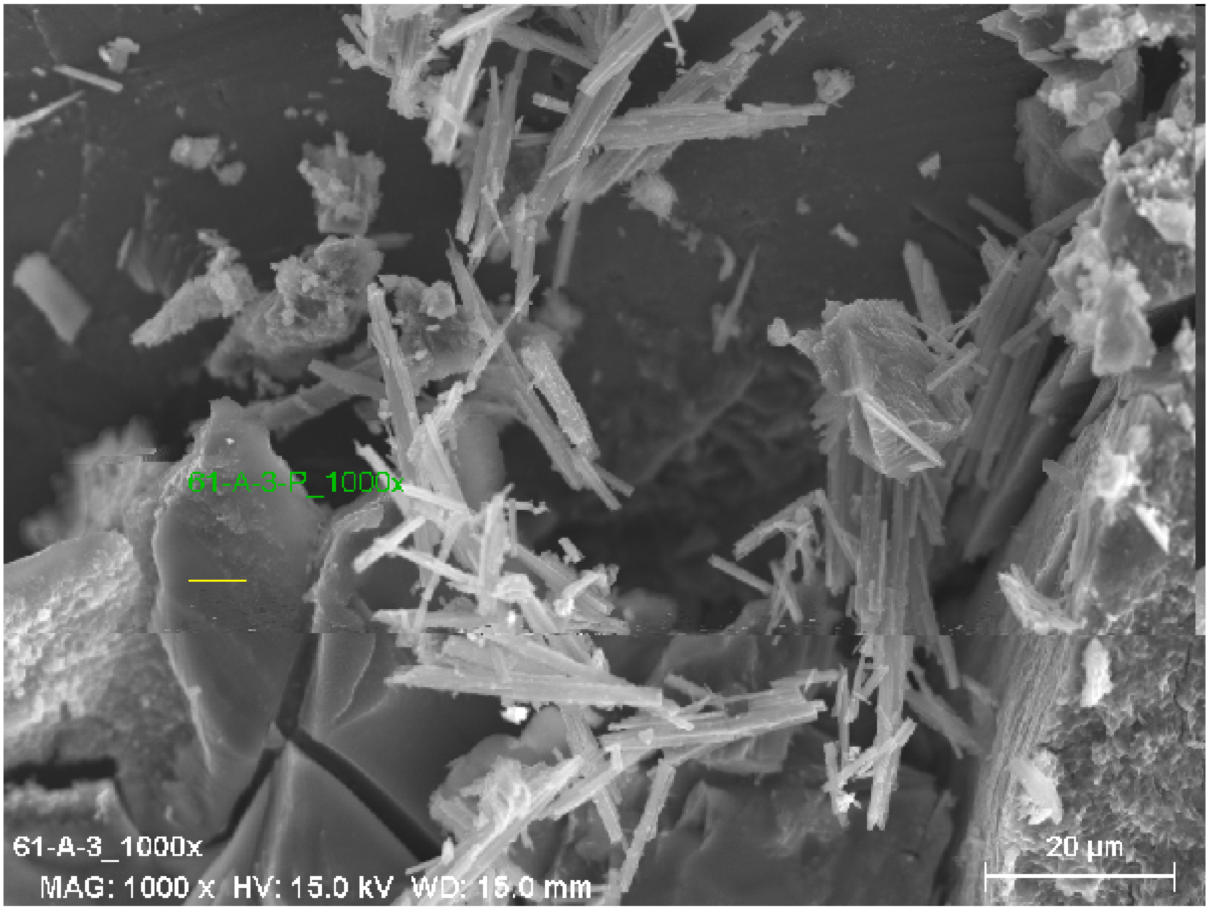

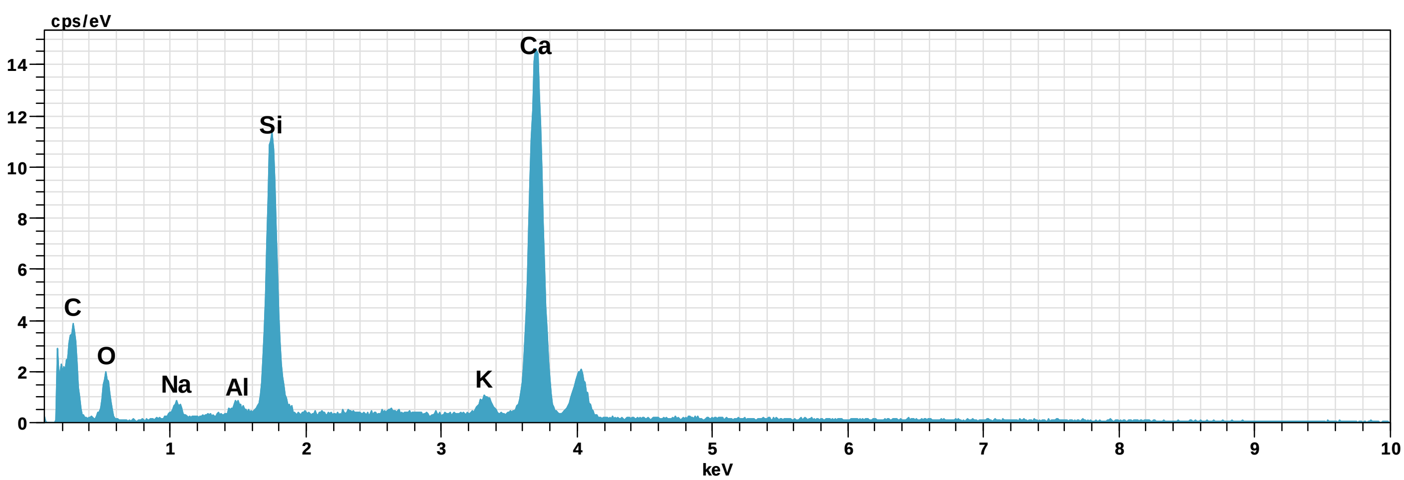

Figure 45. SEM image and EDS spectrum (1000X) of the northwest tip of the SEM study sample (Particle #3) shown in Figures 41 through 43. This spectrum is an analysis of the massive material within the framed area shown in the above image. The material is ASR gel reaction product.

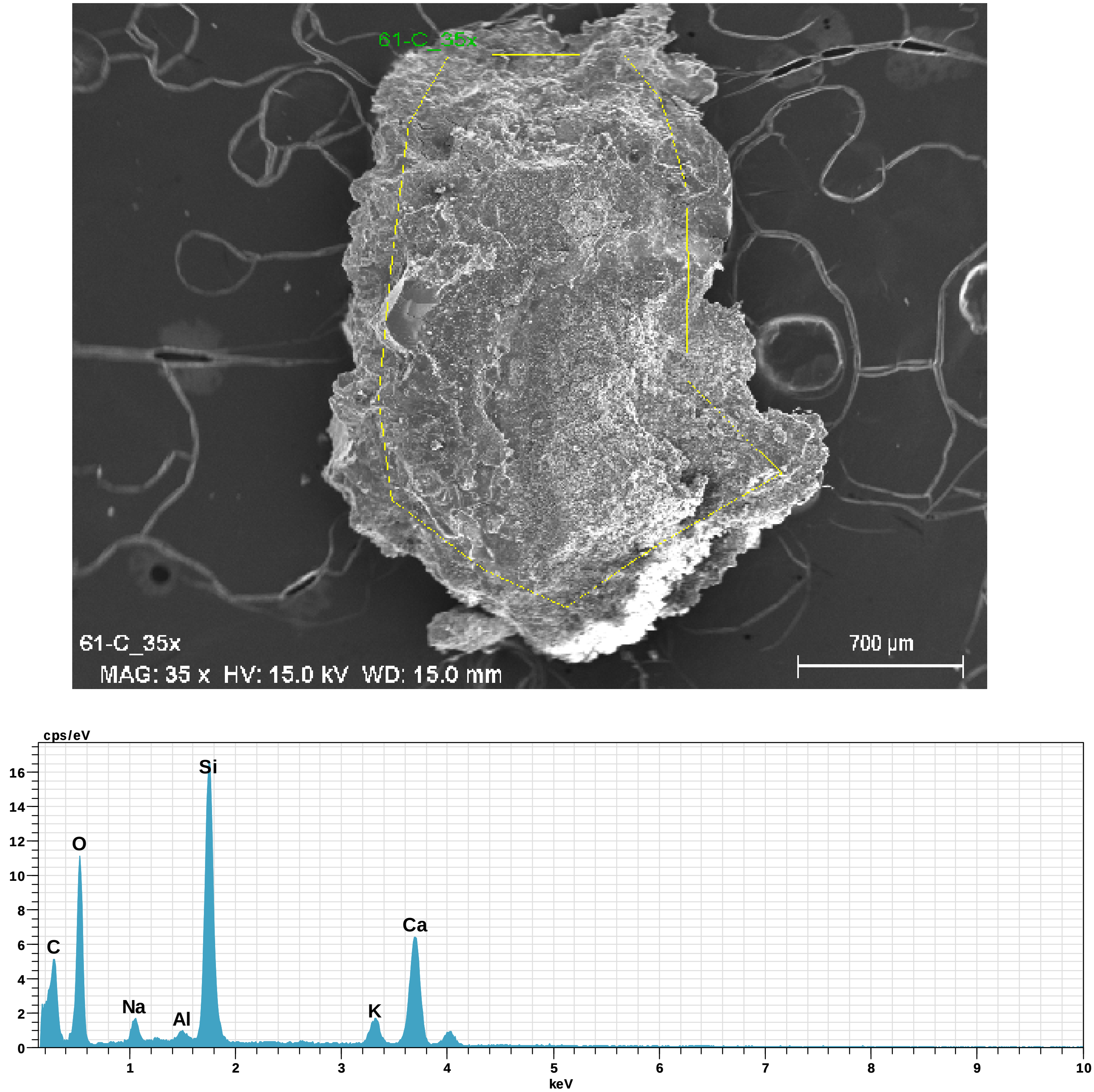

Figure 46. SEM image and EDS spectrum (35X) of Chert fine aggregate Particle #2, which is shown in the top photograph of Figure 40 as it is present on a pre-existing fracture surface of Core 3. Contributions to the elemental chemical analysis include silica from the chert particle itself, and ASR gel.

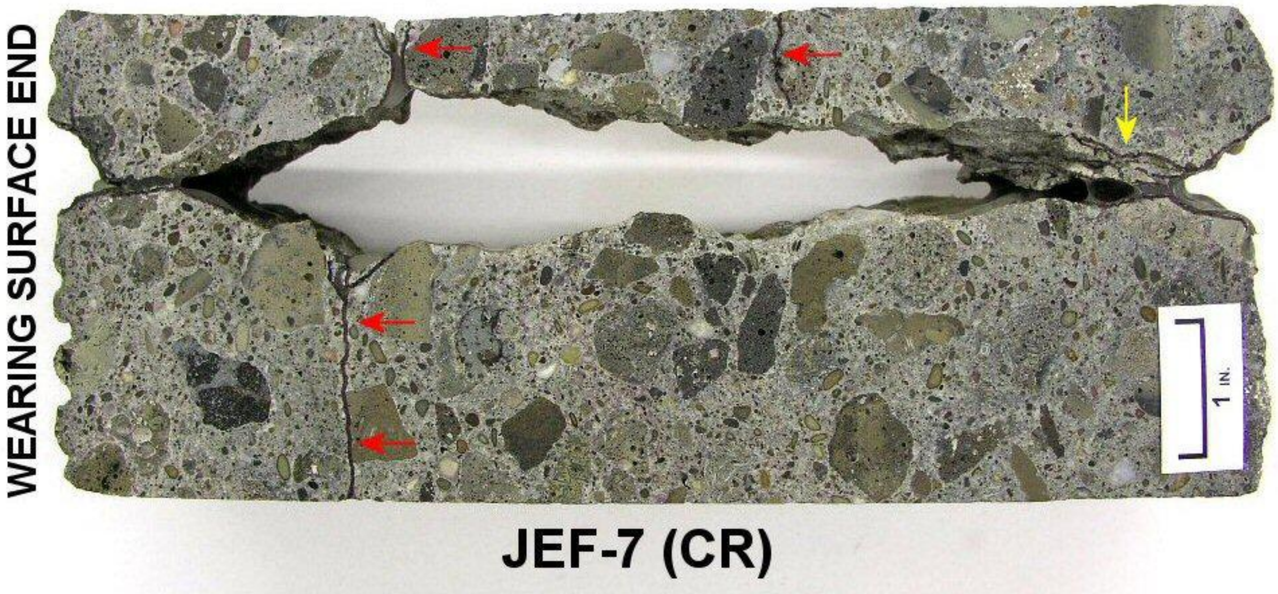

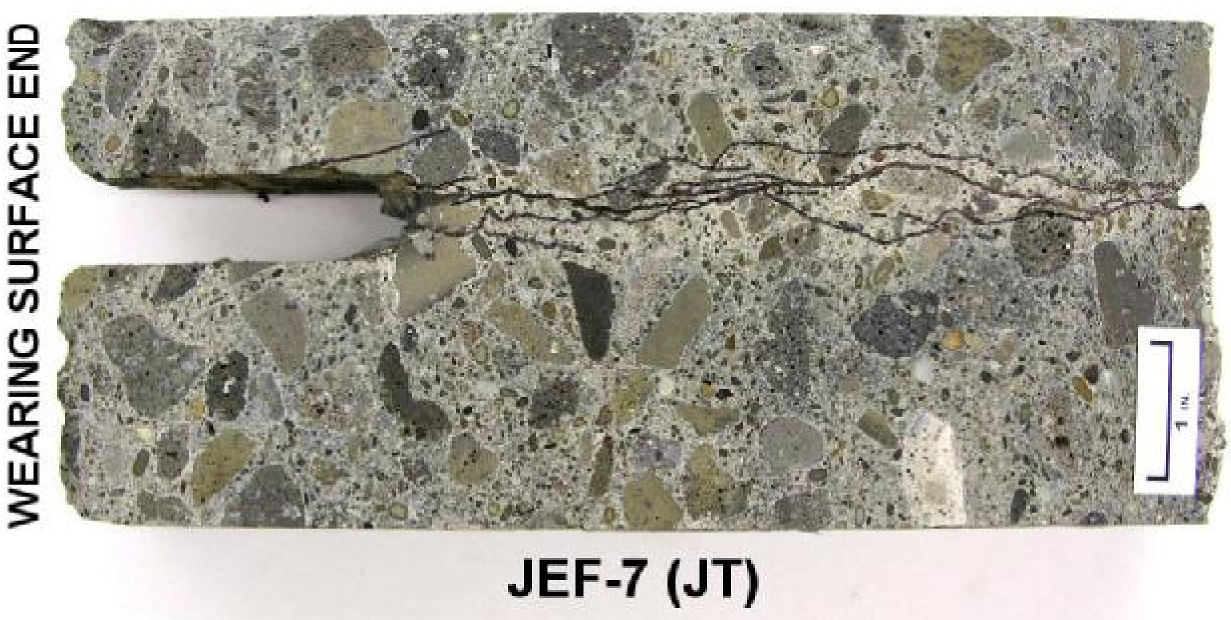

Figure 47. Lapped surface views of a core taken through a transverse crack (CR) and a core taken through a transverse control joint (JT) on a slag aggregate pavement on State Route 7 in Jefferson County, Ohio. The pavement was 19 years old at the time of coring and had been given an "Excellent" performance rating. Cracks in the core concretes are marked with a black marking pen.

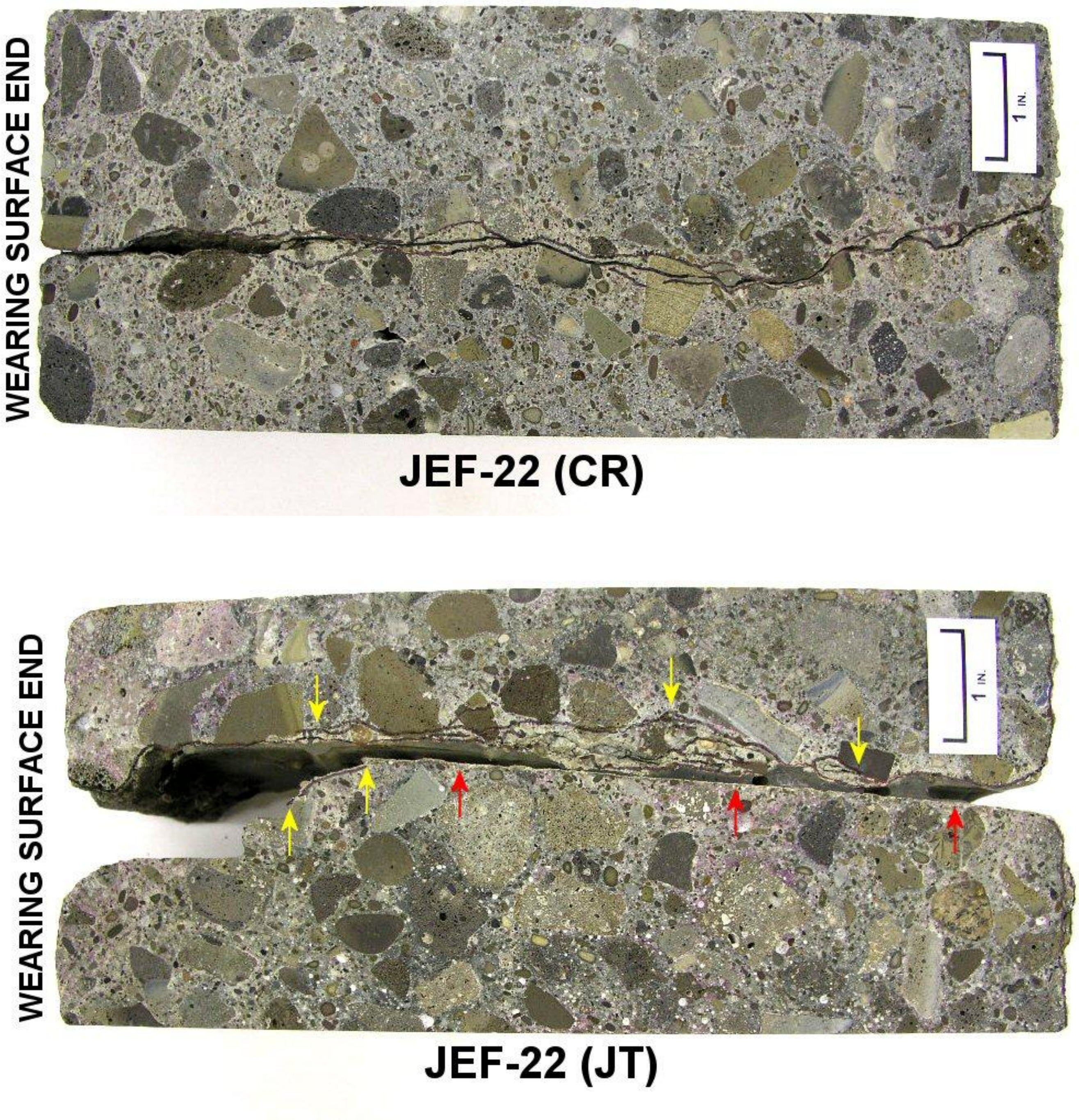

Figure 48. Lapped surface views of a core taken through a transverse crack (CR) and a core taken through transverse control joint (JT) on a slag aggregate pavement on State Route 22 in Jefferson County, Ohio. The pavement was 19 years old at the time of coring and had been given an "Average" performance rating. Cracks in the core concretes are marked with a black marking pen

Figure 49. Lapped surface views (7X) perpendicular to the plane of the wearing surface in the Joint Cores taken from the Jefferson County slag aggregate pavements showing freeze/thaw-related cracking in the cementitious phase and slag aggregate particles (S). The red arrows point to a few of the numerous entrained are voids that are filled with ettringite deposits. The epoxy (yellow dots) is the adhesive used to reassemble the two halves of the as-received cores. The wearing surface is at the top in the photographs.

.

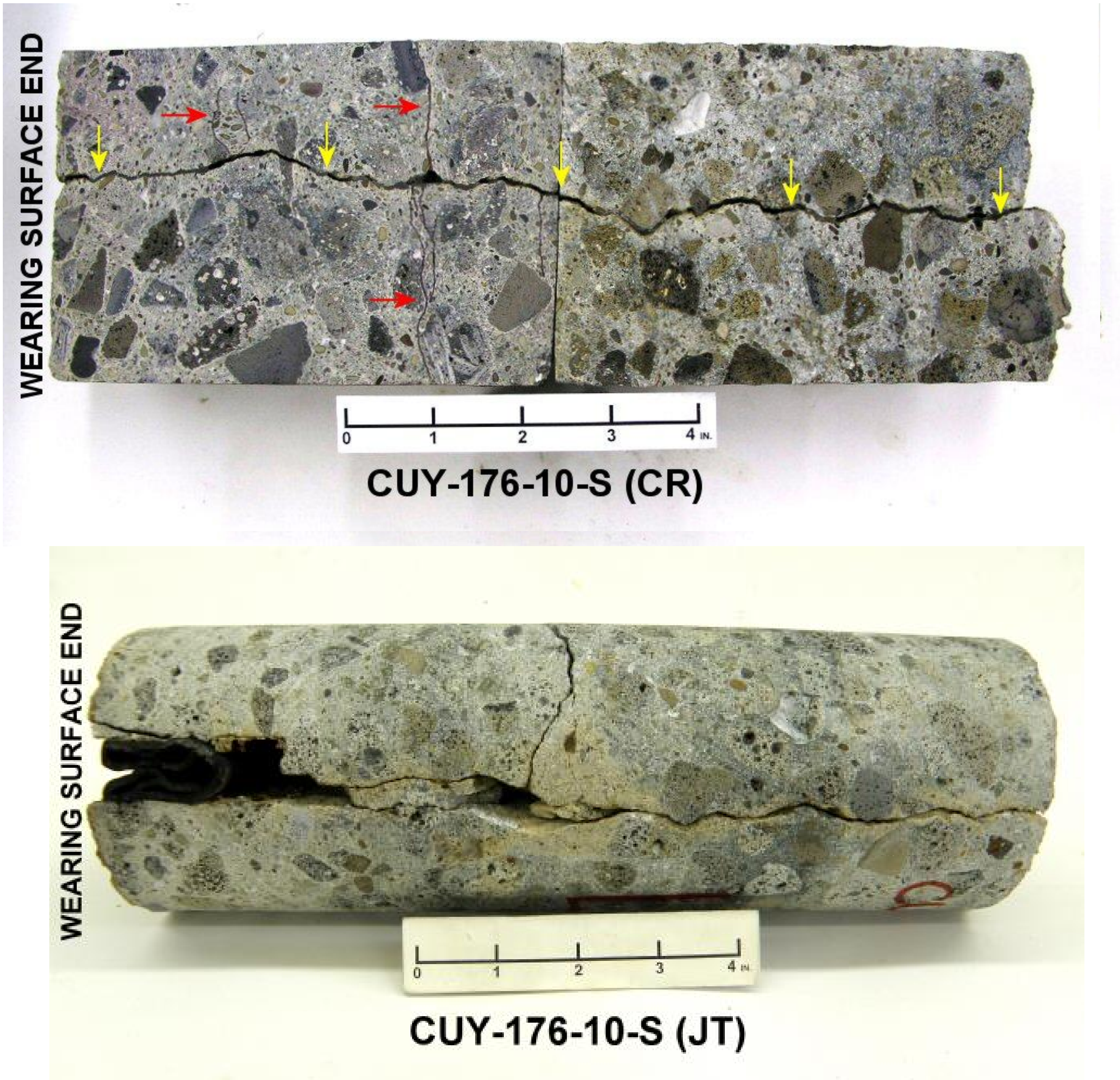

Figure 50. Cores taken from State Route 176 in Cuyahoga County, Ohio. The top photograph is a lapped surface of a core taken through a transverse crack (CR) in the pavement. The transverse crack is marked with the yellow arrows and sub-surface horizontal cracks are marked with red arrows. The bottom photograph is a core taken through a transverse control joint in the condition in which it was received at our laboratory. There is spalling along the joint crack and some sub-surface horizontal cracking about 5 in. (13 cm) below the wearing surface.

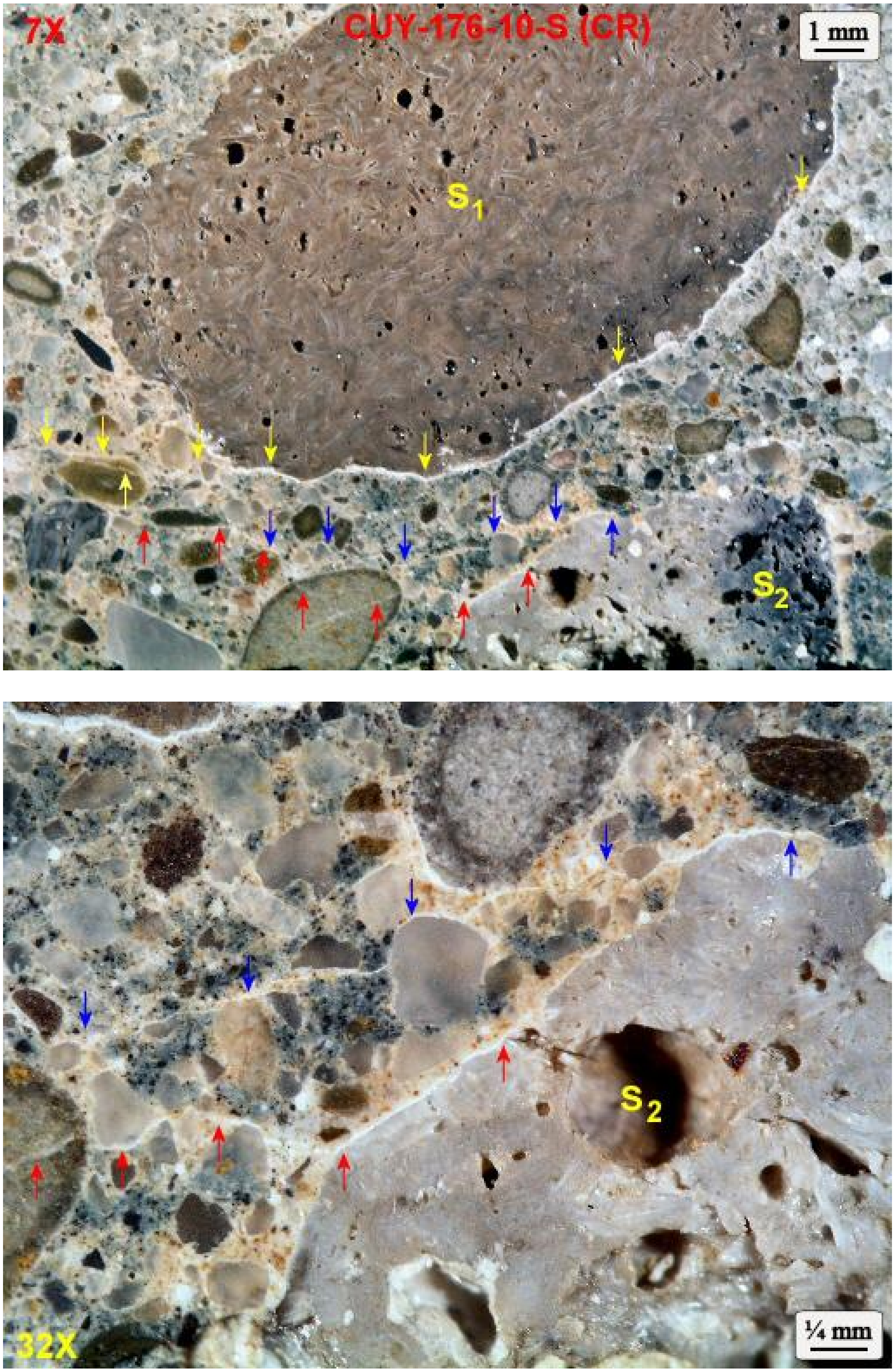

Figure 51. Lapped surface views (7X and 32X) of the Mid-Slab Crack Core taken from the southbound mainline pavement on SR 176 in Cuyahoga County, Ohio. The wearing surface is at the top in the photographs. The location is 5 in. below the wearing surface. The arrows point to the paths of very tight cracks that pass around slag aggregate particles (S1 and S2) and through a number of siltstone particles. The cracks are lined over much of their length with ettringite deposits.

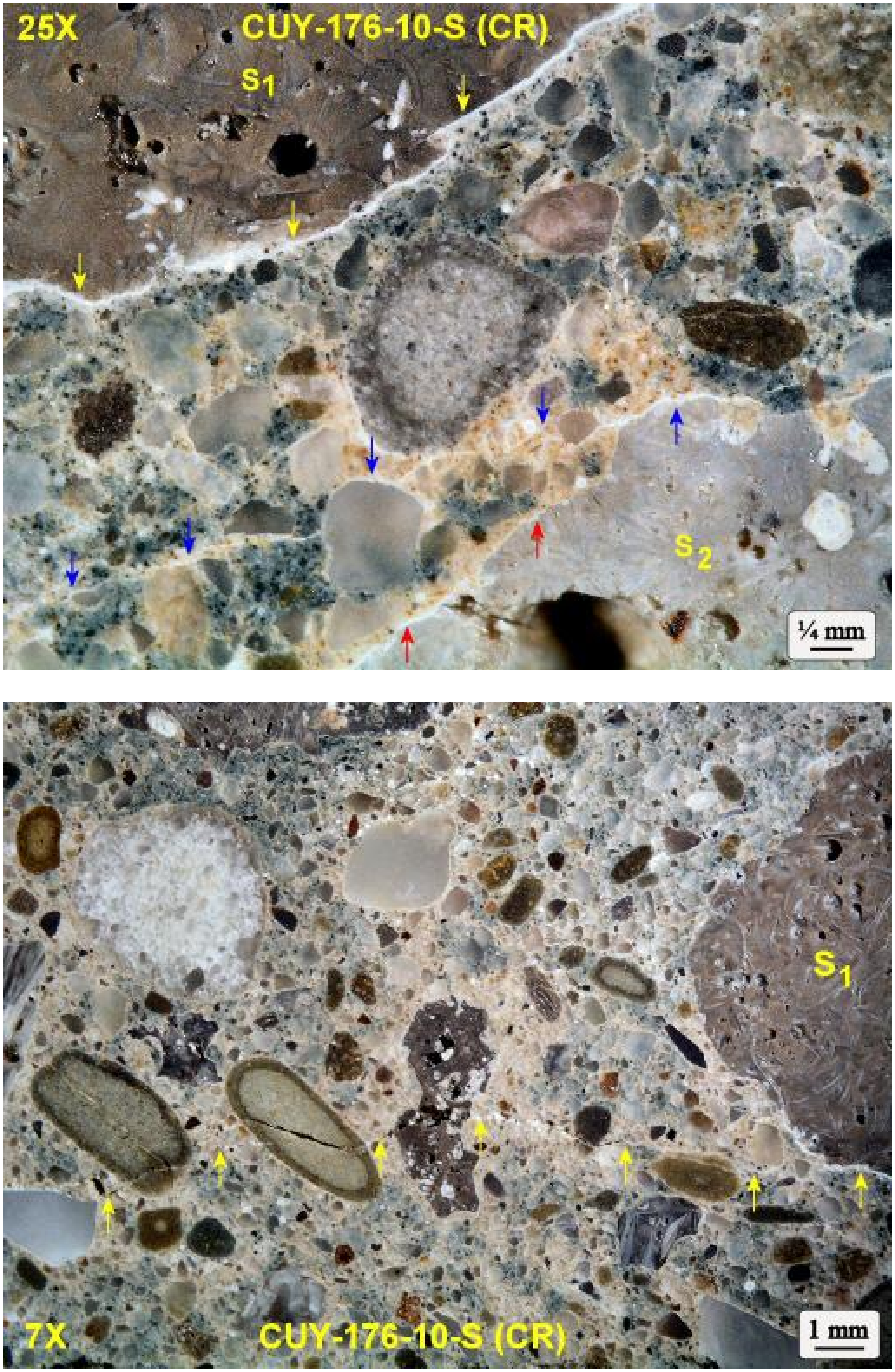

Figure 52. Lapped surface views (7X and 25X) of the Mid-Slab Crack Core taken from the southbound mainline pavement on SR 176 in Cuyahoga County, Ohio. The wearing surface is at the top in the photographs. The location is 5 in. below the wearing surface. The arrows point to the paths of very tight cracks that pass around slag aggregate particles (S1 and S2) and through a number of siltstone particles. The cracks are lined over much of their length with ettringite deposits.

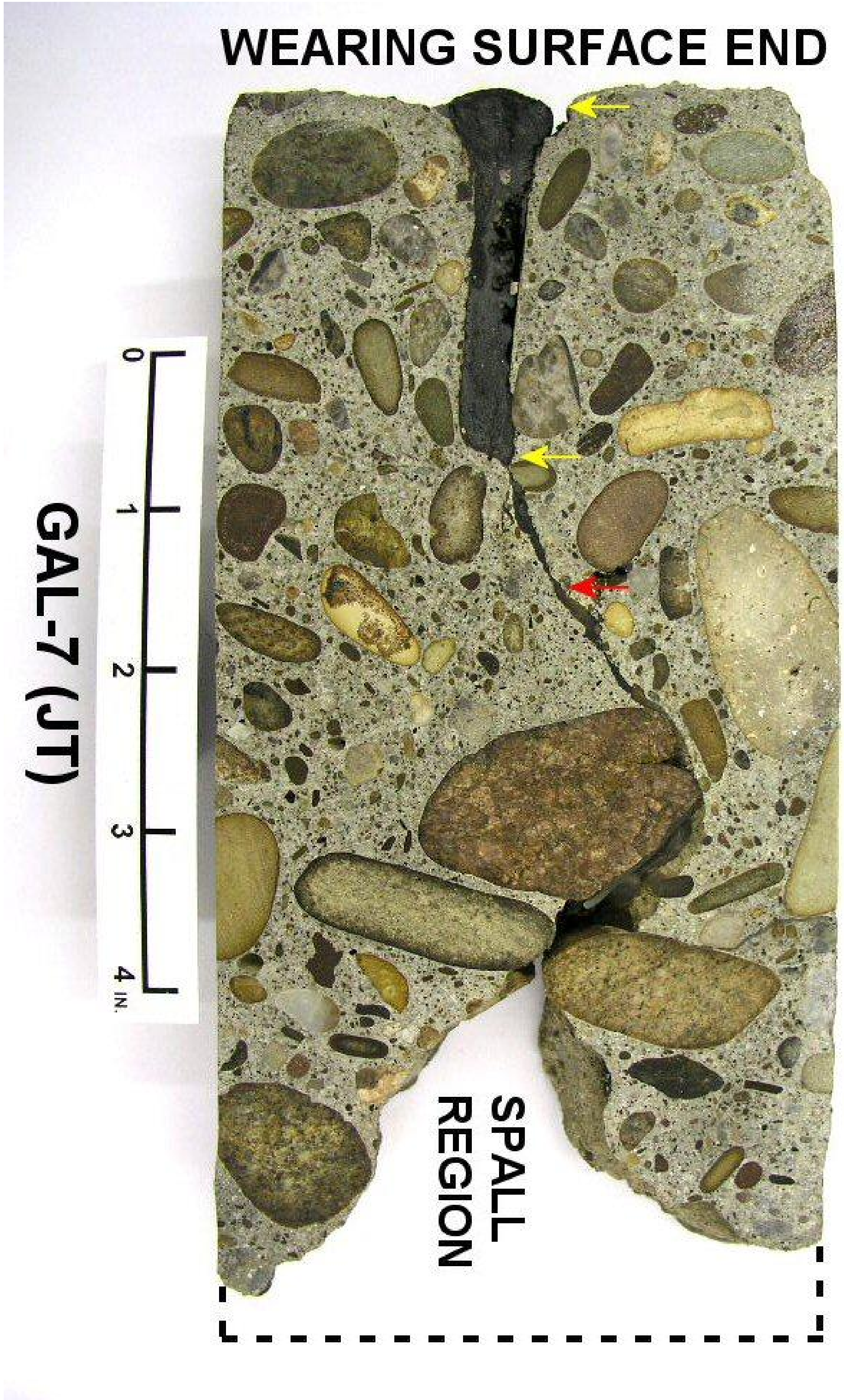

Figure 53. Lapped surface view of Core 2 taken through a transverse control joint on an ODOT PCC pavement on State Route 7 in Gallia County, Ohio. The pavement was constructed in 1946. This is an original joint, as is the joint sealant material, which is a sand-filled bituminous material.

ORITE • 141 Stocker Center • Athens, Ohio 45701-2979 • 740-593-2476
Fax: 740-593-0625 orite@bobcat.ent.ohiou.edu http://webce.ent.ohiou.edu/orite/